Master thesis
Spring 2011
Plate buckling in Movable Scaffolding Systems

Thomas Mørch Larsen
Mechanics Division
Department of Mathematics
University of Oslo
thomasml@math.uio.no

May 27, 2011

Preface

This is a master thesis written in order to qualify for the degree of M.Sc., Master of Science in Solid Mechanics, at the University of Oslo, Department of Mathematics, Mechanics Division. The thesis itself has been conducted in near collaboration with the engineering company Strukturas A/S, localized in Langesund. In that extent I would like to thank my external supervisor Øyvind Karlsen for providing professional guidance over the course of the last five months. I would as well give big thanks to my internal supervisor Professor Jostein Hellesland.

Langesund, 27.05.2011

Thomas Mørch Larsen

Abstract

The main objective of the thesis is to determine the capacity against buckling of the main girder web at a launching stage. As the webs and the flanges of the main girder must defined as slender structural elements (class 4) instability will govern design resistance. The first part of the thesis will give the reader an understanding of the boundary conditions and phenomenon that will determine the loading conditions this steel girder is subjected to. All these observations will then be implemented to a nonlinear buckling analysis in ANSYS Workbench 12.1. This particular analysis will be executed in order to satisfy design guidelines given in *NS-EN 1993 1-5: Plated structural elements*[1] regarding material properties, imperfections and boundary conditions for this buckling phenomenon. With this type of analysis we can evaluate the post critical resistance of a plate. The geometry and loads which will be used as input in ANSYS will be retrieved from a reference project which is a MSS-system used to build a bridge in Portugal in 2004 , project identification: 25111 - VIZELA CALVOS. After obtaining results from this analysis the main girder‘s web panel will collapse at loading from the launching wagon equal to:

$$F_{Rd} = \frac{F_{Rk}}{\gamma_{m1}} = \frac{4267,8kN}{1,1} = 3879kN \tag{1}$$

This particular result was satisfying as it demonstrated that the web panel had enough capacity and that the stiffening arrangement proved to be efficient as it provoked a local buckling mode in a subpanel. The utilization of the web against instability was rather satisfying at this project. A request from Strukturas regarding additional nonlinear analysis with ANSYS obtained with a new stiffening arrangement was as well executed. This will provide useful information regarding capacity at other MSS projects. The alternative stiffening arrangement included a transverse stiffener rigid for shear buckling. With this configuration the collapse load was found to be:

$$F_{Rd} = \frac{F_{Rk}}{\gamma_{m1}} = \frac{6451,3kN}{1,1} = 5832kN \tag{2}$$

Including a transverse stiffener will provide this web with additional stiffness against instability. The main reason for this is that the stiffener will provide the web panel with additional restraint and the critical buckling modes must be obtained with unsymmetrical loading. This is as well evident in design codes in NS-EN 1993 1-5 where plate panels can be treated separately if rigid transverse stiffeners are implemented. These rigid transverse stiffeners will decrease the buckling length and subsequently increase resistance.

When these nonlinear analysis were executed the next objective of the thesis is to study the design formulas in NS-EN 1993 1-5. It soon became evident that there were some important issues regarding the calculation of resistance due to patch loading. Concentrated transverse loading applied perpendicular to the flange in the plane of

the web is referred to as patch loading in Eurocode 3 and would in this case be the support reaction from the launching wagon. The inner web of the main girder has a special configuration with transverse stiffener c/c 750mm to add stiffness in these local regions at the flange and adjacent part of the web. As the ANSYS analysis state that the most critical mode is a local buckling mode between longitudinal stiffeners, the design formulas does not differ between failure modes. Bearing all this in mind that the transverse stiffeners configuration will contribute to spread the load at a larger area on the critical subpanel it's safe to conclude that these design formulas must be discarded.

The main girder's web may as well suffer from instability due the influence of direct stresses and shear buckling. Their effect have been examined and it turns out that they will not govern the web resistance. These results were not unexpected because the main girder will experience a larger bending moment and support reactions at the concreting stage due to self weight of the concrete. As a consequence of these discoveries the nonlinear analysis in ANSYS will reflect that the patch loading will cause the most confusion regarding ULS capacity of the web panel.

Symbols

α - Breadth-length ratio plate panel (a/b)
$\beta_{A,c}$ - Ratio between gross area and effective area
γ_F - Load factor
γ_{m0}/γ_{m1} - Material factor
γ_s - Contribution from longitudinal stiffener at patch loading
ϵ - Correction due to yield strength
η - Factor for strain hardening allowed
η_1 - Utilization direct stresses
η_2 - Utilization patch loading
η_3 - Utilization shear stresses
λ_i - Load multiplier assosiated with mode i
$\bar{\lambda_c}$ - Reduced column slenderness
$\bar{\lambda_F}$ - Reduced patch slenderness
$\bar{\lambda_p}$ - Reduced plate slenderness
$\bar{\lambda_w}$ - Reduced web slenderness shear
ν - Poisson's ratio
ξ - Grade of plate like or column buckling
ρ - Reduction factor effective width
ρ_{loc} - Local buckling reduction factor effective width
ρ_p - Global buckling reduction factor effective thickness
σ - Direct stress
σ_1/σ_2 - Principle stress
$\sigma_{cr,p}$ - Critical elastic stress plate buckling
$\sigma_{cr,c}$ - Critical elastic stress column buckling
σ_v - von Mises equivalent stress
χ_c - Global buckling reduction factor thickness for column buckling
χ_F - Reduction factor patch loading
χ_w - Reduction factor shear loading web
ψ - Rate of stress distribution panel/subpanel, shape of critical mode

a - Length of plate panel,distance between rigid transverse stiffener
b - Breadth of plate panel,distance between longitudinal stiffener
b_{eff} - Effective width
b_f - Breadth flange
b_{st} - Breadth stiffener
f_y - Yield strength
h_f - Inner moment arm
h_w - Height web
i - Cross section moment arm

k_σ - Buckling factor direct stresses
k_τ - Buckling factor shear buckling
k_F - Buckling factor patch loading
l_k - Buckling length Euler column
l_y - Loaded yield length
m_1/m_2 - Dimensionless parameters to evaluate flanges stiffness
s_s - Initial loaded length
t - Thickness structural element
t_f - Thickness flange
t_{st} - Thickness stiffener
t_w - Thickness web

A - Cross section area
A_c - Gross cross section area
A_{eff} - Effective cross section area
A_{sl} - Cross section area stiffener
E - Young's modulus
E_T - Tangent modulus
F_{cr} - Elastic critical load for patch loading
F_{Ed} - Design patch load
F_{Rd} - Design patch load resistance
F_y - Yield load for patch loading
G - Shear modulus
I_p - Second moment of area of the stiffener around the edge fixed to plate
I_{sl} - Second moment of area of the stiffener with contributing plating
I_t - St. Venants torsion constant for stiffener
I_w - Warping cross section constant stiffener
K - First order elastic stiffness matrix
M_{Ed} - Design moment
$M_{f,Rd}$ - Design moment resistance flange
S - Second order geometric stiffness matrix
V_{Ed} - Design shear force
$V_{b,Rd}$ - Design shear force resistance
$V_{f,Rd}$ - Design shear force resistance flange
$V_{w,Rd}$ - Design shear force resistance web
W_{eff} - Effective section modulus

Contents

1 Introduction

Movable scaffolding systems (often abbreviated MSS) are commonly used in conjunction with span-wise construction of reinforced concrete bridges. The scaffolding systems themselves are often complex structural steel structures, that may be subjected to a number of different load cases and that may involve different support conditions. The engineering company Strukturas A/S has specialized in such systems, and has delivered bridge-building equipment for projects around the world for the last 30 years. The company has located some structural problems in the scaffolding systems that would benefit from a closer study.

One of the problem areas, related to local plate buckling, is of interest here. The major structural load carrying elements of the scaffolding system considered, consist of two steel girders with plated box cross-sections. When the scaffolding system is launched forward to the next bridge span, plate buckling localized to the web plate of the boxed cross-section at the front support, can be a problem. In this situation it is important to find the position of the scaffolding system which will provide the most unfavorable loading of the web-plates.

Further, for this critical position, it is important to establish buckling capacity and strength characteristics of the web plates. Due to uncertainties in the design requirements in Eurocode 3, it is difficult to establish the buckling capacity with the help of closed-form design formulas for plates with a complex geometry and loading. The effect of biaxial loading and both longitudinal and transverse stiffeners provides for a very complex stress pattern. Also, uncertainties regarding boundary conditions and the size of the plate element to be analysed, complicate the problem even further. In order to deal with the problem considered, there is a need to study design codes and the theory these are based upon, in more detail. This is in part the motivation for the present master thesis, which will be performed in close collaboration with Strukturas A/S.

2 MSS - Movable Scaffolding System

2.1 Structure

Strukturas A/S has during the last three decades developed systems which will be used to cast concrete decks in bridge structures. The company's MSS has been used in numerous projects around the world with great sucess. The reason behind this sucess, lies in the system's vast opportunities to be modified and be able to cast different cross-sections. A MSS-system can be used to cast cross-sections like single- and doublebox, but as well double T-sections are often used. The reason for that these type of scaffolding systems are so efficient and sucessfully used in these type of projects can be explained by the following:

- Highly optimized engineering will reduce weight of structure due to use of high quality steel
- Easy assembly with few structural elements
- Easy handling of the system which reduce need for manpower
- The system has been used in several different projects and been over time modified with new designs which are proven to give an excellent result
- You are easily able to change the geometry of the cross-section of a bridge deck and span length of the structure to new projects

Figure 1 and 2 shows a typical MSS structure in elevation and plan ready to cast a new span with concrete. These illustrations will give you an indication of which components such a system exist of and their placement. To get a fundamental understanding of how the system works it is appropriate to illustrate a typical work cycle. That means the operations which must be executed in order to cast one bridge deck until the next.

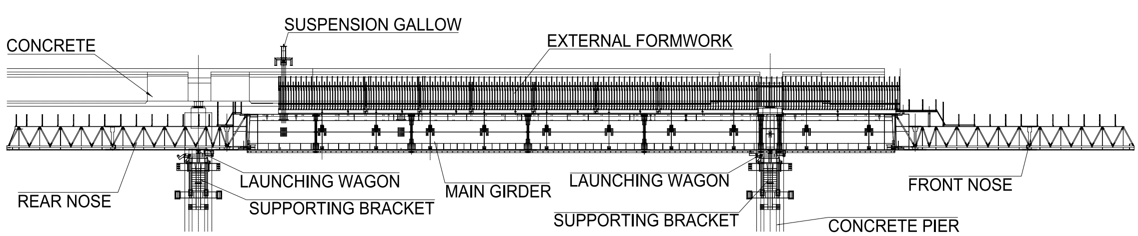

Figure 1: MSS-system seen in elevation

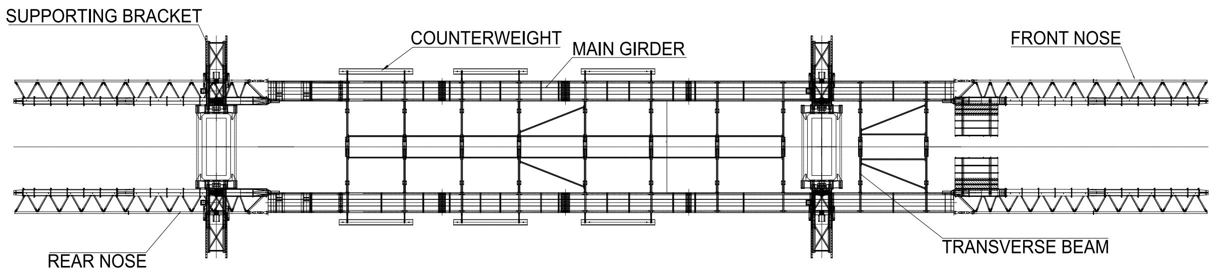

Figure 2: MSS-system seen in plan

Work cycle:

- Lowering of the system roughly 200 mm by means of the main hydraulic jacks at the front pier bracket and rear suspension gallow
- Opening of the centre joints which connect the system transversely at transverse beams, and move the main girder into a position where the transverse beams can pass the piers
- In case of double T-sections, lowering of internal formwork is needed
- The MSS is ready for launching. Since both the halves are independent, a flexible longitudinal movement is achieved

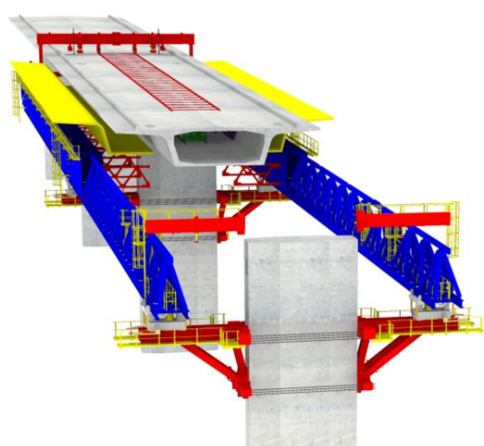

Figure 3: MSS-system ready to launch forward

- Both main girders are moved transversely and all transverse beams are reconnected
- During the longitudinal launching operation the suspension gallow is moved to its next position

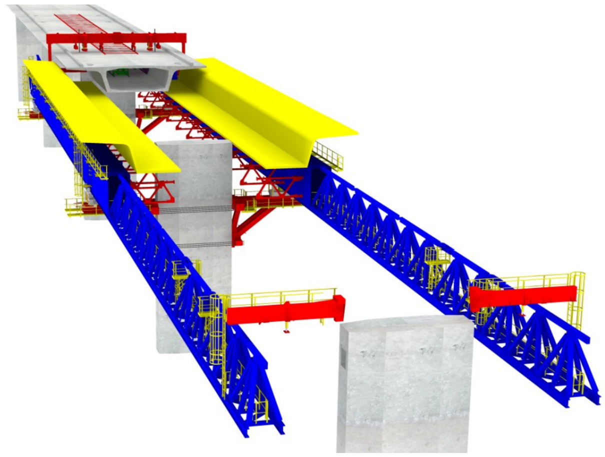

Figure 4: MSS-system launched forward

- Both main girders are raised to their final position by the main hydraulic jacks
- Vertical jacking and levelling of the formwork for the next concreting operation
- For box section bridges it is necessary to move the internal formwork after positioning the reinforcement and tendons of the bottom slab and webs
- Three pairs of brackets are used. The rear pair will be moved during the concreting operation in order to complete one work cycle

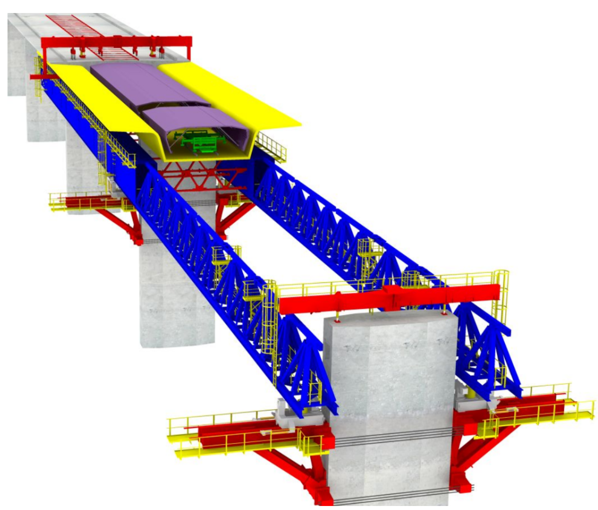

Figure 5: MSS-system ready to cast another span

2.2 Components

2.2.1 Supporting bracket

The system will be mounted to the concrete piers with the help of a supporting bracket. High quality steel is attached over the pier so can you achieve a stabile support in a desirable plan for casting of bridge decks. The forces from the bracket will act as compression forces at the concrete piers. The supporting bracket mainly consist of welded profiles with an optimized geometry for load cases from launching and concreting.

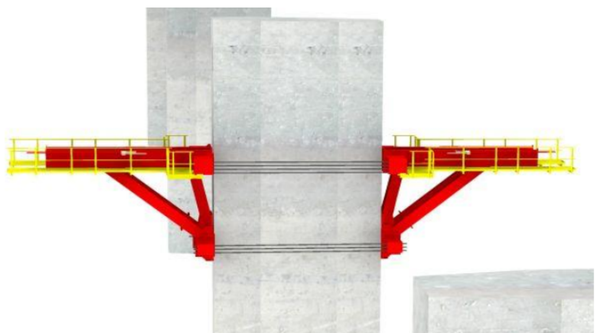

Figure 6: Supporting bracket connected to piers

2.2.2 Main girder

A MSS-system consist of two main girders which are the structure‘s most important element regarding load shedding. These two girders will endure forces from concreting, self-weight from structural elements and complicated load cases due to launching of system. A main girder is designed with plated elements which are welded together to form a box cross-section. In addition to this welded plates the main girders consist of stiffeners which purpose is ensure a higher buckling capacity. Due to launching of the MSS-system many load cases can occur and Strukturas A/S wish to analyze this thoroughly. This is the presented motivation for this master thesis and effort will be made to clarify this matter in the upcoming chapters. The two main girders are connected with transverse beams in a concreting state. Due to transport logistics the main girder is fabricated in smaller segments.

2.2.3 Transverse beams

The transverse beams connects the main girders together and closes the system in concreting state. The beams consist of square profiles which are welded together to form a truss which are connected to the main girders with a bolted connection. An

Figure 7: Segment of main girder

ordinary MSS-system will normally consist of 7-11 transverse beams. The quantity will depend on the span length of the bridge construction. Often are these beams fabricated with a hinged connection which purpose is to prevent collision with concrete piers when the system is launched. With this hinge the transverse beams can rotate closer to the main girders and extra space can be exploited.

Figure 8: Transverse beams at launching, not connected

2.2.4 Rear and front nose

The noses in a MSS-system are connected to the main girder with a hinged connection and consist of bar elements which together form a truss. The purpose for these noses is that they will constitute the rear and front part of the system and enables casting of bridges with horizontal curvatures. Due to the hinged connection between the main girder and noses enables us to cast bridges with low horizontal radius.

2.2.5 Suspension gallow

Suspension gallow is a device which enables lifting of the system 200 mm at the rear just before concreting is initialized. The gallow is placed at the top of the "old" concrete cross-section, which means concrete that was casted from last span. The gallow itself is a beam that is connected with two main hydraulic jacks. There are casted holes in the concrete which enables us to mount high quality steel at the main girder and the gallow. With this solution the main hydraulic jaks can lift the system.

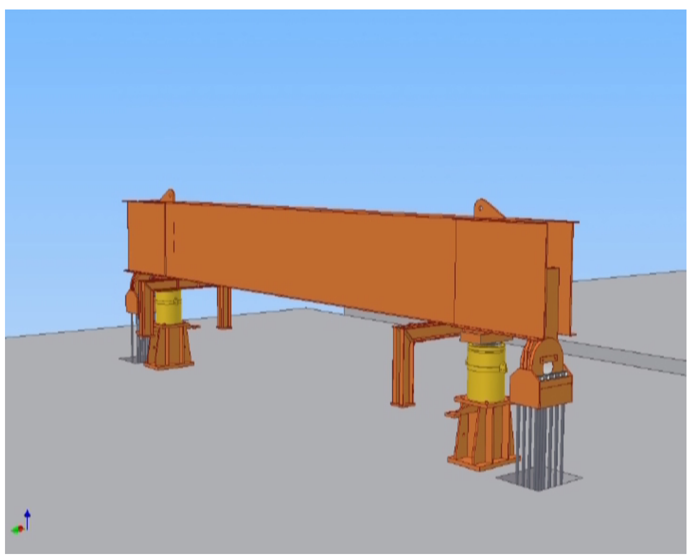

Figure 9: Suspension gallow

2.2.6 Launching wagon

This wagon is a frame construction localized at the supporting bracket and has primarily three main tasks it must execute:

- Launch the system longitudinally to next span
- Lower and lift the system 200 mm at front support
- Move system transversely at supporting bracket so that launching can be executed

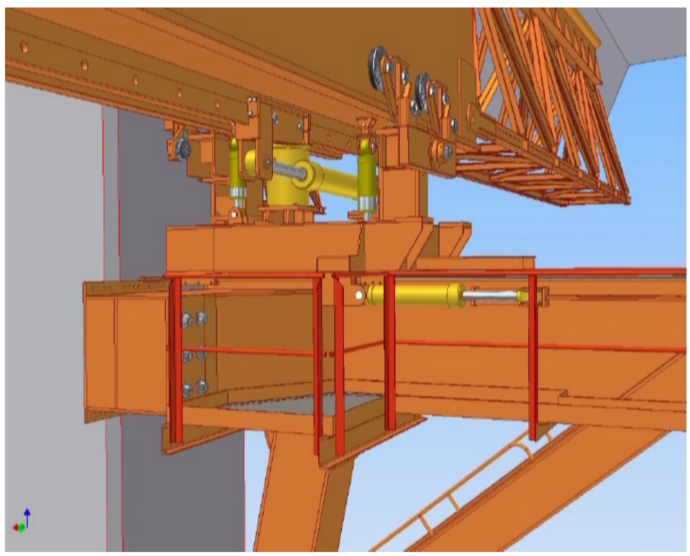

Figure 10: Launching wagon localized at supporting bracket

2.2.7 Formwork

The formwork for bridge cross-sections will be fabricated in accordance to which plans the bridge designers have made for the specific project. The geometry of a bridge cross-section will vary from project to project and Strukturas A/S have due to long experience worked out a whole range of practical solutions regarding this topic. A formwork system always consist of an external part which forms the exterior of the cross-section. This is designed with steel profiles and plywood panels which provide a smooth surface to cast on. In some cases the plywood panels can be changed to thin steel plates. This formwork is mounted to screw-jacks on the transverse beam and support struts to the main girder. The screw-jacks can provide cambering of the bridge cross-section. This way you can compensate for deformations due to self-weight of the concrete structure.

Figure 11: Box cross-section external formwork

There is often a need to fabricate an internal formwork as well, for example with box cross-section. In this case you must produce formwork panels inside the external formwork to achieve complete ambient scaffolding. With these type of scaffolding system you must as well fabricate an internal rolling wagon. This wagon main task is to transport internal panels on rails to the next span.

Figure 12: Internal rolling wagon mounted on rails

2.2.8 Counterweight

In a MSS-system it is important that the centre of gravity (CoG) is within given values considering stability of the structure. A practical solution for this is to introduce counterweights. They exist of a massive concrete cross-section which are mounted to the main girder. The CoG is only of importance in stages when the system is launched forward to next span. In concreting position the system is locked and stabile because loading are applied on several supports. When the system is unlocked at the transverse beams the structure will only be supported by three points. One on the rear support and two at the front support. When the system is launched forward these support conditions change and it is of great importance that the CoG is sufficiently within given values for stability.

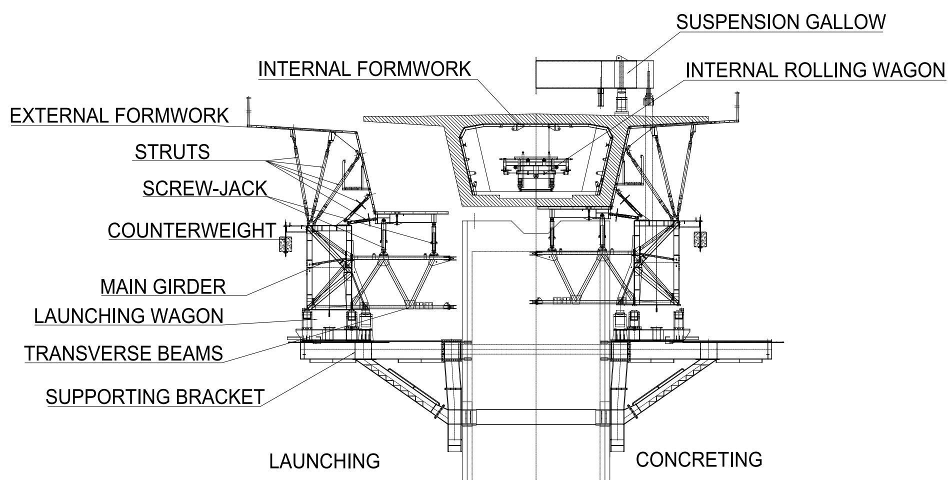

Figure 13: Section of MSS at critical buckling position

3 Plate buckling in MSS-systems

3.1 Geometry and mechanism for load-carrying

Due to uncertainties regarding capacity of plated structural elements in a MSS-system this master thesis‘ main purpose is to clarify this issue. If this should be executed in the proper manner it is feasible to study the important features a MSS-system has in the launching stages. It is of great importance to understand how the system transfer load between structural elements and characterize the most unfavorable loading situation for buckling. This chapter will give the reader an understanding of the geometry and loading condition at this particular situation from a reference project chosen by Strukturas A/S. This project is a MSS-system used to build a bridge in Portugal in 2004 , project identification: 25111 - VIZELA CALVOS.

The phenomenon buckling may appear on the web plates of the main girder in a launching stage. When the MSS is launched in the longitudinal direction by means of hydraulic jacks the main girder will experience a complex state of stress. This stress pattern is caused by two loading conditions:

- Hogging moment due to CoG is localized near a support
- Vertical support reaction from the launching wagon

Figure 14: Web panel in fabrication

The main girder consist of thin steel plates welded together to form a box cross-section. Typical plate thickness is 10-20 mm. In addition the main girder consist of different types of stiffeners which all serve the purpose to achieve a higher buckling capacity.

Figure 15 illustrates a section of the main girder where the stiffening arrangement is shown. The inner web plate is stiffened with the following stiffeners:

- Two longitudinal stiffeners with dimension 16x200 mm, top and bottom
- Longitudinal stiffener with dimension 28x200 mm, middle
- Transversal stiffener c/c 750 mm with dimension 14x200x600 mm, bottom
- Transversal stiffener c/c 2000 mm with dimension 14x200x600 mm, top

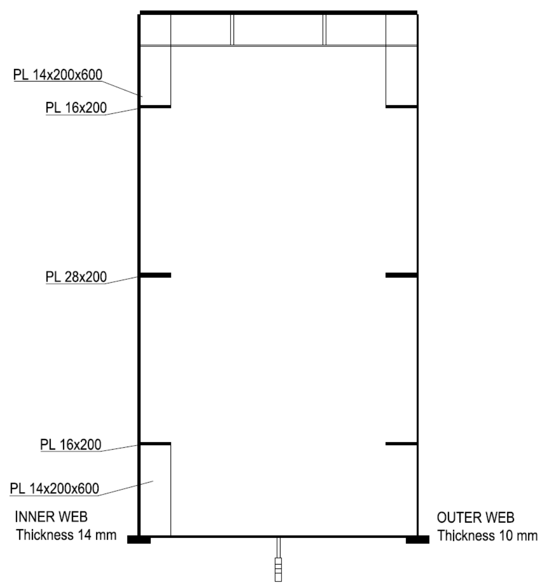

Figure 15: Main girder section

The main girder is connected to the transverse beams, as mentioned in chapter 2.2.3. At the reference project VIZELA the longitudinal distance between the transverse beams is 6000 mm. At these positions there will be added extra diagonal stiffening inside the main girder. The reason for this type of detailing is the need to compensate for a torsional moment due to to eccentric loading on transverse beams. This diagonal stiffening consist of beams connected inside the main girder.

One central component which influence the loading condition at the main girder is the launching wagon. This is a frame construction which is located at the top of the supporting bracket. As mentioned in chapter 2.2.6 this component is used to launch the system by using hydraulic jacks. This is of course an important feature in order for the scaffolding system to be sucessfull. But it has as well significant influence on the support reaction of the MSS.

At the launching wagon there are two support areas for each launching rail located at the main girder. These support areas consist of a neoprene pad which the main girder and the noses will transfer load through. The support is equiped with a pin bolt Ø120 so the system only will experience vertical support reactions. This type of support is referred to as a pinned support in the literature. If there should occur a rotation of the support, for example casting of bridges in slopes, it will be able to rotate so that load shedding will stay symmetrical. We can therefore be certain that the support reaction will occur as an uniform line pressure on the main girder‘s web.

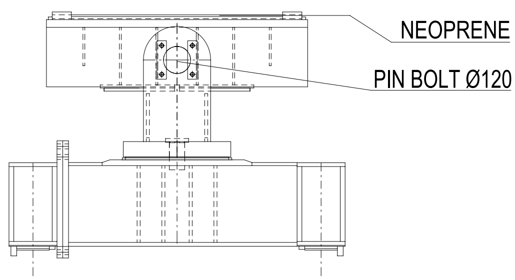

Figure 16: Pinned support at launching wagon

When the MSS-system is launched forward it will endure multiple loading conditions. As the longitudinal CoG is localized near the front pier this support reaction will experience the largest forces. It will therefore be central that this situation is characterized, but with as well given thought on which launching stage provides the largest hogging moment. The transversal CoG is as well of great interest in this case. This will determine the load shedding between inner and outer web plate. With inner web we study the web plate localized nearest to the transverse beams. The transversal CoG is ideally in the region of 300-350 mm from inner web plate. Keeping in mind that wind loads can influence this, Strukturas‘ conservative design rules state that this distance should be taken as 150 mm. However in this master thesis it is chosen that the transversal CoG will provide full loading on the inner web, this will only be correct in extreme situations. But given that it can occur conservative design is required.

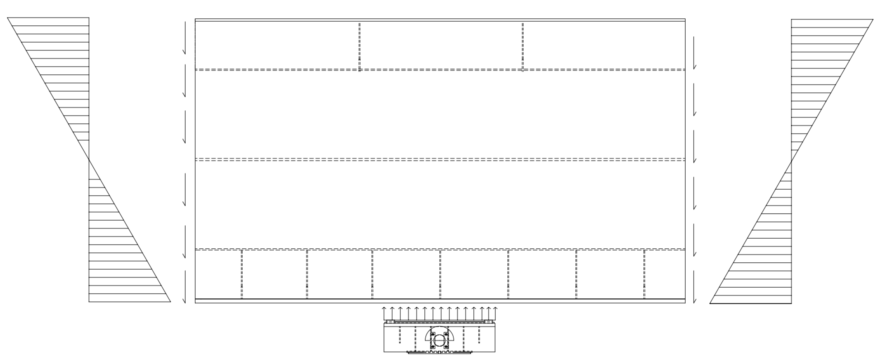

Figure 17: Web plate on the main girder with illustrated loading

Figure 17 illustrates the forces the web plate have to endure. The line pressure from support reaction at the launching wagon must be in equilibrium with the shear forces acting at sections where transverse beams are located. This type of loading will provide for significant shear stresses acting through the web. This combined with stresses caused by the hogging moment will provide a complex stress pattern. It‘s obvious that the lower part of the web will be of interest regarding instability due to the fact that compressive forces is located in this area. It will as well be of interest to look at the stiffening arrangement and the possibility to optimize the structure in order to be able to withstand more forces and ultimately reduce weight of structure. Questions which are going to be asked are:

- Are the longitudinal stiffeners correctly placed?
- Do they have the right dimensions?
- Do they prevent a global buckling phenomenon?
- Which effect will the transversal stiffeners have?
- Will there be reasons to change their arrangement?

3.2 Loading from reference project

This chapter will characterize the amount of loading the web plates will experience due to self-weight of the MSS-system at launching. Given values for weights of structural elements are taken from Strukturas‘ own design manual for this specific project. Values for loads are multiplied with a load factor $\gamma_F = 1,35$.

Structural element	**Type of loading**	**Size**	**Notation**
Rear nose	Line load	8,3 kN/m	q_{RN}
Main girder + Transverse beam	Line load	28,7 kN/m	q_{MG+TB}
Formwork	Line load	13,3 kN/m	q_{FW}
Counterweight	Point load	6,75 kN	F_{CW}
Front nose	Line load	8,3 kN/m	q_{FN}

Table 1: Loading due to self-weight at launching

The most unfavorable loading situation is characterized when the MSS-system‘s front nose will enter the front support. This situation will cause the largest hogging moment and support reaction on the main girder‘s web. Due to the hinged connection to the front nose and relativly large difference between self weight of the main girder, transverse beams and the formwork it is viewed as conservative design to assume that the front

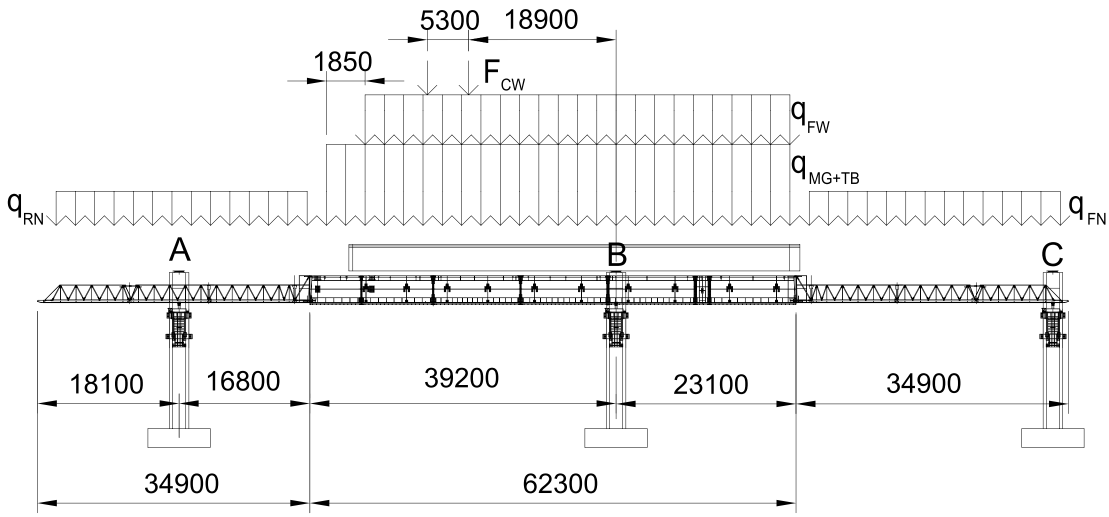

Figure 18: Loading situation analyzed for plate buckling

support will not endure reaction forces before the front nose tip has been launched 2 meters away from this support.

Figure 18 illustrates a stage of launching when the front nose has just past support C. This support will be disregarded due to reasons mentioned. To find the reaction at support B the following equilibrium equation will be executed:

$$\sum M_{SupportA} = 0 \tag{3}$$

$$-q_{RN} \cdot 4,9m \cdot 0,675m + q_{MG+TB} \cdot 63,2m \cdot 47,95m + q_{FW} \cdot 59,8m \cdot 49,8m \tag{4}$$

$$+F_{CW} \cdot 37,1m + F_{CW} \cdot 31,8m + q_{FN} \cdot 34,9m \cdot 96,55m + F_B \cdot 56m = 0$$

$$F_B = 2763kN \tag{5}$$

This will produce a hogging moment at support B which is calculated in the following manner:

$$M_B = q_{FN} \cdot 34,9m \cdot (23,1m + \frac{34,9m}{2}) + (q_{MG+TB} + q_{FW}) \cdot 23,1m \cdot \frac{23,1m}{2} \tag{6}$$

$$M_B = 22564kNm \tag{7}$$

When this hogging moment is characterized, the next step is to calculate the corresponding stresses which can be used as input in ANSYS. To do this I have used an Excel-sheet that Strukturas has developed. Figure 19 illustrates section properties and forces the main girder is exposed to over support B. The hogging moment will induce tensional stress at 99,9 N/mm^2 at top of girder to compressive stresses at 100,2 N/mm^2 located at the lowest region of the girder web plate. As you can see from figure 19 the Excel-sheet only evaluates compressive stresses where y=0, which is at the bottom of a stiffener (280×20mm) localized on the compressive flange. The height of the web is 3400mm and the thickness of the compression flange is 16mm. The distance from the mass centre to bottom of stiffener(280×20mm) in y-direction is 2015mm. As the stress distribution is linear the compressive stress at the boundary of the bottom web is:

$$\sigma = 118,1 * \frac{2015 - 280 - 16}{2015} = 100,2 N/mm^2 \tag{8}$$

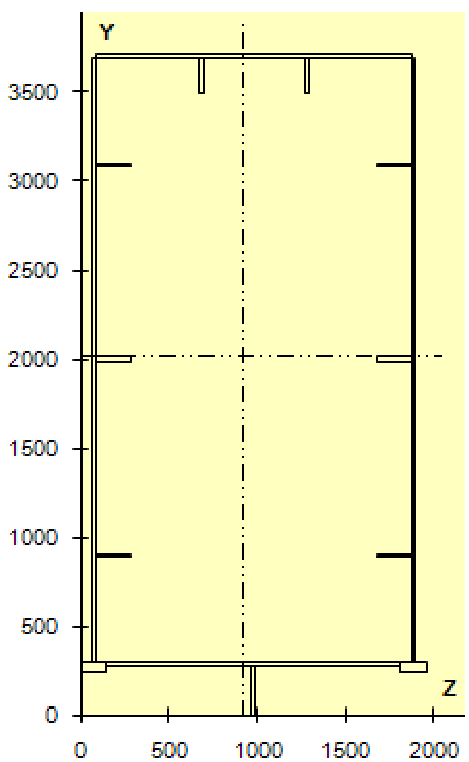

Section properties:

A =	204664	mm^2
g =	1637	kg/m
b =	1962	mm
h =	3720	mm
z_t =	921,2	mm
y_t =	2015,0	mm
I_z =	385,01E+09	mm^4
I_y =	112,54E+09	mm^4
$Wz_{(y=h)}$ =	225,81E+06	mm^3
$Wz_{(y=0)}$ =	191,07E+06	mm^3
$Wy_{(z=o)}$ =	122,16E+06	mm^3
$Wy_{(z=b)}$ =	108,12E+06	mm^3

Section forces:

N =		kN
Mz =	-22564	kNm
My =		kNm

Stresses:

$\sigma_{Mz(y=h)}$ =	99,9	MPa
$\sigma_{Mz(y=0)}$ =	-118,1	MPa

Figure 19: Sectional properties main girder calculated by an Excel-sheet

4 ANSYS modelling of buckling capacity

4.1 Ultimate limit state

4.1.1 Introduction

When a plated structural element experience a complex stress pattern due to biaxial loading and stiffeners arrangement it is difficult to predict the ultimate limit state (ULS) strength with closed-form design formulas. *Eurocode 3* [1], Annex C, has therefore developed a set of design rules which purpose is to make you be able to model a complex plate geometry with a FEM model in ULS. After studying *Commentary and worked examples to EN 1993-1-5* [2] and *Design of plated structures* [3] I have gained knowledge on how to perform a FEM-model in accordance to given guidelines in Eurocode 3. Elastic-plastic resistance in ULS shall be modelled with nonlinear behavior regarding material and deformations with as well initial imperfections included. Special considerations should be made regarding:

- Modelling structural elements and it‘s boundary conditions
- Choice of computational software and documentation
- The use of imperfections
- Loading in ULS

In order to deal with plate buckling problems the structure has to be modelled with shell or solid elements, which will provide a model with a significant number of degrees of freedom (DOF). This will of course have effects on the computational time used to analyze the structure. It is fairly time-consuming to create a model which fully represent the physical behavior of the structure and efforts must be made regarding the applied boundary conditions. This is especially important when you only model a part of a complete structure. Plate buckling at the inner web plate localized at the main girder has to be modelled this way simply because it‘s part of a complete system which endures complex loading situations and interaction between structural elements. To model the whole system is way time-consuming and computational capacity is not present. Careful considerations regarding the loading situation and boundary conditions has been made in collaboration with structural engineers at Strukturas A/S. This has been done with the notion that the Eurocode states that boundary conditions must be applied in a manner which will lead to conservative results. The results and reasoning behind the choices will be presented in chapter 4.2.

4.1.2 Geometrical imperfections

In cases where instability governs the results may be quite sensitive to the assumed imperfections. The model has to include imperfections corresponding to the most likely instability modes. For plated structures the instability modes can be either local or global. These modes are introduced from a linear eigenvalue problem which illustrate the most critical buckling shapes. The magnitude of these initial deformations are often taken as the tolerance limits for fabrication. Based on engineering judgement the suggested level of the applied imperfections should be 0,8 times the tolerance limit, although there are a lack of existing reliable data which can verify this matter.

There might as well be a need to take into account which effects the residual stresses, due to welding of the steel components, will have. The magnitude of these stresses tends to vary systematically but as well randomly. They are represented by a self-equilibriated stress pattern in each plate of the structure. It‘s possible with some FEM-experience to model these stresses but this is regarded as a waste of time because their effect is almost negligible for slender plates.

To take into account imperfections caused by fabrication tolerances and as well residual stresses Eurocode 3 has developed a set of equivalent geometric imperfections. This way you only have to characterize which buckling mode is critical from a linear eigenvalue problem. Is it a global or local buckling mode? Figure 20 illustrates these given values for imperfections on a plated element with width a and length b.

Type of imperfection	Component	Shape	Magnitude
global	member with length ℓ	bow	see EN 1993-1-1, Table 5.1
global	longitudinal stiffener with length a	bow	min (a/400, b/400)
local	panel or sub-panel with short span a or b	buckling shape	min (a/200, b/200)
local	stiffener or flange subject to twist	bow twist	1 / 50

Figure 20: Imperfections used in analysis

Eurocode 3 states that different combinations of imperfections has to be executed in analysis. The rule state that one leading imperfection should be taken with full magnitude and the others may be taken as 70 % of full value. The rule should be applied such that one imperfection a time is tried as leading, which means that several combinations have to be investigated. This particular part of a buckling analysis is regarded as too time-consuming in the industry, and FEM programs such as ANSYS has developed easier ways to include these imperfections. By defining a geometry update from a linear eigenvalue analysis with a factor which satisfy all given values from figure 20 at most critical modes you will achieve the most unfavorable imperfection. This will save engineering companies for computational time needed to run such analysis.

4.1.3 Material properties

Material properties in the FEM-model will of course have influence on the plate buckling capacity. In the Eurocode multiple possibilities are presented regarding this subject. Figure 21 illustrates which two possibilities you have regarding modelling material properties, with yielding plateau or strain hardening. The two stress-strain curves which only represent yielding plateau will have shortcomings with respect to capacity of the plated element. The yielding plateau is modelled with continuous strain and this will not reflect the physical behavior correctly. The actual behavior is however discontinuous and with this model the material is not in an elastic state or in a strain hardening state. This will lead to a prediction of local buckling too early. When the plate will deform due to buckling the secondary stresses will have great influence on the stress-pattern. The consequence of modelling with a yielding plateau is that the plate loses much of it‘s bending stiffness when stresses exceed the yield limit.

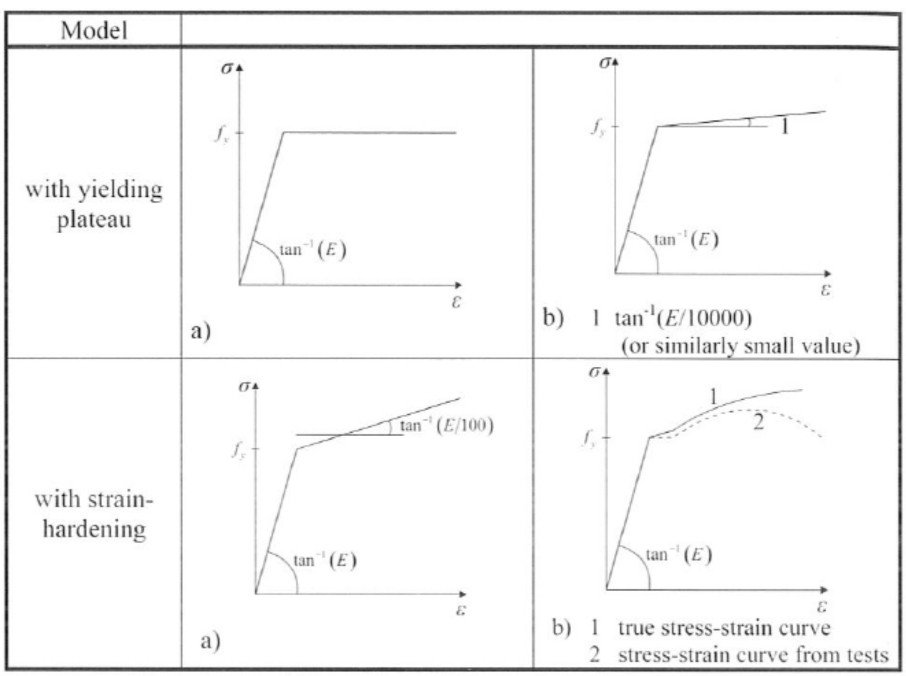

Figure 21: Sress-strain relations at buckling analysis

Modelling with strain-hardening with hardening part of curve E/100 is sufficient in most cases for reaching the maximum load when buckling is governing. One important criteria is that the plate doesn‘t experience strains larger than 5 %. This assumption is wrong as it may neglect the Bauschinger effect, which is of importance if large strain reversals occur. You have as well possibilities to model a true stress-strain diagram based on uniaxial test data which often are implemented in modern software. However ANSYS doesn‘t have this data accessible and there have been a lack of reliant data at my disposal so this material property will not be chosen. With as well the notion that no significant strain reversals will occur in the buckling analysis the material property chosen is with a strain hardening equal to E/100.

4.1.4 Loads and partial factors

The FEM model must include several loading and material factors in order to be sufficiently reliant. Relevant load factors and load combination factors must be present in the model. This set of loads is then increased by a load multiplier α in steps until failure occur. The use of a single load multiplier is a simplification, due to the fact that different loads have different probabilities of occurrence. Methods for taken this into account is not available. The use of a single load multiplier is consistent with design procedyre.

The load magnification factor α_{Rd} is the factor which the structure has endured full collapse. This factor will have to be scaled with a new factor which is caused by uncertainties of modelling and material response. The partial factor is defined as following:

$$\gamma_{M1} = \gamma_C \cdot \gamma_R \tag{9}$$

γ_C will cover the model uncertainty, while γ_R to cover scatter of resistance of the model. Engineering assumptions however leads to γ_{M1}=1,1 when instability governs and no reliable bench marks test are present.

4.2 Methodology

To analyze the web plate at the main girder I‘ve used ANSYS Workbench 12.1. This is a new generation FEM software which allows you to easily import geometries from different 3D CAD programs. To model this particular geometry, DesignModeler has been used, which is an integrated part of ANSYS Workbench. The web plate has been modelled with a flange 50mm*150mm which is a launching rail for the main girder. This is an important inclusion in the analysis due to the fact that the flange‘s stiffness will contribute to spread the support reaction at the launching wagon to a larger area at the web.

The first step is to set up a Static Structural analysis with an elastic material and small deformation theory. At this stage the mesh has to be developed. This is a part which

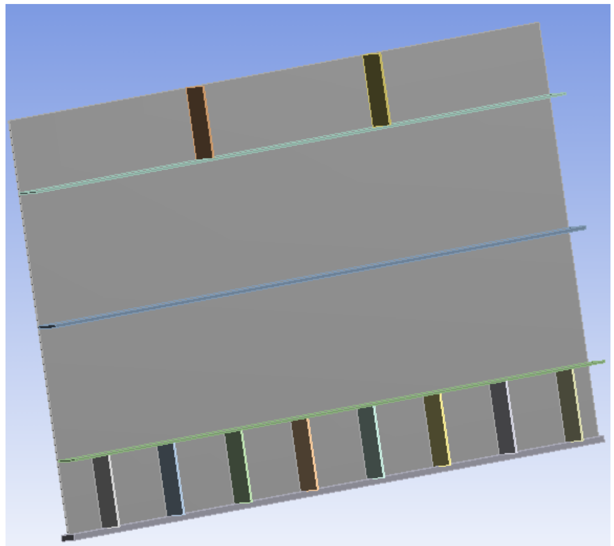

Figure 22: Geometry web at main girder

is done automatically and integrated into this module in ANSYS WB. Quadratical elements are produced with sizes that automatical fulfill convergence criterion, although some refinement has been executed to obtain sensitivity. The model is designed with SOLID 186 elements. According to *ANSYS Workbench 12.1 Release Documentation*[11] this is the prefered element type for this nonlinear analysis with large strains present. SOLID186 is a higher order 3-D 20-node solid element that exhibits quadratic displacement behavior. The element is defined by 20 nodes having three degrees of freedom per node: translations in the nodal x, y, and z directions. The element supports plasticity, hyperelasticity, creep, stress stiffening, large deflection and large strain capabilities.

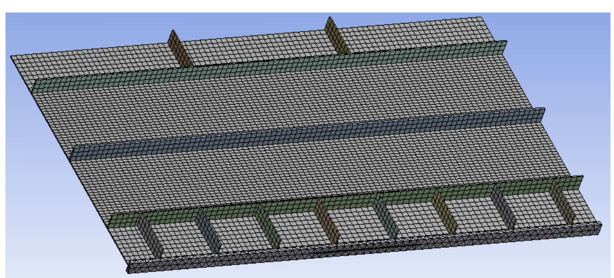

Figure 23: Meshed web plate

Then boundary conditions will have to be applied. This will be done in a manner which lead to conservative results. All the edges will be prevented to endure displacement out of plane. As well will boundaries (shear sections at transverse beams) be prevented to displace vertically. The lower boundary where transversal stiffeners are placed c/c 750mm will experience rotational stiffness. They are connected to the lower flange of the box girder and when they pass the support at the launching wagon there will be no possibilities for the stiffeners to rotate about their main axis. A result of this observation the lower part of the flange will be modelled as completely stiff and will not experience any rotation. There will as well be some rotational stiffness related to the upper flange of the main girder. This is however neglected as it's hard to predict the influence. With this assumptions the web plate must be modelled in a conservative manner. In order not to experience rigid-body motion in the model it must be fully constrained. This is done by defining a single point which can not displace horizontally.

When this web is loaded there are one main factor which is not easy to predict. It is evident that both the support reaction and the stresses from the hogging moment will not act simultaneously with full value. Full load at web plate due to CoG in the transversal direction is located over the web will only appear in extreme situations which of course is not desirable due to stability of MSS. These extreme situations can be caused by launching scaffolding systems in bridges designed with low horizontal radius, influence from wind loads and margins of error in CoG calculations. The maximum bending moment over the support will not be present over the entire cross-section, so the stress pattern due to this moment will be slightly exaggerated. This is however viewed as a small margin of error in the analysis because the bending moment will not govern resistance of the web panel.

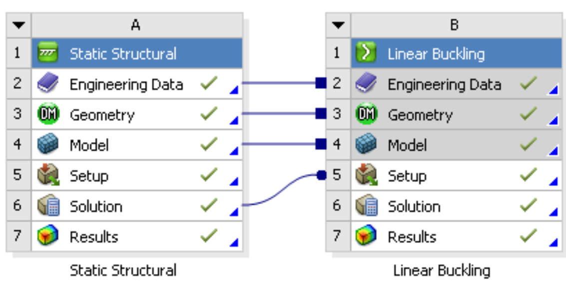

Figure 24: Project step in ANSYS Workbench

The solution from Static Structural will be transfered to a Linear Buckling analysis where the three first critical modes will be detected. These results are not interesting in this context, where ULS capacity of the web plate is the object for the analysis. Anyway slender plates exposed to shear forces tend to have significant post critical reserve present. The eigenvalue formulation will only be used to find the shape of the critical mode so that imperfections can be applied in the most unfavorable manner. The most convenient way to do this in ANSYS Workbench is to duplicate the Static Structural to a new independent analysis. This way you can obtain a new analysis based on the same meshing and geometry, but with opportunities to include large deformation theory and imperfections. The imperfections will be included with the command UPGEOM and based on the result file from the Linear Buckling analysis.

```
/PREP7
FACTOR=X
UPGEOM,FACTOR,1,1,LINBUCK, RST
/SOLU
```

Figure 25: ANSYS input file for including imperfections

The factor X will be scaled in order to satisfy design rules from the Eurocode. The imperfections are pivotal in order to initiate buckling. If the loading of a structure is perfectly in plane (that is, membrane or axial stresses only), the out of plane deflections are necessary to initiate buckling behavior. If this is not present the analysis will fail to predict buckling behavior. In order to obtain results from a nonlinear buckling analysis you will have to model a collapse failure of the structure. This will be done by introducing a large support reaction which most definitely will provoke a plastic collapse. The analysis will as well have to be divided into substeps so results can be obtained at multiple loading situations. Collapse will be present when the structure will experience singularaties in it‘s stiffness matrix. The easiest way to obtain this result, and be sure that you are evaluating the collapse, is to set up a force-displacement graph which indicates the ultimate limit state loading that collaps will occur.

Material properties will as well have to be changed in order for post critical behavior to be present in analysis. Metals will deform elastically until the yield strength f_y is reached, after this stress state is reached careful considerations must be made regarding modelling of plastic response of the metal. Experiments show that if you plastically deform a solid , then unload it, and then try to re-load it to induce plastic flow, it‘s resistance to plastic flow will have increased. This is known as strain hardening. According to *ANSYS Mechanical Structural Nonlinearities*[9] two main hardening possibilities can be modelled in ANSYS:

- Kinematic hardening
- Isotropic hardening

With kinematic hardening the yield area remains constant in size and translates in the direction of yielding. This configuration is ideal for small strain cyclic loading. If you experience cyclic behavior with large strains the Bauschinger effect will be inappropriate. The unloading curve will decrease with a value $2f_y$ at unloading, so for large strains you will experience a different starting point for the stress-strain relation at the next cycle. The Bauschinger effect is defined as the subsequent yield in compression that is decreased by the amount that the yield stress in tension is increased.

Isotropic hardening configuration will make the yield surface increase in size, but remain

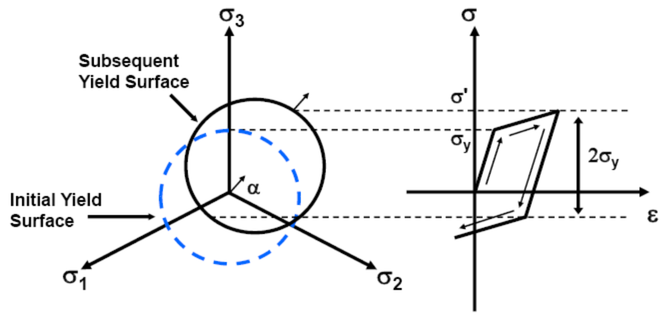

Figure 26: Kinematic hardening

the same shape, as a result of plastic hardening. This is sufficient in this analysis which will not experience cyclic loading. With cyclic loading the solid will harden up until it respond elastically. This hardening model is appropriate for a large strain simulation, as this buckling analysis will be. It will as well not account for the Bauschinger effect, but as the analysis will not simulate cyclic loading this will not lead to inappropriate results.

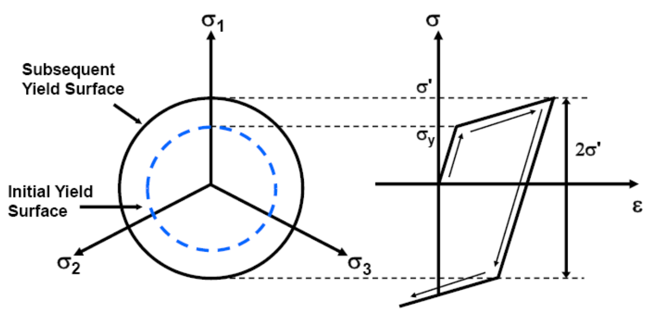

Figure 27: Isotropic hardening

As you can see this model must utilize isotropic hardening properties because of the large strains present in the model. Two input parameters will have to be established when bilinear isotropic hardening is used. The yield strength f_y= 355 N/mm^2 and tangent modulus E_T=2100 N/mm^2. Figure 28 shows the material input in the nonlinear ANSYS analysis.

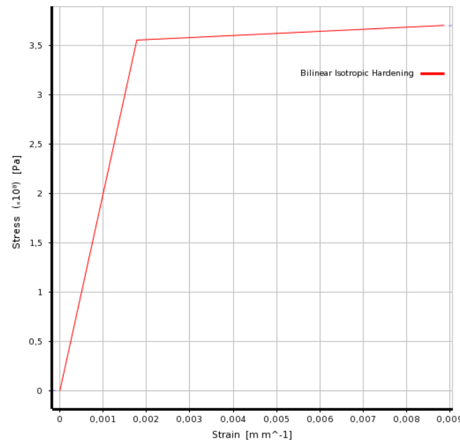

Figure 28: Material properties using bilinear isotropic hardening

When obtaining solutions from the nonlinear buckling analysis some preliminary theory regarding convergence of the solution must be studied. ANSYS uses a method called the Newton-Rapson Method. This method is based on an iterative series of linear approximations with corrections. Each iteration is known as an equilibrium iteration. If you analyze a force-displacement curve like figure 29 you see how the method evaluates convergence.

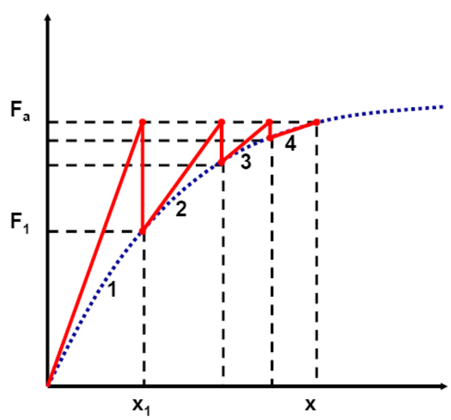

Figure 29: Newton-Rapson Method obtaining equilibrium iterations

In the Newton-Rapson Method, the total load F_a is applied in iteration 1. The corresponding displacement is x_1. From the displacements, the internal forces F_1 can be calculated. If $F_a \neq F_1$, then the system is not in equilibrium. Hence, a new stiffness matrix (slope of red line) is calculated based on the current conditions. The difference F_a - F_1 is defined as the the residual forces. These residual forces must be within given values for the solution to converge. This process is repeated until $F_a = F_1$. In figure 29 this is achieved at equilibrium iteration 4, and the solution is converged.

The residual is a measure of force imbalance of the structure. When using this method the goal is to iterate until the residual becomes acceptably small. As a general rule any sudden changes to any aspect of a system will cause convergence difficulties. To be sucessfull using this method at complex structures you must understand how the loads can be incrementally applied at substeps. Linear analysis will be easier to perform sensitivity studies on by altering mesh density or other model parameters like boundary conditions and the applied loads. Nonlinear analysis is more complex and results are more difficult to verify. Parameters like load increments and mesh density become more expensive to verify due to elapsed time in analysis. Trial and error is sometimes required with the Newton-Rapson Method because it endures some important shortcomimgs. It will not be able to evaluate results when the tangent stiffness K_T is equal to zero.

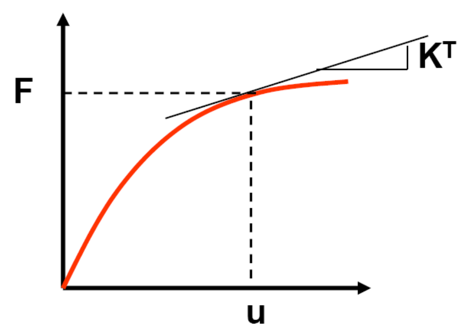

Figure 30: Newton-Rapson method evaluating tangent stiffness

When using multiple substeps, you need to achieve a balance between accuracy and economy: more substeps (that is, small time step sizes) usually result in better accuracy, but at a cost of increased run times. ANSYS provides automatic time stepping that is designed for this purpose. Automatic time stepping adjusts the time step size as needed, gaining a better balance between accuracy and economy. Automatic time stepping activates the ANSYS program's bisection feature. Bisection provides a means of automatically recovering from a convergence failure. This feature will cut a time step size in half whenever equilibrium iterations fail to converge and automatically restart from the last converged substep. If the halved time step again fails to converge, bisection will again cut the time step size and restart, continuing the process until convergence is achieved or until the minimum time step size (specified by the user) is reached.

Alternative methods have been developed to make ammends for the shortcomings at the Newton-Rapson. The Arc-Length Method is a convergence method that will enable the user to detect post buckling. To handle zero or negativ tangent stiffness,the Arc-Length Method multiplies the incremental load with a load factor, which is between 1 and -1. The Arc-Length method causes the Newton-Rapson equilibrium iterations to converge along an arc, thereby often preventing divergence, even when the slope of the force-displacement curve becomes negative. This method is not used due to the fact

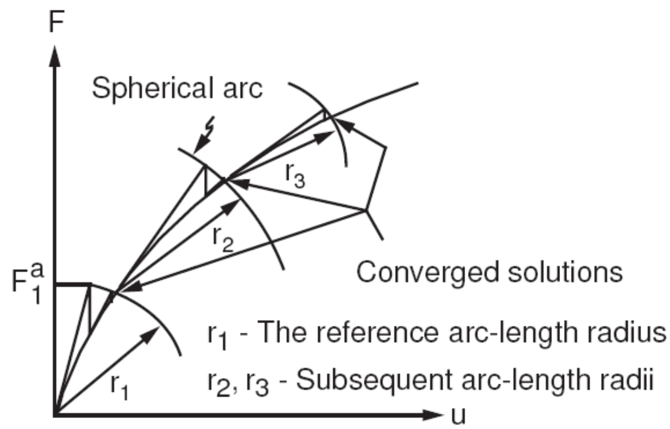

Figure 31: Arc-Length Method evaluating equilibrium iterations

that ANSYS provides the user with the bisection option at Newton-Rapson. This is regarded as the best way to evaluate convergence and as well the method that will run analysis in the fastest manner.

4.3 Results

Analysis has been executed in the manner described in chapter 4.2. The results from the first Static Structural analysis indicate that first order static analysis will give results which are in accordance to what expected. The equivalent von Mises stresses indicate a stress level which is below the yield strength f_y. This is expected due to the fact that this loading situation will not provoke the largest bending moment at the main girder. This actual situation will be when the bridge cross section is casted and at a different stage at the work cycle.

As the solver in ANSYS uses von Mises stresses as the yield criterion some theory regarding this matter must be briefly explained. The von Mises yield criteria is used to relate multiaxial stresses to an uniaxial case. The reason for the need of this yield criterion can be explained as:

- Tensile testing on specimens provide uniaxial data, which can easily be plotted on one-dimensional stress-strain curves
- The actual structure usually exhibits multiaxial stress state. The yield criterion provides a scalar invariant measure of the stress state of the material which can be compared with the uniaxial case

In general a stress state can be separated in two components:

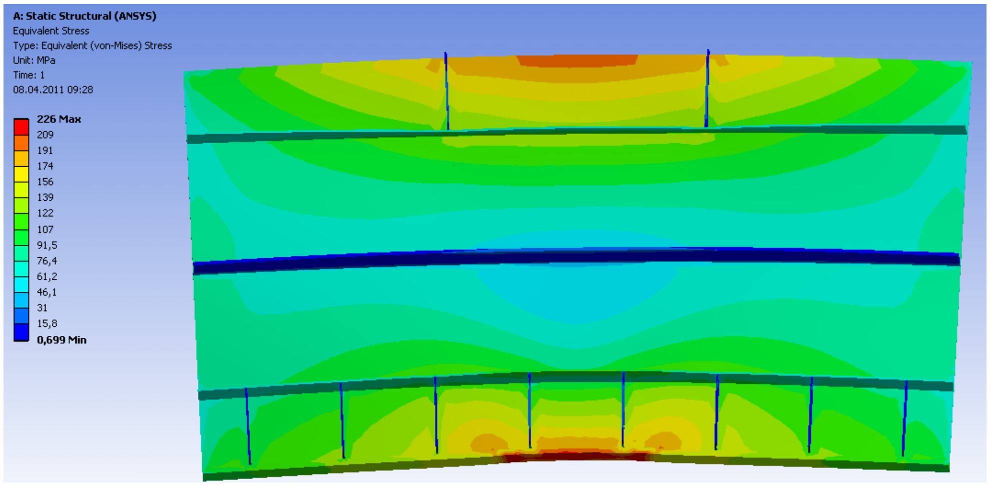

Figure 32: von Mises stresses in the main girder

- Hydrostatic stress - generates volume change
- Deviatoric stress - generates angular distortion

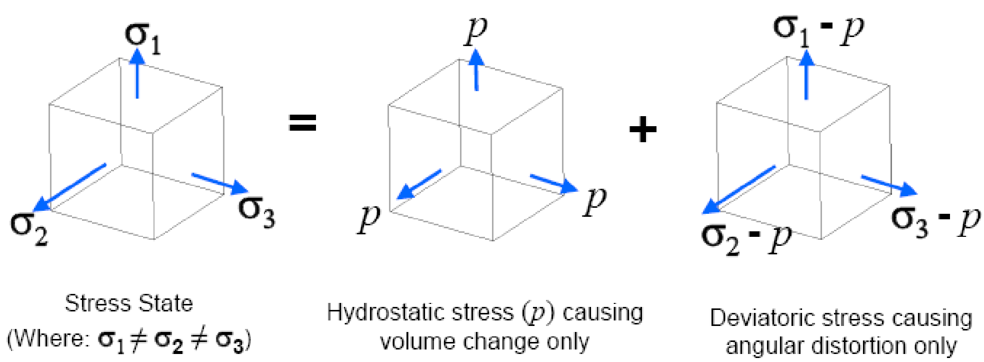

Figure 33: von Mises yield criterion

The von Mises yield criterion predicts that yielding will occur whenever the distortion energy in a unit volume equals the distortion energy in the same volume when uniaxially stressed to the yield strength. When von Mises equivalent stress exceeds the uniaxial material yield strength, general yielding will occur.

The von Mises stresses in ANSYS is calculated by making all of the stresses in a single point at the plate to an equivalent tensile stress. This is a very practical approach to analyze if the structure will experience stress patterns that exceed the yield strength. A scalar invariant (von Mises equivalent stress) is derived as:

$$\sigma_v = \sqrt{\frac{(\sigma_1 - \sigma_2)^2 + (\sigma_2 - \sigma_3)^2 + (\sigma_3 - \sigma_1)^2}{2}} \tag{10}$$

σ_1, σ_2 and σ_3 are principal stresses. A principal stress is defined as a multiaxial stress state that can be defined with the use of only normal stresses. If you plotted in 3D the principal stress space indicates that the von Mises yield surface is a cylinder.

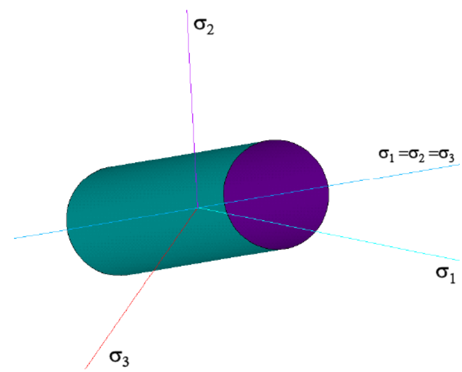

Figure 34: von Mises yield surface in 3D

As you can see the cylinder is aligned with the axis σ_1=σ_2=σ_3. At the edge of the cylinder yielding will occur and hardening rules are used to describe this behavior. An important thing to notice is that yielding will not occur with increasing hydrostatic pressure (σ_1=σ_2=σ_3).

As figure 32 indicates the maximum von Mises stress is localized at the support reaction from the launching wagon. At this location you will have maximum effect from the compressive stresses due to the hogging moment and as well the support reaction. At this point the maximum equivalent stresses is 226 N/mm^2. Another important result set from this Static Structural analysis is the shear stress distribution in the web. This is caused by the support reaction and the shear sections set up as a boundary conditions to simulate vertical forces from transverse beams.

These shear sections indicates that the shear stresses will be distributed symmetrically to each transverse beam. This has as well been verified by checking support reactions. Figure 35 illustrates the symmetric shear distribution in the girder web.

The solution from the Static Structural analysis will be transfered to a separate Linear Buckling analysis which will detect the first three critical buckling modes. The results from this analysis is giving on the form of a single load multiplier λ_i. This load multiplier is calculated by obtaining the following relation:

$$[K] + \lambda_i[S]\{\psi\} = 0 \tag{11}$$

[K] is the first order elastic stiffness matrix while [S] is the second order geometric stiffness matrix which is calculated based on the stress rate from the Static Structural analysis. The vector $\{\psi\}$ contains the form of the buckled modes. With this specific

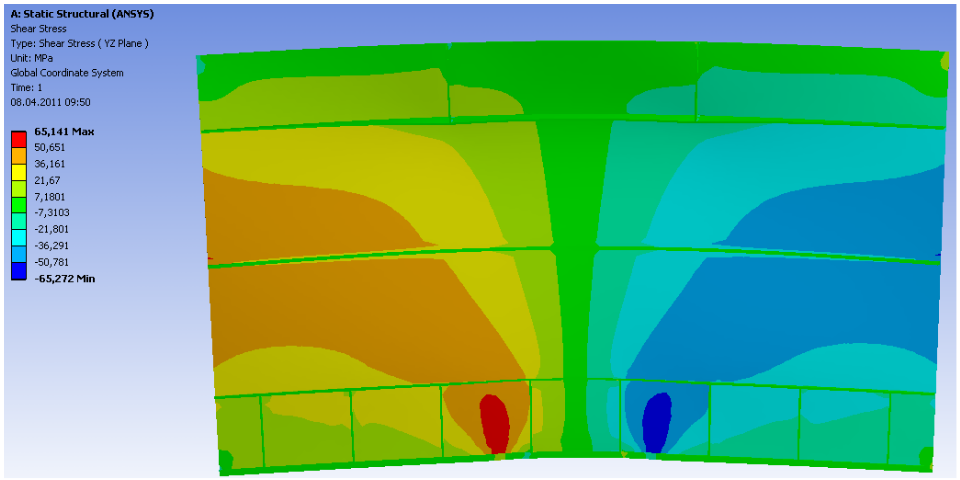

Figure 35: Shear stresses provoked by support reaction

loading condition it is difficult to acess the parameter λ_i due to the fact it is based on the stress state of biaxial loading. Although this has no practical influence because we are purely interested in the shape of the modes, it can be interesting to compare the eigenvalue analysis with the nonlinear. The first critical mode‘s shape is illustrated in figure 36.

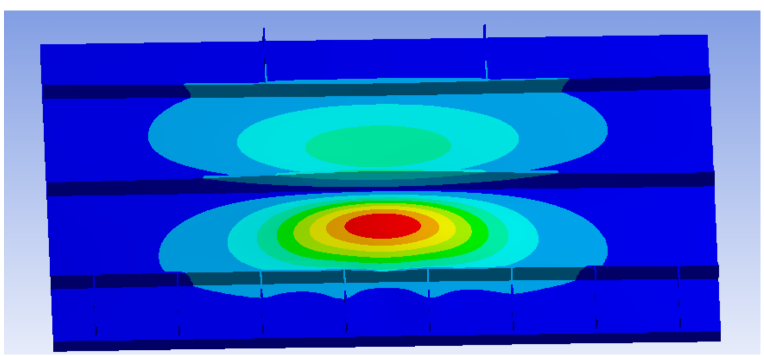

Figure 36: First critical mode original arrangement

This is the mode that clearly stands out because of the low load multiplier assosiated with it. This particular eigenvalue configuration gives a load multiplier λ_1=1,383. This result indicates there is capacity present in the plate, but no conclusion will be drawn after a complete collapse is modelled. It is as well useful to take notice of the stiffeners configuration in this mode. The longitudinal stiffeners are strong enough to withstand to buckle with the plate which indicates a decent configuration. An important effect that will govern resistance of the main girder at launching, is the effect the support reaction. As you can see no local failure mode due to the support reaction is initialized and the transversal stiffener c/c 750 mm sucessfully transfer the load to the second subpanel. This effect is important for ULS capacity. Figure 37 and 38 illustrates the next two critical modes.

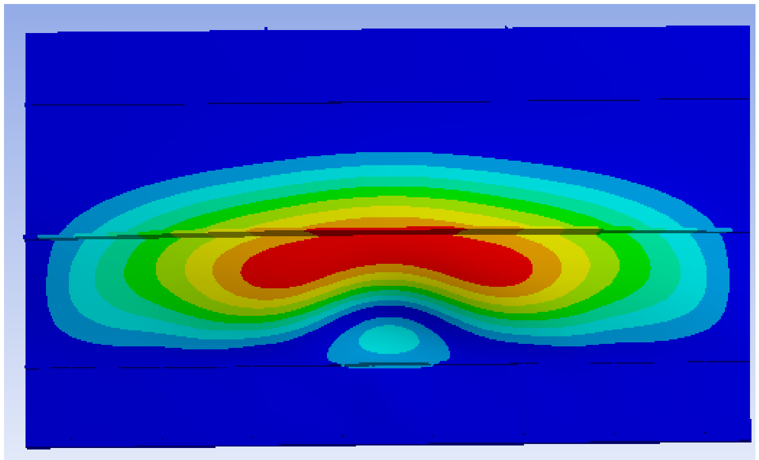

Figure 37: Second critical mode original arrangement

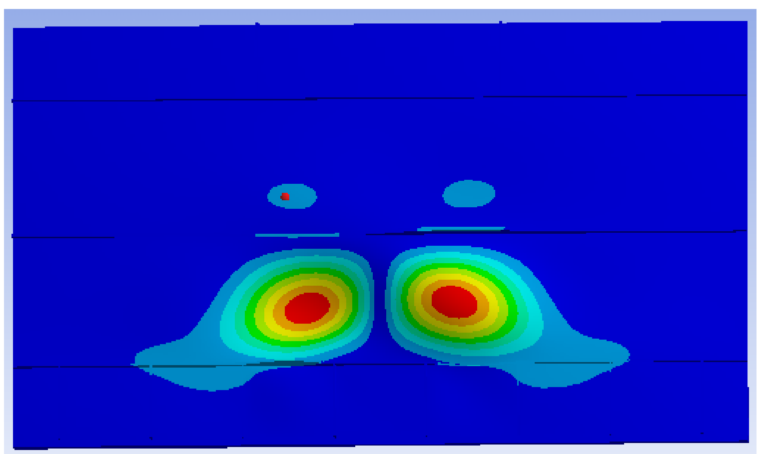

Figure 38: Third critical mode original arrangement

The critical modes have load multipliers associated with the buckled shapes illustrated in table 2.

The design requirements for a FEM model with biaxial loading is often obtained by a single load magnification amplifier α_{Rd} of the complete stress field. This is however neglected in this analysis due to only uncertainties of the capacity caused by the support reaction and not stresses caused by the hogging moment. This would lead to that the stresses caused by the hogging moment will remain constant at all substeps at the analysis, while the the support reaction will be defined at substep intervals with an increasing value. With this set-up configuration for the analysis you will be able to

Critical mode	Load multiplier
1	1.383
2	1.784
3	2.013

Table 2: Load multipliers original arrangement

only evaluate the size of the support reaction that will lead to a collapse of the panel. This is the loading that will be the most difficult to predict resistance against with design formulas (see chapter 5.2.4).

These results will be transfered to a new Static Structural analysis where large deflections and bilinear isotropic hardening will be implemented. With included imperfections these results were found with the nonlinear analysis:

Imperfections	Characteristic load F_{Rk}
Mode 1	4267.8 kN
Mode 2	4676.2 kN
Mode 3	5117.6 kN

Table 3: ULS capacity inner web original arrangement

The results has been seen deduced from a force-displacement curve. The force taken as the support reaction at launching wagon while the displacement is out-of plane displacement for the panel. Imperfections have been implemented with the factor X= 5,5, this will ensure that the criterions regarding imperfections due to local buckling of sub panels and local imperfection of stiffeners were satisfied. Figure 39 shows the plate panel subjected to imperfections, as you can see critical subpanel between longitudional stiffeners in the compression zone will experience an imperfection with a maximum amplitude equal to 5,5mm. The amplitude is obtained by evaluating the design demand for a local buckling mode which states that the amplitude should be min(a/200,b/200). In this case a=6000mm and b=1100mm which lead to an amplitude equal to 1100/200=5,5mm. This configuration also ensures that the two longitudinal stiffeners that experience compressive stresses will have a minimum bow twist of 1/50. Design guidelines in NS-EN 1993 1-5 also states that a global imperfection should be tested. This is not executed in this thesis due to two main factors:

- The critical mode is a local buckling mode which clearly indicates that stiffeners will not buckle with the plate. This is confirmed in chapter 6.1 where no reduction of inner webs capacity is needed to account for global buckling.
- Time available to process the analysis.

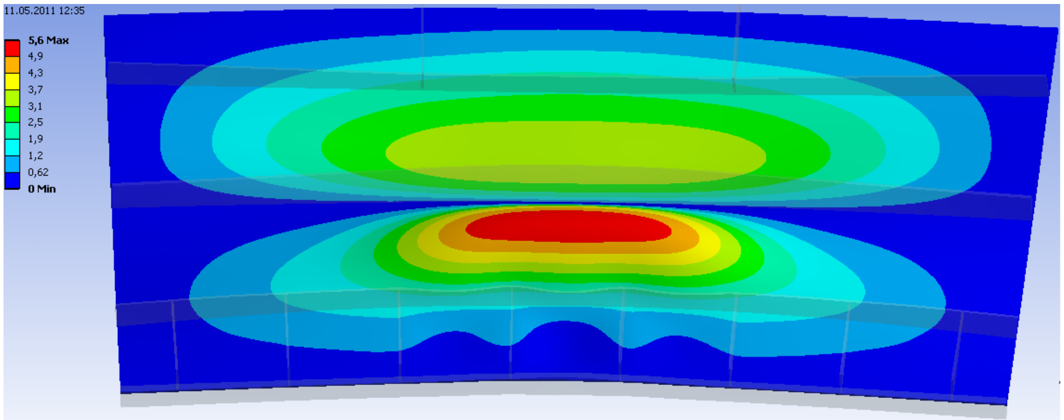

Figure 39: Imperfections related to mode 1 on plate panel

Some problems were encountered when the element transformation based on the critical buckling shapes were initialized. It turned out to be a distortion on some of the elements problem caused by a too coarse mesh. After reviewing some theory in ANSYS User Manual [11] it is a problem related to solid elements at buckling analysis. When you have a loading that will induce essential stresses and gradients over the thickness of a plate like a concentrated load on a flange you need to add elements. It is recommended to use at least three elements over the thickness of the plate. This was executed at the launching rail and no more distortion warnings were encountered.

The force-displacement curve for additional displacement at the original arrangement will be illustrated in figure 40. With additional displacement the displacement related to imperfections are neglected in the graph. The support reaction implemented in the analysis was set to 5000kN, and as you can see from figure 40 this will most definitely provoke a singularity.

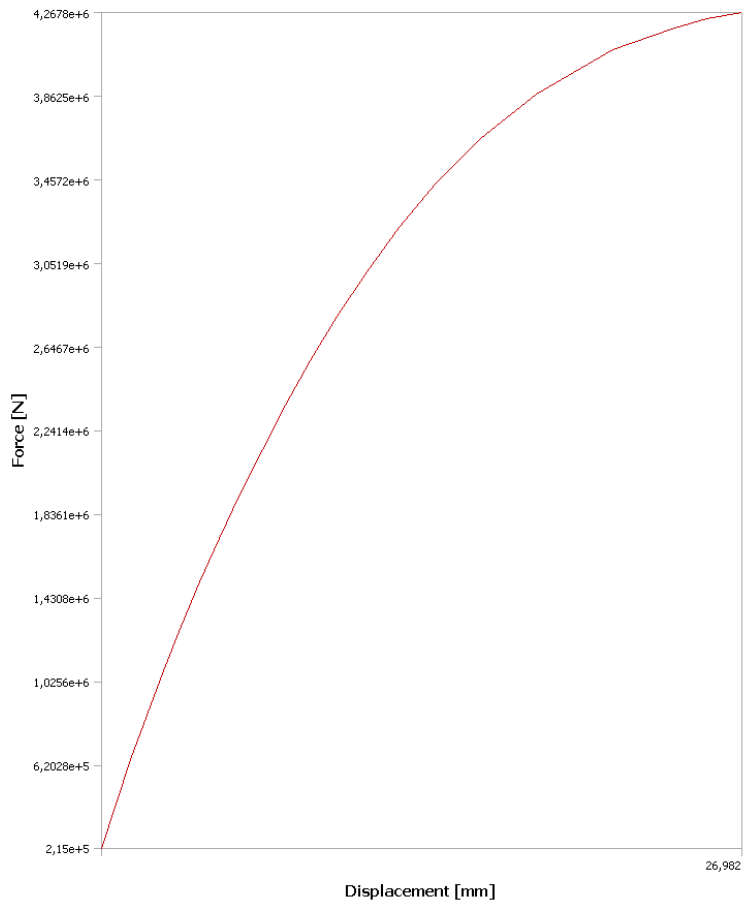

Figure 40: Force-displacement curve for additional displacement

When the support reaction have the value 4267,8 kN the Newton-Raphson will not converge and singularaties in the stiffness matrix is reached. By studying the force-displacement diagram you will see that there is a significant drop of stiffness before the characteristic collapse load is reached. At the collapse load the tangent of the curve is equal to zero and no more capacity is left in the plate. One larger value of the support reaction would lead to unrealistic high values of displacement. By this analysis we can conclude that the collapse load and ULS capacity of the plate is:

$$F_{Rd} = \frac{F_{Rk}}{\gamma_{m1}} = \frac{4267,8kN}{1,1} = 3879kN \tag{12}$$

Some sensitivity analysis has been performed by obtaining difference in ULS capacity caused by difference in load increments. As ANSYS provides the bisection alternative you can define initial substeps in analysis. If you apply a load that will pose no threat for convergence ANSYS will only evaluate at this given conditions. If you apply a large load that must certainly will endure plastic collapse the maximum substep option will reset the load increment. Initial analysis were performed with inital substeps equal to

10, which mean you will apply the support reaction in 10 equal increments. Maximum substeps were set to 100, this would mean that if the Newton-Rapson could not converge at some point given by initial substeps the iteration would restart. The new load increment would be 20 and this would continue until you reach the maximum given substep interval or convergence. With this method you can obtain a solution which is very close to the point of plastic collapse. Regarding the sensitivity test initial substeps were altered to 5 and 20 to obtain differences in results. This would however lead to only small deviations in the analysis. Both of the tests would provide a result within 1% margin of error.

One additional sensitivity analysis was executed to evaluate the effect of imperfections. This analysis was based on a larger initial imperfection. By using the UPGEOM command with the factor X=10 analysis were performed. This would lead to a characteristic collapse load F_{Rk} equal to 4156,3 kN. If you compare with the original analysis this will lead to a margin of error equal to 2,6 % which is not much considering that the imperfections were almost doubled.

4.4 Alternative stiffening arrangement

Results from analysis in chapter 4.3 clearly states that there is enough capacity in the web of the main girder. The support reaction will have to reach a value of F_{Rd}= 3879 kN before total collaps of the main girders web will occur. The most critical buckling mode indicate that buckling will occur locally between longitudinal stiffeners. This shows that the stiffening arrangement serves it‘s purpose by inducing a higher capacity. However Strukturas is as well interested to see the effect of introducing a new transverse stiffeners between transverse beams at c/c 3000mm. This transverse stiffener will be rigid for shear buckling and with a dimension 16×200mm (see chapter 5.3.2). The support reaction will not be localized symmetrically at the plate panel. It will be placed between transverse beam and the rigid transverse stiffener. This must be the most unfavorable loading condition for this arrangement. This has been validated by comparing results from linear buckling analysis where the support reaction has been placed at several positions along the launching rail.

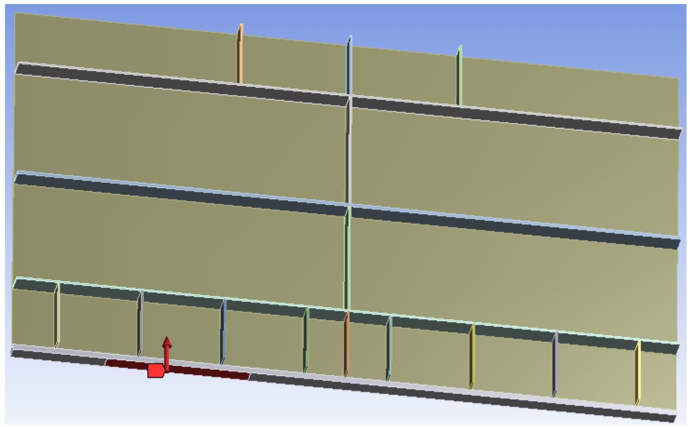

Figure 41: Geometry and loading at alternative arrangement analysis

This type of loading will ensure that the shear forces in the web will not be distributed symmetrically. Certainly more shear forces will be consumed in the transverse beam localized nearest to the support reaction‘s location. This assumption is confirmed in figure 42.

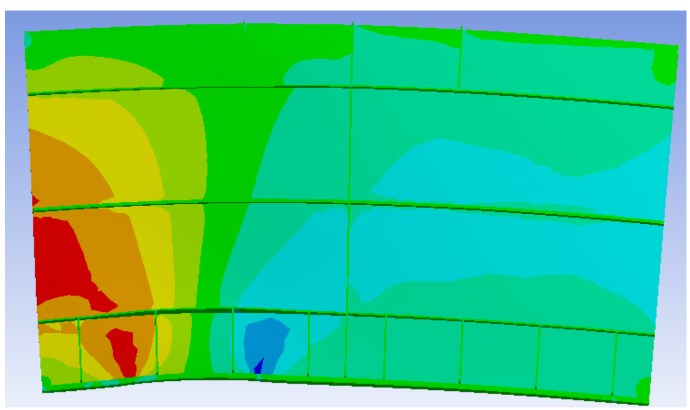

Figure 42: Shear distribution web alternative arrangement

The same procedyre as the original analysis will be executed, by transferring data from Static Structural to Linear Buckling. In the Linear Buckling analysis three most critical modes is characterized. The load multipliers λ_i for these modes are listed in table 4.

Critical mode	**Load multiplier**
1	1.647
2	2.224
3	2.596

Table 4: Load multipliers with alternative stiffening

By experience only imperfections based on the first critical mode will give the lowest failure collaps in a new Static Structural analysis. This conclusion can be drawn by looking at the difference in elastic buckling load between mode 1 and 2. Clearly a higher capacity is assosiated with mode 2 than 1. Figure 43 indicates that local buckling occur between longitudinal stiffeners once again, but the transversal stiffener will as well prevent a buckling mode over the length of the panel.

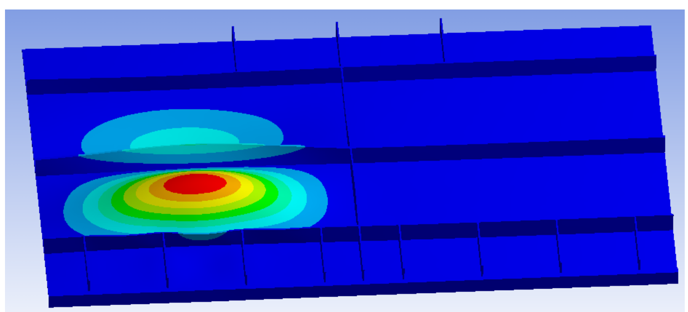

Figure 43: First critical mode alternative arrangement

Imperfections will of course be important in this analysis as well. The same design requirements related to imperfections as the original arrangement must be implemented. The maximum amplitude of local buckling of subpanels must be 1100/200 = 5,5mm. The longitudinal stiffeners must experience a minimum bow twist equal to 1/50. This will be done by using the UPGEOM command with the factor X=5,5. To interpret this factor is rather simple as it is based on a linear relation. The linear buckling analysis will not be able to determine the exact amplitude corresponding to the critical buckling shape. The post processor in ANSYS will only give results that state that the critical mode will have a maximum amplitude equal to 1. If you multiply this configuration with the factor X=5,5 you will obtain a new configuration. In this configuration the single node that experienced the largest displacement at the panel at linear buckling analysis will have moved 5,5mm.

Once again the ULS capacity will be interpreted from a force-displacement curve. The force is again the support reaction while the displacement is out of plane for the buckled sub panel. Figure 44 illustrates this force-displacement graph for additional displacement. As you can read from this diagram there is no additional stiffness present when the collapse load is reached and ULS capacity will be:

$$F_{Rd} = \frac{F_{Rk}}{\gamma_{m1}} = \frac{6451,3kN}{1,1} = 5832kN \tag{13}$$

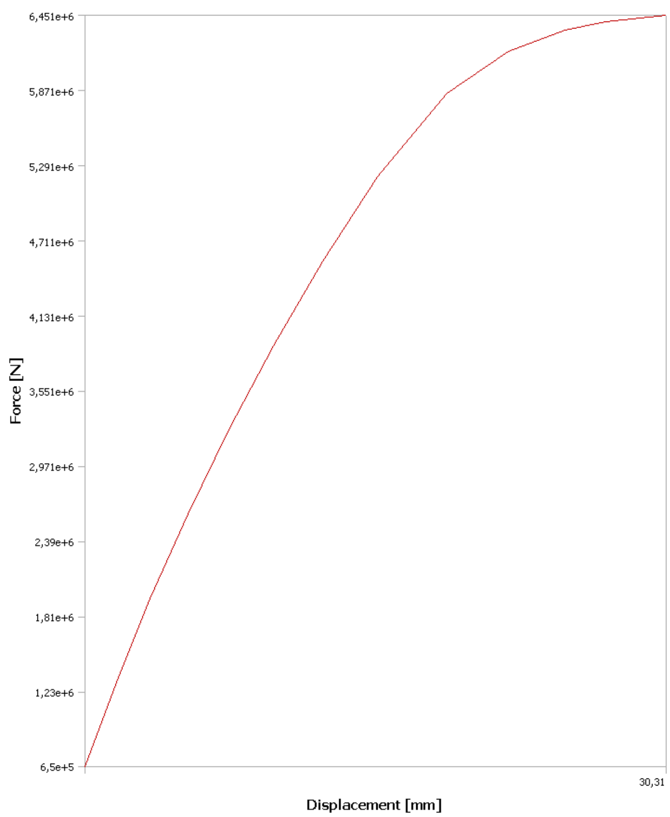

Figure 44: Force-displacement curve with implemented transverse stiffener

As expected this configuration will provide a higher capacity against buckling. The additional transversal stiffeners makes the panel restraint at the middle of the critical subpanel as it is designed to do. As a result of this configuration the panel becomes stiffer and only a more local failure mode is possible.

5 Eurocode 3: Design formulas

5.1 Introduction

Eurocode 3 NS-EN 1993 1-5 [1] provides two methods for considering plate buckling effects. These two methods are referred to as the reduced cross section approach and the reduced strength approach. Despite different procedures to find the ultimate strength of a panel in compression it can be shown that it exist good conformity between capacities calculated by each of the methods. Especially for cases with uniaxial compression, but as well good enough conformity at bi-axial compression. However of the two methods the reduced cross section method is the most acknowledged and used in the engineering industry.

Slender plates in compression have significant post critical resistance that must be utilized in design. For an ideal plated element that does not experience any imperfections pre and post critical behavior is evident. For imperfect plates pre- and post critical behavior is more gradual and of course relies of the size of imperfections. An imperfect plate reaches the critical stresses σ_{cr} while there is still capacity left in the structure. In the post critical stress state a stress distribution will occur. The buckled middle part will experience a decrease in axial stiffness while the stresses will increase near the plates edges. The ultimate resistance will occur when the maximum edge stress has reached the yield strength. To deal with this nonlinear stress distribution the two methods are developed.

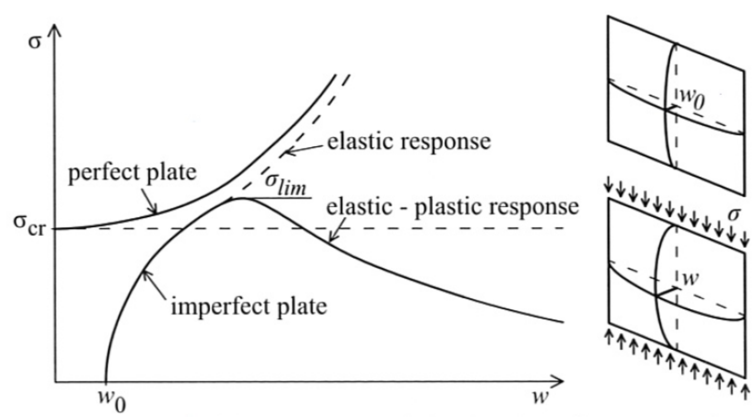

Figure 45: Post-critical behavior slender plates

The reduced cross section method is based on the appropriate reduction of the cross section in the central part, taken effective widths b_{eff} adjacent to edges as fully effective with stresses equal to f_y. The middle buckled part will not contribute to any stiffness of the plate. The reduced stress method is based on the average stress σ_{avg} of the actual stress distribution σ_{act}. This reductions, both in cross section and stress, is of course in a way that maintains equilibrium of the plated element:

$$P_{ult} = \int_0^b \sigma_{act} dx = b_{eff} * f_y = b * \sigma_{avg} = \rho * b * f_y \tag{14}$$

This will provide a plate buckling reduction factor equal to:

$$\rho = \frac{b_{eff}}{b} = \frac{\sigma_{avg}}{f_y} \tag{15}$$

As one of this thesis objective is to analyze the ULS capacity of the main girder‘s web with given design formulas in Eurocode 3 a reasoning for choice of used method must be given. In this thesis I have chosen only to analyze the web panel with the reduced cross section method. The reason for this is that the reduced strength method has some disadvantages that will be critical in design. The main disadvantage is that this method does not consider load shedding between highly stressed to less stressed plate elements. Common engineering practice may be to state that only the flanges will resist the bending moment while the webs must resist shear forces. This is however not possible with the presented method. The result is that the weakest plate element will govern design resistance of the entire cross section. This method would correspond with the reduced cross section for a single plate element like the web. But for Strukturas and other engineering companies this approach will provide meaningless results as the resistance of the entire cross section only is of interest. These arguments will lead to that only the reduced cross section method will be used in this thesis.

Generally buckling in Eurocode 3 is based on the use of reduced slenderness curves. According to *Knekning av søyler og rammer*[10] this approach will make buckling curves independent of yield strength and Young‘s modulus. An important reference for the buckling curves in the standard is the Euler hyperbel. The critical elastic stress for an Euler column is defined as:

$$\sigma_{cr} = \frac{\pi^2 EI}{l_k^2 A} \tag{16}$$

This equation is based on critical elastic stress of an ideal centric buckling of a column with ideal elastic material properties. In this relation l_k is the buckling length, which means the distance between point of no curvature in a deformed second order configuration. This distance is dependent on the boundary conditions of the column. The relation for a column‘s slenderness is defined as:

$$\lambda = \frac{l_k}{i} \tag{17}$$

i is the cross sectional moment arm and is defined as:

$$i = \sqrt{\frac{I}{A}} \tag{18}$$

By substituting the relations for the slenderness and cross sectional moment arm the following relation for elastic critical stress can be determined:

$$\sigma_{cr} = \frac{\pi^2 E i^2}{l_k^2} = \frac{\pi^2 E}{\lambda^2} \tag{19}$$

The reduced slenderness is defined as:

$$\bar{\lambda} = \frac{\lambda}{\lambda_F} = \frac{\lambda}{\pi}\sqrt{\frac{\sigma_F}{E}} \tag{20}$$

Where λ_F is the slenderness that will cause yielding and will be calculated from:

$$\sigma_F = \frac{\pi^2 E}{\lambda_F^2} \Longrightarrow \lambda_F = \pi\sqrt{\frac{E}{\sigma_F}} \tag{21}$$

By substituting $\lambda = \pi\bar{\lambda}\sqrt{\frac{E}{\sigma_F}}$ into equation 19 you can obtain the following relation:

$$\frac{\sigma_{cr}}{\sigma_F} = \frac{1}{\bar{\lambda}_F} \tag{22}$$

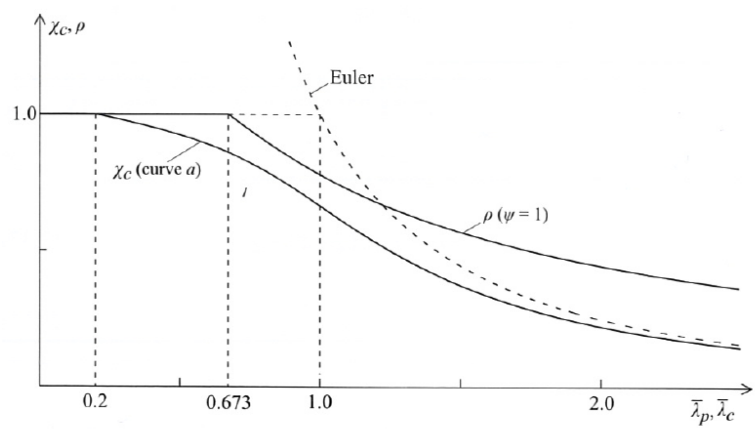

Figure 46: Slenderness effects plate and column buckling

As the Eurocode 3 obtain buckling curves for columns and plates they will of course be possibilities to relate this to the Euler hyperbel. The curves in the standard consider the effect of residual stresses and imperfections. These effects varies at cross section shapes and for columns Eurocode 3 has developed curves for several cross section shapes. For plates post critical reserve will as well be evident. As figure 46 illustrates reduction factors of cross sections caused by slenderness you will be able to differ between column like and plate like buckling of class 4 cross sections. For plate like buckling a reduction of the cross section is needed when $\bar{\lambda}_p > 0,673$. This point ($\bar{\lambda}_p = 0,673$) will correspond to λ=1 for the Euler hyperbel. Which mean that plate like buckling can endure larger slenderness than the Euler hyperbel due to post critical reserve. For column like buckling this is not the case and the reduction curve is always smaller than the Euler hyperbel.

5.2 The reduced cross section approach

5.2.1 Cross section class

This particular method is based calculating ULS capacity of slender structural steel elements in cross section class 4 in accordance to table 5.2 *Eurocode 3: Part 1-5- General rules and rules for buildings* [4]. In class 4 cross sections local buckling occur within the yield strength f_y is reached. To take account for this a reduction of the capacity must be executed. For internal compression parts like webs subjected to bending the following criterion for class 3 must be fulfilled, if not the inner web is a class 4 cross section:

$$b/t \leq 124\epsilon \tag{23}$$

$$3400/14 \leq 124\sqrt{\frac{235}{355}} \tag{24}$$

This criterion is not fulfilled and the inner web must be treated as a class 4 cross section. For the outer web the exact same procedyre must be executed:

$$b/t \leq 124\epsilon \tag{25}$$

$$3400/10 \leq 124\sqrt{\frac{235}{355}} \tag{26}$$

This leads to that both of the webs must be treated as class 4 cross sections. For the bottom flange which is loaded with uniform compression the following criterion must be fulfilled:

$$b/t \leq 42\epsilon \tag{27}$$

$$1800/16 \leq 42\sqrt{\frac{235}{355}} \tag{28}$$

This criterion is not either fulfilled and the entire cross section is a class 4 cross section. This means the capacity of the main girder must be utilized in respect to effective widths calculated from methods from the following subchapters.

5.2.2 Plate buckling effects due to direct stresses

A class 4 cross section subjected to direct stresses must use a reduced cross section according to an effective width calculation in order to withstand stresses. Each plate that the cross section consist of must be treated independently and as simply supported around all boundaries. Based on these effective widths the effective cross section area A_{eff} and effective section modulus W_{eff} are calculated. These effective widths are based on plate buckling effects, but in some cases contribution from shear lag must be included. Shear lag is a first order effect of shear deformations due to normal stresses in flanges. This effect is caused by longitudinal stresses in a girder and how they transform to transverse stresses in the flange. This particular effect can be neglected if you have large span lengths typically 50-60 m with steel girders. This is neglected in the calculations of ULS capacity of the main girder due to the fact that we have span lengths of 56,1m.

When the effective cross section is determined it will be treated as an equivalent class 3 cross section, assuming linear elastic strain and stress distribution over the reduced cross section. The ultimate resistance is reached with the onset of yielding in the center of the compressed plate furthest from the centroid of the cross section.

Slender plates will have significant post-critical resistance present. For shorter panels with low aspect ratios $\alpha = a/b$ this resistance gradually will vanish. This is down to the fact that the plate panel will buckle like a one-dimensional column. Column buckling does not exhibit any post critical resistance and this must be considered. For unstiffened panels column buckling will occur at aspect ratios α smaller than 1, while for longitudinally stiffened panels this can occur for values over 1. Design formulas in NS-EN 1993-1-5 takes these factors into consideration and ULS capacity is calculated based on both types of buckling. In some cases an interpolation between the buckling states are as well needed.

For longitudinally stiffened plates the first order of business is to determine the effective width based on the stress distribution over the subpanels between longitudinal stiffeners. Every element is regarded as simply supported in this particular process. In this process we neglect the effect of stiffeners and local buckling is considered. The elastic critical buckling stress for an unstiffened subpanel is:

$$\sigma_{cr,p} = k_\sigma \frac{\pi^2 E}{12(1-\nu^2)}(\frac{t}{b})^2 \tag{29}$$

In this particular formula b is the vertical distance between longitudinal stiffeners and t is the thickness of the structural element analysed. The buckling factor k_σ is a function of the stress pattern on the structural element. For uniform compression this factor is 4 and stress distribution from bending at a double symmetrical cross section the factor is 23,9. For other stress states table 4.1 and 4.2 in NS-EN 1993 1-5 will provide formulas to calculate this factor. The slenderness of the plate is defined as the following:

$$\bar{\lambda_p} = \sqrt{\frac{f_y}{\sigma_{cr,p}}} \tag{30}$$

For internal compression elements like flanges and webs at a boxed cross section the reduction factor for effective width ρ_{loc} is determined from formula 4.2 and 4.3 in NS-EN 1993-1-5.

$$\rho_{loc} = 1.0, for : \bar{\lambda_p} \leq 0,673 \tag{31}$$

$$\rho_{loc} = \frac{\bar{\lambda}_p - 0,055(3+\psi)}{\bar{\lambda}_p^{\,2}}, for: \bar{\lambda}_p > 0,673 \tag{32}$$

ψ is a factor based on the stress distribution at the considered subpanel. This factor can be calculated by dividing the maximum compressive stress σ_1 with the minimum compressive stress σ_2 at a subpanel. If a subpanel is localized where tensile stress is present σ_2 should be taken as the maximum tensile stress. The calculation for a non symmetrical cross section subjected to bending is illustrated in figure 47.

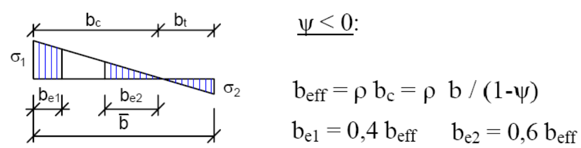

Figure 47: Effective widths of a stiffened subpanel

Based on the plate slenderness the effective width is determined from this relation:

$$b_{eff} = \rho_{loc} * b \tag{33}$$

When this effective b_{eff} widths is calculated for local buckling of subpanels we can use these widths to calculate a global buckling analysis for the considered structural element. At this particular step separate checks for plate- and column like buckling must be executed, as well as criterions for interaction between these buckling states. This particular inclusion is based on how the plate will buckle. For a longitudinally stiffened panel column buckling can occur at aspect ratios $\alpha = a/b$ equal to 1 at large plate orthotropy. This means that the longitudinal and transversal stiffeners are placed frequently and their stiffness is important to withstand instability. Column buckling does not have any post critical reserve and design codes reflects this matter. In order to model column buckling the longitudinal edges must be free so the plate can buckle like a column.

For plate like buckling the procedyre is the same as for an unstiffened panel. The critical elastic buckling stress must be determined for the whole analyzed plate. This must be a global buckling mode that induces this critical stress. To determine this critical stress I have used a program based on PMPE (Principle of Minimum Potential Energy) called EBPlate[7]. This is a customized program to calculate elastic critical stresses based on small deformation theory and elastic material properties. One important issue regarding this program is if you want to obtain the parameter $\sigma_{cr,p}$ for longitudinal stiffened panels you must ensure that global buckling is considered. The way to do this is to prevent local buckling so the panel will experience the effect of smeared stiffeners. That means that stiffness of the longitudinal stiffener is spread out across the breadth of the plate element.

The plate slenderness is defined now as the following:

$$\bar{\lambda_p} = \sqrt{\beta_{A,c}\frac{f_y}{\sigma_{cr,p}}} \tag{34}$$

The parameter $\beta_{A,c}$ will be determined in the following manner:

$$\beta_{A,c} = \frac{A_{c,eff,loc}}{A_c} \tag{35}$$

$A_{c,eff,loc}$ is the sum of effective areas of subpanels and stiffeners excluding edge parts, while A_c is the gross area of the compression zone excluding edge parts of the stiffened plate. For a linear stress pattern due to bending figure 48 indicates the effective and gross area for a stiffened web panel.

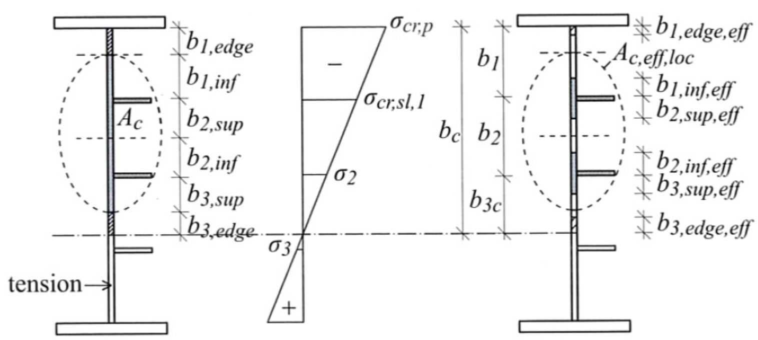

Figure 48: Effective widths of a stiffened panel

$$A_{c,eff,loc} = A_{sl} + \sum_i \rho_{loc,i} b_{loc,i} t \tag{36}$$

Where A_{sl} is the cross section area of stiffeners localized in the compression zone.

The plate slenderness $\bar{\lambda_p}$ will be calculated based on the effective and gross area. The next step now is to determine the elastic critical stress for column buckling. This particular elastic stress is obtained by evaluating the single longitudinal stiffener with contributing plating that experience the largest compressive stress.

$$\sigma_{cr,sl} = \frac{\pi^2 E I_{sl,1}}{A_{sl} a^2} \tag{37}$$

In this relation $I_{sl,1}$ is the second moment of area of the gross cross section of the stiffener in the compression zone and adjacent part of of the plate for out of plane bending of the plate. A_{sl} is the gross cross section area of the stiffener in the compression zone and adjacent part of plate. With adjacent parts the effective widths of the plate calculated for local buckling should be accounted for. This elastic critical stress for column buckling can never be larger than plate buckling. The reason for this is that plate buckling is an obtained solution for a panel which is simply supported along all edges, while column buckling is treated as unsupported along the longitudinal edges.

The elastic critical stress for column buckling is considered at the location of the most compressed longitudinal stiffener. In order to obtain equal premises to evaluate the difference between plate like and column like buckling this stress must be obtained at the the most compressed edge of the plate. $\sigma_{cr,c}$ is found by evaluating the critical elastic stress based on the initial stress distribution at the most compressed edge.

Column slenderness is defined as:

$$\bar{\lambda_c} = \sqrt{\beta_{A,c}\frac{f_y}{\sigma_{cr,c}}} \tag{38}$$

The parameter $\beta_{A,c}$ will be determined in the following manner:

$$\beta_{A,c} = \frac{A_{sl,1,eff}}{A_{sl,1}} \tag{39}$$

Where $A_{sl,1,eff}$ is defined as the effective cross section of the stiffener in the compression zone and adjacent part of plate. $A_{sl,1}$ is the corresponding gross area. When this column slenderness is determined an interaction between column and plate buckling must be checked. If interaction is relevant and global buckling may induce instability the thickness of the effective area calculated for local buckling must be reduced by a factor ρ_c:

$$\rho_c = \xi(2-\xi)(\rho-\chi_c)+\chi_c \tag{40}$$

The factor ξ indicated the relation between elastic critical stresses obtained for plate and column buckling. It is calculated in the following manner:

$$\xi = \frac{\sigma_{cr,p}}{\sigma_{cr,c}} - 1 \tag{41}$$

The factor χ_c is determined from figure 6.4 in NS-EN 1993 1-1. This particular figure indicates the reduction of columns capacities at buckling due to effects of slenderness. If an interaction is not necessary ($\xi > 1$) the reduction of effective thickness should be obtained by using the plate slenderness $\bar{\lambda_p}$. This particular reduction ρ will have the same formulas as for local buckling of subpanels.

$$\rho = 1,0, for: \bar{\lambda_p} \leq 0,673 \tag{42}$$

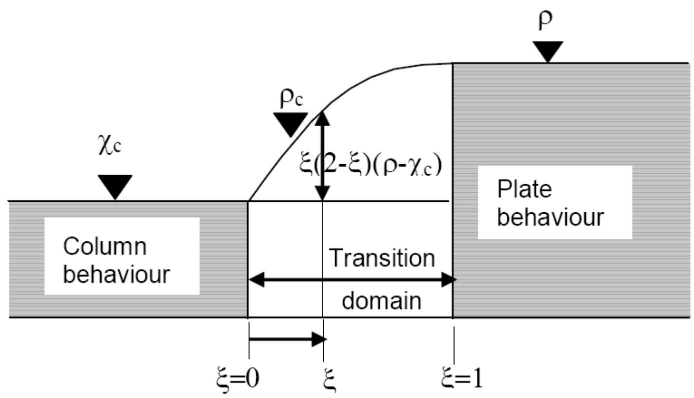

Figure 49: Interpolation between column buckling

For $\bar{\lambda_p} \leq 0,673$ global buckling will not be critical for the structural element and no reduction is necessary. While for $\bar{\lambda_p} > 0,673$ global buckling will govern design and a thickness reduction must be executed:

$$\rho = \frac{\bar{\lambda_p} - 0,055(3+\psi)}{\bar{\lambda_p}^2}, for: \bar{\lambda_p} > 0,673 \tag{43}$$

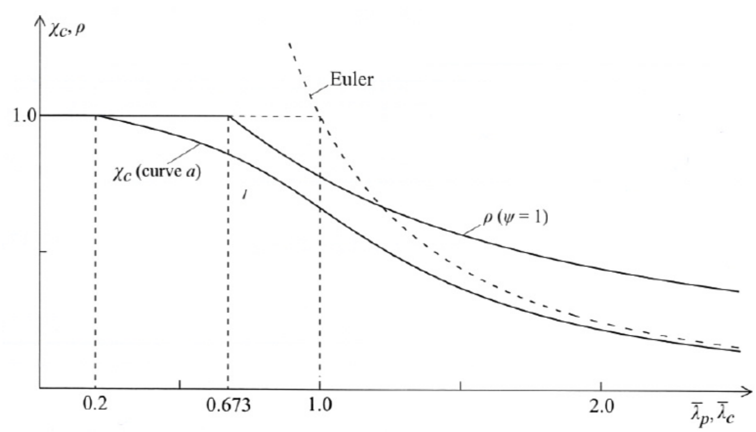

Figure 50: Slenderness effects plate and column buckling

As you can see from figure 50 the reduction factor related to column buckling χ_c is always smaller than for plate like buckling. This is related to that plate slenderness is always smaller than column slenderness. This is due to that $\sigma_{cr,p} > \sigma_{cr,c}$ because of the unsupported longitudinal edges at column buckling.

This method for effective width must be executed on all webs and flanges that experience compressive stresses. When this is done you will obtain an effective cross section. Finally you can include a new strength criteria for the effective cross section and threat the equivalent cross section as class 3. The maximum compressive stress $\sigma_{x,Ed}$ must not exceed the yield stress:

$$\eta_1 = \frac{\sigma_{x,Ed}}{f_y/\gamma_{m1}} \leq 1,0 \tag{44}$$

The compressive design stress is based on beam theory and obtained by the calculated effective cross section:

$$\sigma_{x,Ed} = \frac{M_{Ed}}{W_{eff}} \tag{45}$$

5.2.3 Shear buckling

Slender web panels in shear posess a significant post buckling resistance. Design formulas in the Eurocode 3 is based on the rotated stress field. The basic idea of this theory is to look at resulting principal tension σ_1 and compression σ_2 induced by shear stresses in the web. These stresses will have their corresponding value 45 °from direction of the acting shear stresses. When these principle compressive stresses reach the elastic critical stress state a shear buckle forms in the direction of the principle tensile stresses. Due to buckling no significant increase of compressive stresses is possible while tensile stresses can still increase in the post critical state. This will lead to a rotation of the stress field for equilibrium reasons.

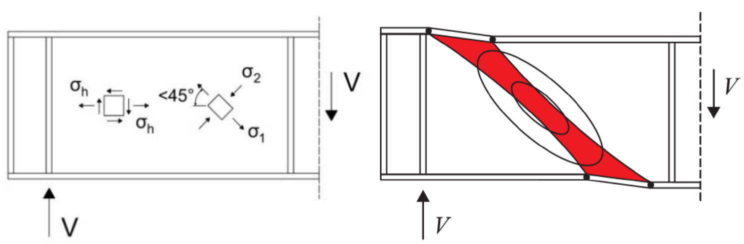

Figure 51: Rotated stress field

When this increasing tensile force forms in the web it is important that it is sufficiently anchored. This will be done by using rigid intermediate transverse stiffeners. In this case the flanges restrain the intermediate transverse stiffener and provide anchorage for the tensile forces. When the tensile force reaches the ultimate load for fracture a plastic hinge mechanism forms in the flanges.

Formulas for the rotated stress field theory has been implemented into NS-EN 1993 1-5. Formula 5.1 gives resistance to shear for unstiffened or stiffened panels:

$$V_{b,Rd} = V_{bw,Rd} + V_{bf,Rd} \leq h_w t_w \frac{\eta f_{yw}}{\sqrt{3}\gamma_{m1}} \tag{46}$$

This design resistance generally tells you that the total shear resistance $V_{b,Rd}$ gets both contribution from the web $V_{bw,Rd}$ and the flanges $V_{bf,Rd}$. This can however not be larger than plastic shear resistance of the web alone.

For a steel girder subjected to shear loading the verification of shear capacity by the following criterion:

$$\eta_3 = \frac{V_{Ed}}{V_{b,Rd}} \leq 1,0 \tag{47}$$

V$_{Ed}$ is the design shear force in the web.

One preliminary step which can save you time is to obtain if a shear resistance check is needed. For unstiffened webs this criterion must be fulfilled:

$$\frac{h_w}{t_w} \geq 72\frac{\epsilon}{\eta} \tag{48}$$

η is attributed to strain hardening which can be tolerated before the steel structural element will get excessive deformations. For steel grades with $f_y \leq 460$ N/mm^2 η=1,2.

For stiffened webs the following criterion must be fulfilled:

$$\frac{h_w}{t_w} \geq 31\frac{\epsilon}{\eta}\sqrt{k_\tau} \tag{49}$$

k$_\tau$ is the shear buckling coefficient and for longitudinally stiffened web panels with aspect ratio $a/h_w \geq 1,0$ it is defined as the following:

$$k_\tau = 5,34 + 4,00(\frac{h_w}{a})^2 + k_{\tau,sl} \tag{50}$$

$k_{\tau,sl}$ is the contribution from the longitudinal stiffeners and defined as the following:

$$k_{\tau,sl} = 9(\frac{h_w}{a})^2 + (\frac{I_{sl}}{t^3 h_w})^{3/4} > \frac{2,1}{t}(\frac{I_{sl}}{h_w})^{1/3} \tag{51}$$

Contribution from the web to the cross sections shear resistance:

$$V_{bw,Rd} = \chi_w h_w t_w \frac{f_{yw}}{\sqrt{3}\gamma_{m1}} \tag{52}$$

In this case χ_w is the reduction factor for shear buckling. This particular reduction factor considers components of pure shear and anchorage of membrane forces via transverse stiffeners. The axial and flexural rigidity of the transverse stiffener will lead to different results at post critical behavior. Requirements for rigid transverse stiffeners is given in chapter 5.3.2.

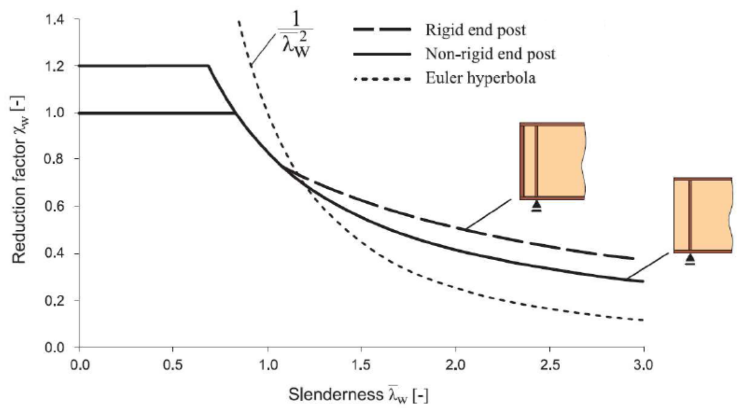

Figure 52: Reduction curves for shear buckling

The plate slenderness for shear buckling $\bar{\lambda_w}$ should be calculated for global shear buckling of the entire web panel with the effect of longitudinal stiffeners and local shear buckling of subpanels. Plate slenderness for shear buckling is defined as:

$$\bar{\lambda_w} = max(\frac{h_w}{37,4 t_w \epsilon \sqrt{k_\tau}}; \frac{h_{wi}}{37,4 t_w \epsilon \sqrt{k_{\tau i}}}) \tag{53}$$

$k_{\tau i}$ and h_{wi} corresponds to shear buckling at subpanels between longitudinal stiffener, and will not consider additional stiffness from stiffeners which means $k_{\tau,sl}$ =0.

For a rigid end post and rigid intermediate transverse stiffeners in a continuous girder the reduction factor χ_w is defined based on values of plate slenderness for shear buckling:

$$\chi_w = \eta, for: \bar{\lambda_w} < \frac{0,83}{\eta} \tag{54}$$

$$\chi_w = \frac{0,83}{\bar{\lambda_w}}, for: \frac{0,83}{\eta} \leq \bar{\lambda_w} < 1,08 \tag{55}$$

$$\chi_w = 1,37/(0,7 + \bar{\lambda_w}), for: \bar{\lambda_w} \geq 1,08 \tag{56}$$

Contribution from the flanges can be accounted for by assessing the formation of plastic hinges in the flanges. Due to the rotated stress field the flanges will endure tensional stresses at transverse stiffeners. The shear resistance from flanges are given as:

$$V_{bf,Rd} = \frac{b_f t_f^2}{c} * \frac{f_{yf}}{\gamma_{m1}}(1 - (\frac{M_{Ed}}{M_{f,Rd}})^2) \tag{57}$$

The distance c between the two plastic hinges in the flange is defined as:

$$c = a(0,25 + \frac{1,6 b_f t_f^2 f_{yf}}{t_w h_w^2 f_{yw}}) \tag{58}$$

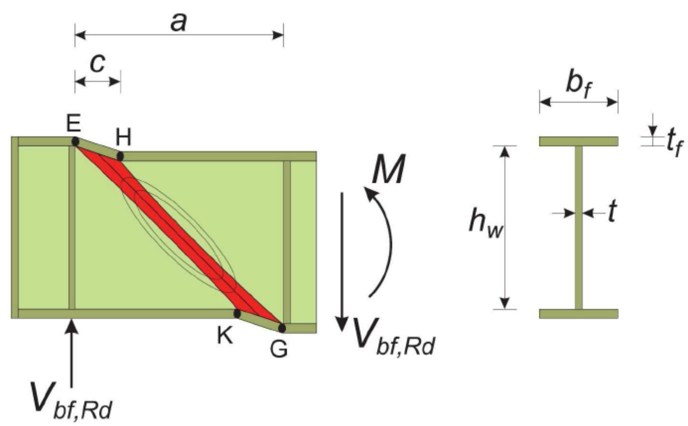

Figure 53: Shear resistance due to flanges stiffness

The moment resistance from the flanges are determined in the following manner:

$$M_{f,Rd} = \frac{M_{R,k}}{\gamma_{m0}} = min(A_{f,1} f_{yf,1} h_f; A_{f,2} f_{yf,2} h_f)/\gamma_{m0} \tag{59}$$

Where h_f is the inner moment arm, that will mean the vertical distance between mid-planes of each of the flanges.

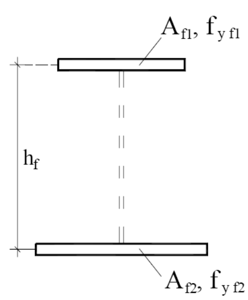

Figure 54: Moment resistance steel girder

5.2.4 Patch loading

Concentrated transverse loading applied perpendicular to the flange in the plane of the web is referred to as patch loading in NS-EN 1993 1-5. For a MSS-system the ULS capacity subjected to patch loading of the box girder is not easy to predict. This is due to the fact that this patch load will occur at multiple loading states and transverse stiffeners may not be appropriate at the needed locations. A patch load may induce three types of failure modes at a steel girder.

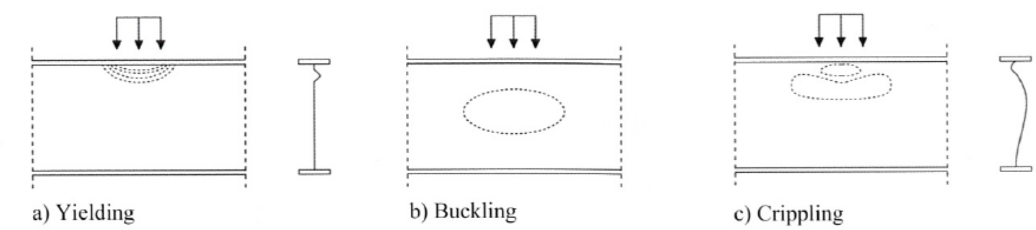

Figure 55: Failure modes at patch loading

Yielding, buckling and crippling of the web are the three failure modes that patch loading can produce. Eurocode 3 does not threat these modes separately because there are many parameter that can influence the ULS capacity, like geometry and difference in material strength of web and flange as well as stiffeners arrangement. The design formulas are based on empirical relations to ensure conservative capacities based on test data and parametric studies.

Before the presentation of the design formulas is presented it can be of great importance to discuss which factors these formulas does not consider. It is obvious that transverse stiffeners c/c 750mm located at the bottom of the web will add stiffness against the concentrated support reaction at the launching wagon. Earlier experience with the design codes is that they will give too conservative results. This is due to the fact that the transverse stiffeners contribution is neglected in the analysis. Results from the ANSYS model indicates that no local buckling mode at the flange or the bottom the web will be of importance, only failure mode b) between longitudinal stiffeners. However it is interesting to study the design codes although it‘s expected that they will lead to resistances well below the actual capacity.

The ultimate transversal load capacity that can be transmitted through the flange and into web is defined as:

$$F_{R,d} = \chi_F * \frac{F_y}{\gamma_{m1}} = \chi_F \frac{l_y t_w f_{yw}}{\gamma_{m1}} \tag{60}$$

In this relation χ_F is the reduction factor for transverse loading while l_y is the effective loaded length. The yield load F_y will be reduced with the reduction factor χ_F which is calculated based on patch slenderness of the web. The reduction factor χ_F is based on a reduction curve according to the following relation:

$$\chi_F = \frac{0,5}{\bar{\lambda_F}} \leq 1 \tag{61}$$

$\bar{\lambda_F}$ is the slenderness of the web panel which is reliant on the relation between the yield load F_y and the elastic critical load $F_{cr,1}$:

$$\bar{\lambda_F} = \sqrt{F_y/F_{cr,1}} \tag{62}$$

The elastic critical load is calculated in the following manner:

$$F_{cr,1} = 0,9 k_{F,1} E \frac{t_w^3}{h_w} \tag{63}$$

The buckling factor $k_{F,1}$ depends on what type of transversal load application is used. NS-EN 1993 1-5 distinguishes between three types:

- a: Load application through one flange
- b: Load application through both flanges
- c: Load application through one flange adjacent to an unstiffened end

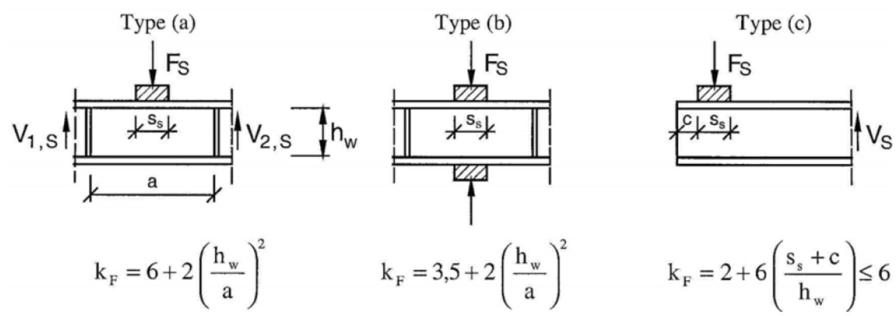

Figure 56: Load applications at steel girders

It is clearly evident that the load application at the main girder through the launching rail is type a. The load will be transfered through a launching flange with breadth b_f= 150mm and thickness t_f=50mm.

For longitudinally stiffened plates like the main girder the buckling factor $k_{F,1}$ can be calculated in the following manner:

$$k_{F,1} = 6 + 2(\frac{h_w}{a})^2 + [5,44\frac{b_1}{a} - 0,21]\sqrt{\gamma_s} \tag{64}$$

The parameter b_1 is the vertical distance between the loaded flange and the first longitudinal stiffener. γ_s determines contribution from longitudinal stiffeners and shall be calculated from the formula:

$$\gamma_s = 10,9\frac{I_{sl,1}}{h_w t_w^3} \le 13(\frac{a}{h_w})^3 + 210(0,3 - \frac{b_1}{a}) \tag{65}$$

$I_{sl,1}$ is the second moment of area of the longitudinal stiffener closest to the loaded flange including contributing parts of the web ($15\epsilon t_w$) for out of plane bending.

To calculate the plate slenderness we need as well to determine the yield load F_y. For this calculation an effective loaded length l_y is introduced. This effective loaded length takes into account the stiffness of the flange and how the patch load will be distributed to the web. The basic idea of these calculations is to determine the stiffness of the flange by introducing two dimensionless parameters m_1 and m_2. These two parameters considers the flange's stiffness by evaluating four plastic hinges. As well will an effective web height $=0{,}14h_w$ be considered in the stiffness calculation.

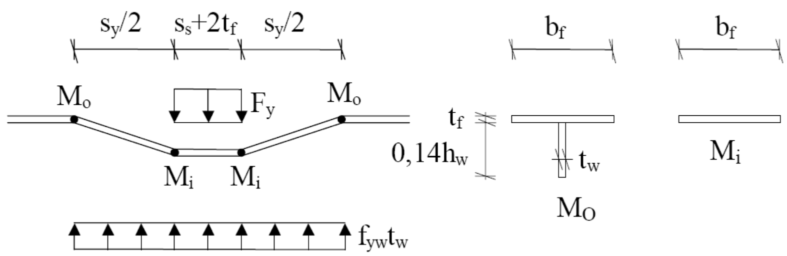

Figure 57: Effective loaded length

The yield load will be calculated by the formula:

$$F_y = l_y t_w f_{yw} \tag{66}$$

While the effective loaded length l_y for load application through one flange is determined by:

$$l_y = s_s + 2t_f(1 + \sqrt{m_1 + m_2}) \leq a \tag{67}$$

s_s is the initial loaded length on the flange. The dimensionless parameters m_1 and m_2 will be determined by:

$$m_1 = \frac{f_{yf} b_f}{f_{yw} t_w} \tag{68}$$

$$m_2 = 0, for : \bar{\lambda_F} \leq 0,5 \tag{69}$$

$$m_2 = 0,02(\frac{h_w}{t_f})^2, for : \bar{\lambda_F} > 0,5 \tag{70}$$

Resistance against patch loading will be an important feature of calculating the ULS capacity of buckling at the main girder at the launching stage. After studying theory on this subject it is evident that some important parameters will not be considered and results tend to be too conservative. According to *JRC Scientific and Technical Reports* [2] the influence of length of launching device at launching state is not fully covered. To increase capacity of the web's capacity against patch loading the length s_s is increased. At Vizela Calvos this particular length is 1300mm. The relation $s_s/h_w = 1300/3400 =$ 0,38 will lead to conservative results by using design formulas in NS-EN

1993 1-5. According to test results the ratio between loaded length and web height will induce larger capacities. These capacities are in the region of 1,4-1,8 times larger then predictions from design formulas.

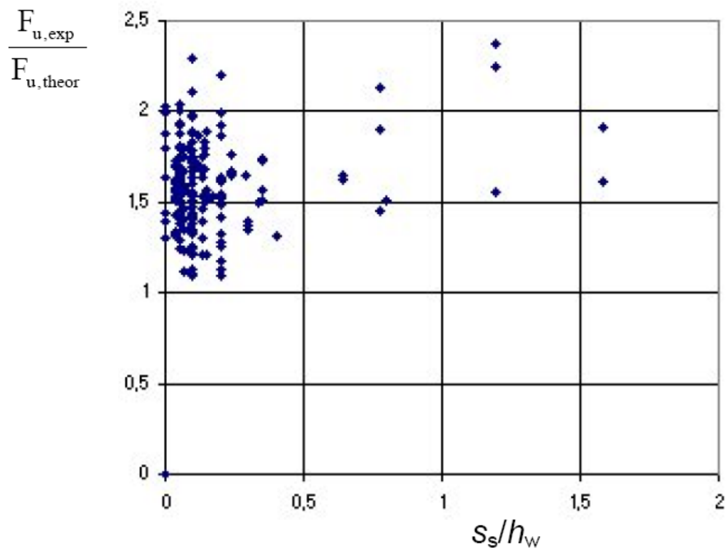

Figure 58: Test results s_s/h_w

The inner web of the main girder will experience additional stiffness against patch loading due to transversal stiffeners placed c/c 750mm at lower region region of the web. Their contributing is important because they will contribute to additional stiffness to prevent the three failure modes and as well distribute the patch load at a larger area. No design parameters will take their contribution into consideration.

Recent research has been conducted on the effect on patch loading. According to *Davaine, Patch loading of longitudinally stiffened bridge girders*[5](2004) the current design formulas in NS-EN 1993 1-5 tend to give too conservative predictions on capacities regarding patch loading at plated girders. A new improved method has been developed and will be implemented into the next NS-EN 1993 1-5. These methods are based on the same principles as before although these formulas are based on more reliable test data to calculate resistances of patch loading.

This research states that the yield resistance F_y was comparable high while the reduction factor χ_F was on the other hand too low. The new proposed design formulas will correct formulas in the following manner:

$$l_y = s_s + 2t_f(1 + \sqrt{m_1}) \leq a \tag{71}$$

This will lead to the conclusion that dimensionless moment parameter m_2 is set equal to zero and the yield load will be reduced. The buckling factor $k_{F,2}$ will as well be corrected to:

$$k_{F,2} = (0,8\frac{s_s + 2t_f}{a})(\frac{a}{b_1})^{0,6\frac{s_s+2t_f}{a}+0,5} \tag{72}$$

$$F_{cr,2} = k_{F,2}\frac{\pi^2 E}{12(1-\nu^2)}(\frac{t_w^3}{b_1}) \tag{73}$$

The new elastic patch load will now be calculated from:

$$F_{cr} = \frac{F_{cr,1}F_{cr,2}}{F_{cr,1} + F_{cr,2}} \tag{74}$$

The reduction factor χ_F will now be calculated with this formula:

$$\chi_F = \frac{1}{\phi_F + \sqrt{\phi_F^2 + \bar{\lambda_F}}} \leq 1,2 \tag{75}$$

Where:

$$\phi_F = 0,5(1 + 0,21(\bar{\lambda_F} - 0,8) + \bar{\lambda_F}) \tag{76}$$

The method from Davaine has been reviewed by Mattias Clarin (2007)[6] and a whole range of FEM testing and available test data have been included. He has made corrections on the method proposed by Davaine where the elastic buckling load should be determined by:

$$F_{cr} = min(F_{cr,1}, F_{cr,2}) \tag{77}$$

5.2.5 Interactions

Bending moment and shear force in a web panel:

For a box girder like the main girder the web panel have to withstand loading due to shear and bending. The main girders capacity has to be verified using:

$$\eta_1 + (1 - \frac{M_{f,Rd}}{M_{pl,Rd}})(2\eta_3 - 1)^2 \leq 1,0 \tag{78}$$

Where $M_{f,Rd}$ is the design plastic moment resistance of the section consisting only of the effective area of the flanges. $M_{pl,Rd}$ is the the design plastic moment resistance of the effective flanges and fully effective web. This interaction does not not to be executed if you can ensure that:

$$\eta_3 = \frac{V_{Ed}}{V_{bw,Rd}} \leq 0,5 \tag{79}$$

$$M_{Ed} \leq M_{f,Rd} \tag{80}$$

As you can see this interaction does not need to be executed if the flanges alone can resist the bending moment and the web alone can have enough resistance to deal with shear forces. This interaction is often lightly to be a vital part of bridge design at supports. At this location you will experience the maximum shear and as well a hogging moment.

Bending moment and patch loading:

If the patch load is acting on the compression zone of the main girder, like the support reaction at the main girder, the following criterion must be fulfilled:

$$\eta_2 + 0,8_{\eta_1} \leq 1,4 \tag{81}$$

This particular interaction does not need to performed if one of the following criterions is fulfilled:

$$\eta_1 \leq 0,5 \tag{82}$$

$$\eta_2 \leq 0,6 \tag{83}$$

5.3 Detailing of stiffeners

5.3.1 Longitudinal stiffeners

For longitudinal stiffeners the calculation of resistance of the web regarding shear buckling, plate buckling effects due to direct stresses and as well patch loading the longitudinal stiffeners contribution are already included. The presence of longitudinal stiffeners certainly increases the plates resistance to buckling and must be an important feature in design. However some attention is needed regarding local torsional buckling of these stiffeners. A general design rule is developed in order to ensure that this phenomenon does not happens for open cross section like flat bars. Formula 9.3 in NS-EN 1993-1-5 states:

$$\frac{I_T}{I_p} \geq 5,3\frac{f_y}{E} \tag{84}$$

Here I_T is St.Venants torsional constant for the stiffener alone, while I_p is a polar second moment of area alone around the edge fixed to the plate. For a steel material with a yield strength f_y=355 N/mm^2 this means a breadth-thickness ratio $b_{st}/t_{st} \leq$ 10,6. This calculation is however based on a uniform compression over the panel equal to f_y and only contribution from St.Venants torsion. The stiffener which may cause concern is the one placed nearest the compression flange and has a dimension 16×200mm. This will give a breadth-thickness ratio of 12,5. The middle longitudinal stiffener which has dimensions 28×200mm has a breadth-thickness ratio of 7,1 and it can be concluded that this stiffener will not experience local torsional buckling. A more general approach is to calculate the elastic critical stress for the stiffener at torsional buckling with contribution from warping and elastic restraint of contributing plating. This particular configuration at the main girder will experience warping restraint at transverse beam location and it's contribution must not be neglected. These formulas are not included in NS-EN 1993 1-5, but *Commentary and worked examples to NS-EN 1993 1-5* [2] have developed a set of design rules to ensure capacity. The elastic critical stress of a stiffener at torsional buckling should fulfill the following requirement for flat bars as stiffening:

$$\sigma_{cr} \geq 2 f_y \tag{85}$$

The yield strength f_y should be taken as the maximum stress the stiffener will experience. The practical way to solve this is to assume that you only can load a box girder with a bending moment so that the flanges will experience the yield stress. With a linear stress distribution the longitudinal stiffener nearest the compression flange will experience maximum compressive stresses equal to:

$$\sigma_{sl} = \frac{1100}{1700} * f_y = 0,647 * 355 = 229,7 N/mm^2 \tag{86}$$

This would lead to that the requirement for the stiffener is:

$$\sigma_{cr} \geq 2 * 229,7 = 459,4 N/mm^2 \tag{87}$$

With only contribution from warping and St.Venants torsion the formula for σ_{cr} is:

$$\sigma_{cr} = \frac{1}{I_p}\left(\frac{\pi^2 E I_w}{l^2} + G I_T\right) \tag{88}$$

I_w is the warping cross section constant of the stiffener alone around the edge of the fixed plate while l is the length of the stiffener between points it is restraint to buckle. In this case l=750mm because of the configuration with transverse stiffeners c/c 750mm at the bottom of the web. The calculation for the needed parameters will be:

$$I_p = \frac{1}{3} t_{st} b_{st}^3 = \frac{1}{3} * 16 * 200^3 = 4,27 * 10^7 mm^4 \tag{89}$$

$$I_t = \frac{1}{3} b_{st} t_{st}^3 = \frac{1}{3} * 200 * 16^3 = 2,73 * 10^5 mm^4 \tag{90}$$

For a isotropic material like steel the shear modulus can be determined to be:

$$G = \frac{E}{2(1+\nu)} = \frac{210000}{2(1+0,3)} = 80769 N/mm^2 \tag{91}$$

The warping cross section constant for a flat bar is determined from table 7.3 in *Arne Selberg, Stålkonstruksjoner, 1972*[8]:

$$I_w = \frac{1}{144} b_{st}^3 t_{st}^3 \frac{b_{st}^2 - t_{st}^2}{b_{st}^2 + t_{st}^2} = \frac{1}{144} * 200^3 * 16^3 \frac{200^2 - 16^2}{200^2 + 16^2} = 2,24 * 10^8 mm^4 \tag{92}$$

The elastic critical stress in the stiffener for torsional buckling is:

$$\sigma_{cr} = \frac{1}{4,27 * 10^7}(\frac{\pi^2 * 210000 * 2,24 * 10^8}{750^2} + 80769 * 2,73 * 10^5) = 535N/mm^2 \quad (93)$$

As you can see this elastic critical stress satisfies the requirement:

$$\sigma_{cr} \geq 2 * 229,7 = 459,4N/mm^2 \quad (94)$$

As a conclusion we can say that the stiffener is prevented to buckle in local torsion. Additional calculation could have been executed to evaluate the contributing plating acting as a continuous elastic support. This is however not done because resistance against torsional buckling is present.

5.3.2 Transversal stiffeners

NS-EN 1993 1-5 only provide formula for transversal stiffeners which are continuous and welded to each flange. This will lead to that the transversal stiffeners at the bottom part of the web will not be considered in any calculations. These stiffeners are located here to contribute to rotational stiffness of the support and ensure capacity against failure modes at patch loading. At the location of the transverse beams the main girder is stiffened with inner beams and a complete set of transversal stiffeners.

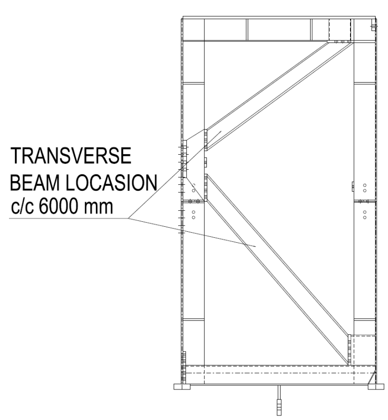

Figure 59: Transverse stiffening at transverse beams c/c 6000mm

This particular stiffening arrangement must of course be defined as a rigid transverse stiffening. A MSS-system has often been used with transverse stiffener located 3000 mm from each transverse stiffening arrangement. These transverse stiffeners have had dimension of 16×200mm. These are stiff enough to qualify as rigid intermediate transverse stiffeners loaded in shear. In practice this would mean that they are stiff enough to transfer tensional stress caused by shear from the web to the flanges.

Intermediate transverse stiffeners rigid for shear must fulfill the following criterions:

$$I_{st} \leq \frac{1,5h_w^3 t^3}{a^2}, for : \alpha = \frac{a}{h_w} < \sqrt{2} \tag{95}$$

$$I_{st} \leq 0,75 h_w t^3, for : \alpha = \frac{a}{h_w} \geq \sqrt{2} \tag{96}$$

I$_{st}$ is the second moment of area of the stiffener for the axis parallel to the web plate and adjacent part of plate (15ϵt) for out out of plane bending. This requirement for shear does not demand very strong stiffeners, but this is the configuration Strukturas is interested in regarding capacity of the main girder‘s web.

Verification of transverse stiffener:

$$\frac{a}{h_w} = \frac{3000}{3400} = 0,88 < \sqrt{2} \tag{97}$$

For calculation of I_{st} see appendix A.

$$3,22 * 10^7 \leq \frac{1,5 * 3400 * 14^3}{3000^2} = 1,80 * 10^7 \tag{98}$$

These requirements assure that at the ultimate shear resistance of the cross section is preserved because the lateral deflection of the intermediate stiffener remains small compared to the web.

This configuration has been implemented in a new analysis at chapter 4.4 to obtain the buckling capacity of the main girders web using ANSYS Workbench.

6 Application of methods in ULS design

6.1 Direct stresses due to bending moment

To perform this method on the main girder effective widths has to be calculated on the structural elements that experience compressive stresses. In this particular case with direct stresses caused by bending, both webs and the bottom flange has to be calculated. The entire cross section before reduction due to effective widths is shown in figure 60. The maximum tensile stress at the upper flange is calculated to 99,9N/mm^2, while maximum compressive stresses in the bottom flange is equal to 100,2N/mm^2.

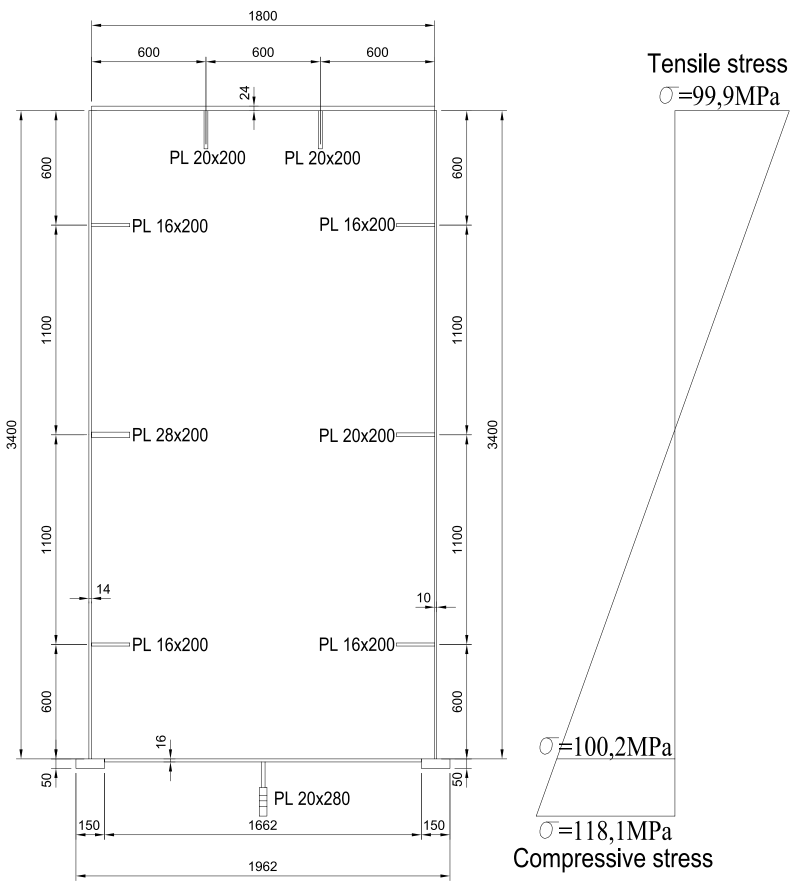

Figure 60: Cross section before reduction

Reduction of web capacity:

Reduction of the inner and the outer web will be performed in accordance to NS-EN 1993 1-5. In order to obtain this solution EBPlate has to be used to find the elastic critical stress $\sigma_{cr,p}$ for smeared stiffeners. These stresses has been found to be:

Structural element	$\sigma_{cr,p}$
Inner web	1262,5N/mm^2
Outer web	863,4 N/mm^2

Table 5: Elastic critical stresses for smeared stiffeners

For input data and results at EBPlate see appendix F. Based on these calculations the corresponding effective widths can be calculated. Figure 61 indicates the effective areas to be calculated to ensure that local buckling will pose no threat of design.

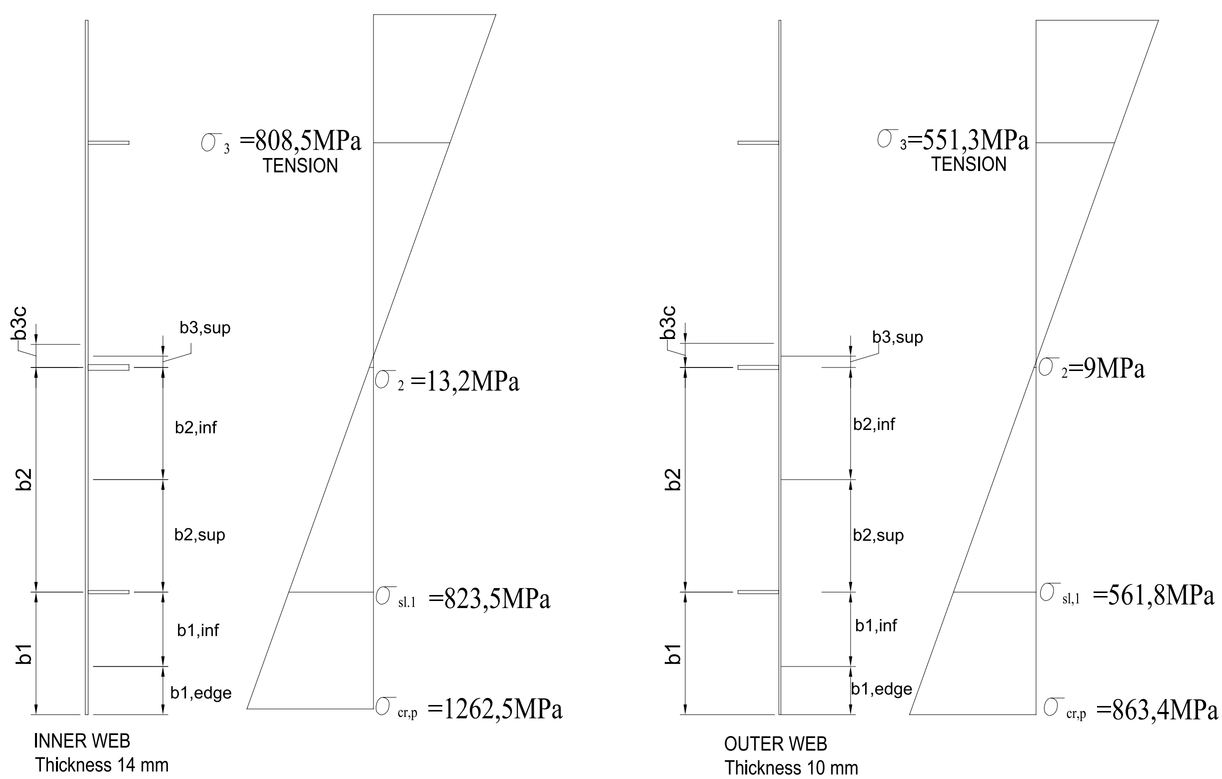

Figure 61: Elastic critical stresses at cross section

The effective widths for each of the webs will be calculated from table 6.

All the conditions ψ are upheld as illustrated in table 6. The next step in the calculation

Width	Width for gross area	Width for effective area	Condition for ψ
$\mathrm{b}_1, edge$	$\frac{2}{5-\psi_1}\mathrm{b}_1$	$\frac{2}{5-\psi_1}\mathrm{b}_{1,eff}$	$\frac{\sigma_{cr,sl,1}}{\sigma_{cr,p}} > 0$
b_1, inf	$\frac{3-\psi_1}{5-\psi_1}\mathrm{b}_1$	$\frac{3-\psi_1}{5-\psi_1}\mathrm{b}_{1,eff}$	$\frac{\sigma_{cr,sl,1}}{\sigma_{cr,p}} > 0$
b_2, sup	$\frac{2}{5-\psi_2}\mathrm{b}_2$	$\frac{2}{5-\psi_2}\mathrm{b}_{2,eff}$	$\frac{\sigma_2}{\sigma_{cr,sl,1}} > 0$
b_2, inf	$\frac{3-\psi_2}{5-\psi_2}\mathrm{b}_1$	$\frac{2}{5-\psi_2}\mathrm{b}_{2,eff}$	$\frac{\sigma_{cr,2}}{\sigma_{cr,sl,1}} > 0$
b_3, sup	$0,4\mathrm{b}_{3c}$	$0,4\mathrm{b}_{3c,eff}$	$\frac{\sigma_3}{\sigma_2} < 0$

Table 6: Effective width calculation webs

is to determine effective widths for the subpanels between longitudinal stiffeners. This calculation will be the same for both of the webs as the distances b_1, b_2 and b_{3c} are the same as well as ψ_1,ψ_2 and ψ_3. Calculations will be made in accordance to table 4.1 in NS-EN 1993 1-5.

$$\psi_1 = \frac{\sigma_{cr,sl,1}}{\sigma_{cr,p}} = \frac{823,5}{1262,5} = \frac{561,8}{863,4} = 0,65 \tag{99}$$

$$\psi_2 = \frac{\sigma_2}{\sigma_{cr,sl,1}} = \frac{13,2}{823,5} = \frac{9}{561,8} = 0,016 \tag{100}$$

$$\psi_3 = \frac{\sigma_3}{\sigma_2} = \frac{-808,5}{13,2} = \frac{-551,3}{9} = -61,2 \tag{101}$$

Then the buckling factor for local buckling of subpanels must be determined:

$$k_{\sigma,1} = 8,2/(1,05+\psi_1) = 8,2/(1,05+0,65) = 4,82 \tag{102}$$

$$k_{\sigma,2} = 8,2/(1,05+\psi_2) = 8,2/(1,05+0,016) = 7,69 \tag{103}$$

For $\mathrm{k}_{\sigma,3}$ the elastic buckling stress $\sigma_{cr,p}$ would tend to infinity because of the distance b_{c3} is small. This means that stiffeners is placed near to the neutral axis and will not experience significant compressive stresses. This tells us that global buckling of this stiffened web will not occur and reducing widths assosiated with this stiffener can be neglected.

The elastic critical stresses for each of the two subpanels at the inner web that experience compressive stresses will be:

$$\sigma_{cr,p,1} = k_{\sigma,1}\frac{\pi^2 E}{12(1-\nu^2)}(\frac{t}{b_1})^2 = 4,82\frac{\pi^2 210000}{12(1-0,3^2)}(\frac{14}{600})^2 = 498N/mm^2 \tag{104}$$

$$\sigma_{cr,p,2} = k_{\sigma,2}\frac{\pi^2 E}{12(1-\nu^2)}(\frac{t}{b_2})^2 = 7,69\frac{\pi^2 210000}{12(1-0,3^2)}(\frac{14}{1100})^2 = 236N/mm^2 \tag{105}$$

The elastic critical stresses for each of the two subpanels at the outer web that experience compressive stresses will be:

$$\sigma_{cr,p,1} = k_{\sigma,1}\frac{\pi^2 E}{12(1-\nu^2)}(\frac{t}{b_1})^2 = 4,82\frac{\pi^2 210000}{12(1-0,3^2)}(\frac{10}{600})^2 = 254N/mm^2 \tag{106}$$

$$\sigma_{cr,p,2} = k_{\sigma,2}\frac{\pi^2 E}{12(1-\nu^2)}(\frac{t}{b_2})^2 = 7,69\frac{\pi^2 210000}{12(1-0,3^2)}(\frac{10}{1100})^2 = 120N/mm^2 \tag{107}$$

This will give the local plate slenderness of the two subpanels at the inner web:

$$\bar{\lambda_{p,1}} = \sqrt{\frac{f_y}{\sigma_{cr,p,1}}} = \sqrt{\frac{355}{498}} = 0,84 \tag{108}$$

$$\bar{\lambda_{p,2}} = \sqrt{\frac{f_y}{\sigma_{cr,p,2}}} = \sqrt{\frac{355}{236}} = 1,22 \tag{109}$$

This will give the local plate slenderness of the two subpanels at the outer web:

$$\bar{\lambda_{p,1}} = \sqrt{\frac{f_y}{\sigma_{cr,p,1}}} = \sqrt{\frac{355}{254}} = 1,18 \tag{110}$$

$$\bar{\lambda_{p,2}} = \sqrt{\frac{f_y}{\sigma_{cr,p,2}}} = \sqrt{\frac{355}{120}} = 1,71 \tag{111}$$

For $\bar{\lambda_p} > 0,673$ the reduction factor for internal compression elements like the web the effective width will be determined by:

$$\rho_{loc} = \frac{\bar{\lambda_p} - 0,055(3+\psi)}{(\bar{\lambda_p})^2} \tag{112}$$

Inner web:

$$\rho_{loc,1} = \frac{\bar{\lambda_{p,1}} - 0,055(3+\psi_1)}{(\bar{\lambda_{p,1}})^2} = \frac{0,84 - 0,055(3+0,65)}{0,84^2} = 0,90 \tag{113}$$

$$\rho_{loc,2} = \frac{\bar{\lambda_{p,2}} - 0,055(3+\psi_2)}{(\bar{\lambda_{p,2}})^2} = \frac{1,22 - 0,055(3+0,016)}{1,22^2} = 0,72 \tag{114}$$

Outer web:

$$\rho_{loc,1} = \frac{\bar{\lambda_{p,1}} - 0,055(3+\psi_1)}{(\bar{\lambda_{p,1}})^2} = \frac{1,18 - 0,055(3+0,65)}{1,18^2} = 0,70 \tag{115}$$

$$\rho_{loc,2} = \frac{\bar{\lambda_{p,2}} - 0,055(3+\psi_2)}{(\bar{\lambda_{p,2}})^2} = \frac{1,71 - 0,055(3+0,016)}{1,71^2} = 0,53 \tag{116}$$

Now we know how much of the subpanels that can be utilized in design. The effective width can be calculated from the formula:

$$b_{eff} = \rho_{loc} * b_c \tag{117}$$

This gives effective widths for the inner web:

$$b_{1,eff} = 0,9 * 600 = 540mm \tag{118}$$

$$b_{2,eff} = 0,72 * 1100 = 792mm \tag{119}$$

The outer web get effective widths:

$$b_{1,eff} = 0,7 * 600 = 420mm \tag{120}$$

$$b_{2,eff} = 0,53 * 1100 = 583mm \tag{121}$$

Finally we can calculate the effective widths with effect of longitudinal stiffeners:

Width	**Width for gross area**	**Effective area inner web**	**Effective area outer web**
$b_1, edge$	$\frac{2}{5-0,65} \times 600 = 275$mm	$\frac{2}{5-0,65} \times 540 = 248$mm	$\frac{2}{5-0,65} \times 420 = 193$mm
b_1, inf	$\frac{3-0,65}{5-0,65} \times 600 = 324$mm	$\frac{3-0,65}{5-0,65} \times 540 = 292$mm	$\frac{3-0,65}{5-0,65} \times 420 = 227$mm
b_2, sup	$\frac{2}{5-0,016} \times 1100 = 441$mm	$\frac{2}{5-0,016} \times 792 = 317$mm	$\frac{2}{5-0,016} \times 583 = 233$mm
b_2, inf	$\frac{3-0,016}{5-0,016} \times 1100 = 659$mm	$\frac{2}{5-0,016} \times 792 = 474$mm	$\frac{2}{5-0,016} \times 583 = 349$mm

Table 7: Final effective width calculation

The next step is to check for interpolation between plate and column like buckling. For plate like buckling the plate slenderness is defined as:

$$\bar{\lambda_p} = \sqrt{\beta_{A,c} \frac{f_y}{\sigma_{cr,p}}} \tag{122}$$

The parameter $\beta_{A,c}$ will be determined in the following manner:

$$\beta_{A,c} = \frac{A_{c,eff,loc}}{A_c} \tag{123}$$

The effective areas and gross cross sections areas for the inner web will be calculated to:

$$A_{c,eff,loc} = b_{1,inf,eff} t_w + b_{2,sup,eff} t_w + b_{2,inf,eff} t_w + b_{2,sup,eff} t_w + A_{sl,1} \tag{124}$$

$$A_{c,eff,loc} = 248 * 14 + 292 * 14 + 317 * 14 + 474 * 14 + 200 * 16 = 21834mm^2 \tag{125}$$

$$A_c = b_{1,inf} t_w + b_{2,sup} t_w + b_{2,inf} t_w + b_{2,sup} t_w + A_{sl,1} \tag{126}$$

$$A_c = 275 * 14 + 324 * 14 + 441 * 14 + 659 * 14 + 200 * 16 = 26986mm^2 \tag{127}$$

$$\beta_{A,c} = \frac{A_{c,eff,loc}}{A_c} = \frac{21834}{26986} = 0,81 \tag{128}$$

The plate slenderness for the inner web:

$$\bar{\lambda_p} = \sqrt{0,81\frac{355}{1262,5}} = 0,48 \tag{129}$$

The effective areas and gross cross sections areas for the outer web will be calculated to:

$$A_{c,eff,loc} = 193*14 + 227*14 + 233*14 + 349*14 + 200*16 = 17228mm^2 \tag{130}$$

The gross area of the subpanels for the outer web will be the same as the inner because they are based on the same stress distribution.

$$\beta_{A,c} = \frac{A_{c,eff,loc}}{A_c} = \frac{17228}{26986} = 0,64 \tag{131}$$

Therefore the plate slenderness for the outer web is:

$$\bar{\lambda_p} = \sqrt{0,64\frac{355}{863,4}} = 0,42 \tag{132}$$

The column slenderness will be calculated from:

$$\bar{\lambda_c} = \sqrt{\beta_{A,c}\frac{f_y}{\sigma_{cr,c}}} \tag{133}$$

The elastic critical stress for column buckling at the inner web:

$$\sigma_{cr,sl} = \frac{\pi^2 E I_{sl,1}}{A_{sl,1}a^2} \tag{134}$$

For calculation of I$_{sl}$ see appendix C.

The parameter $\beta_{A,c}$ will be determined in the following manner:

$$\beta_{A,c} = \frac{A_{sl,1,eff}}{A_{sl,1}} \tag{135}$$

$$A_{sl,1,eff} = A_{sl,1} + b_{1,inf,eff}t_w + b_{2,sup,eff}t_w \tag{136}$$

$$A_{sl,1,eff} = 200*16 + 292*14 + 317*14 = 11726mm^2 \tag{137}$$

$$A_{sl,1} = A_{sl,1} + b_{1,inf}t_w + b_{2,sup}t_w \tag{138}$$

$$A_{sl,1} = 200*16 + 324*14 + 441*14 = 13910mm^2 \tag{139}$$

$$\beta_{A,c} = \frac{11726}{13910} = 0,84 \tag{140}$$

Elastic critical stress for the inner web:

$$\sigma_{cr,sl} = \frac{\pi^2 * 210000 * 3,91 * 10^7}{13910 * 6000^2} = 162N/mm^2 \tag{141}$$

This elastic critical stress is obtained at the longitudinal stiffener in the compression zone. You must obtain the stress at the bottom of the web in order to have equal premises for calculations of plate slenderness.

$$\sigma_{cr,c} = 162N/mm^2 * \frac{1700}{1100} = 250N/mm^2 \tag{142}$$

Column slenderness for the inner web:

$$\bar{\lambda_c} = \sqrt{0,84\frac{355}{250}} = 1,10 \tag{143}$$

Interpolation between plate and column buckling for the inner web the reduction of the thickness:

$$\rho_c = \xi(2-\xi)(\rho - \chi_c) + \chi_c \tag{144}$$

This equation is only valid if the following equation is fulfilled:

$$\xi = \frac{\sigma_{cr,p}}{\sigma_{cr,c}} - 1, for : 0 \leq \xi \leq 1 \tag{145}$$

$$\xi = \frac{\sigma_{cr,p}}{\sigma_{cr,c}} - 1 = \frac{1262,5}{250} = 4,05 \tag{146}$$

This will induce that plate like buckling prevails the reduction of the thickness ρ_p must be calculated in accordance to:

$$\rho_p = 1,0, for : \bar{\lambda_p} \leq 0,673 \tag{147}$$

For the global check the plate slenderness $\bar{\lambda_p} = 0,48$. This will give no reduction of the thickness of the web.

Similar approach must be executed for the outer web. The column slenderness will be calculated from:

$$\bar{\lambda_c} = \sqrt{\beta_{A,c}\frac{f_y}{\sigma_{cr,c}}} \tag{148}$$

The elastic critical stress for column buckling at the outer web:

$$\sigma_{cr,sl} = \frac{\pi^2 EI_{sl,1}}{A_{sl,1}a^2} \tag{149}$$

For calculation of I_{sl} see appendix D.

The parameter $\beta_{A,c}$ will be determined in the following manner:

$$\beta_{A,c} = \frac{A_{sl,1,eff}}{A_{sl,1}} \tag{150}$$

$$A_{sl,1,eff} = A_{sl,1} + b_{1,inf,eff}t_w + b_{2,sup,eff}t_w \tag{151}$$

$$A_{sl,1,eff} = 200 * 16 + 227 * 14 + 233 * 14 = 9640mm^2 \tag{152}$$

The gross area will be the same as the inner web $A_{sl,eff}$=13910mm^2.

$$\beta_{A,c} = \frac{9640}{13910} = 0,69 \tag{153}$$

Elastic critical stress for the outer web:

$$\sigma_{cr,sl} = \frac{\pi^2 * 210000 * 3,56 * 10^7}{13910 * 6000^2} = 147N/mm^2 \tag{154}$$

This elastic critical stress is obtained at the longitudinal stiffener in the compression zone. Equal premises give:

$$\sigma_{cr,c} = 147N/mm^2 * \frac{1700}{1100} = 227N/mm^2 \tag{155}$$

Column slenderness for the outer web:

$$\bar{\lambda_c} = \sqrt{0,69\frac{355}{227}} = 1,03 \tag{156}$$

Interpolation between plate and column buckling for the outer web the reduction of the thickness:

$$\rho_c = \xi(2 - \xi)(\rho - \chi_c) + \chi_c \tag{157}$$

This equation is only valid if the following equation is fulfilled:

$$\xi = \frac{\sigma_{cr,p}}{\sigma_{cr,c}} - 1, for : 0 \leq \xi \leq 1 \tag{158}$$

$$\xi = \frac{\sigma_{cr,p}}{\sigma_{cr,c}} - 1 = \frac{863,4}{227} = 2,80 \tag{159}$$

This will induce that plate like buckling prevails and the reduction of the thickness ρ_p must be calculated in accordance to:

$$\rho_p = 1,0, for : \bar{\lambda_p} \leq 0,673 \tag{160}$$

For the global check the plate slenderness $\bar{\lambda_p} = 0,42$ for the outer web. This will give no reduction of the thickness of the web and indicates that the longitudinal stiffeners will not take part in any buckling. Local buckling between stiffeners at subpanels will govern the design buckling capacity.

Reduction of compression flange capacity:

From EBPlate the elastic critical stress for smeared stiffeners $\sigma_{cr,p}$ is 480 N/mm^2 (see appendix F). This calculation is based on a uniformed compressed plate with breadth 1662 mm and length 6000mm. As you can see from figure 62 the compression flange also consist of two launching rails 50*150mm. Difference in thickness is not possible to model in EBPLate so their contribution is neglected. Their contribution would probably give a hive higher elastic critical load, but no available software is developed to analyze this in a reasonable time period. This will certainly be a conservative design approach as this will cause a higher grade of column buckling where post critical resistance is neglected.

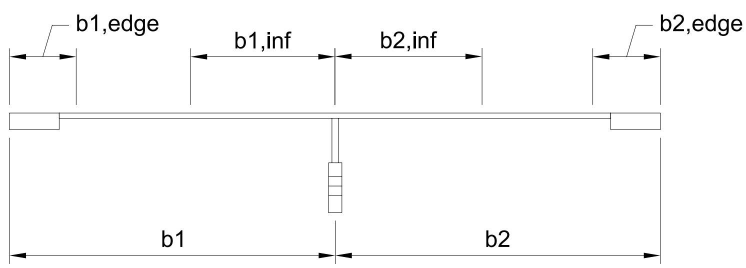

Figure 62: Compression flange

For local buckling of subpanels the elastic critical stress is calculated to:

$$\sigma_{cr,p} = k_\sigma \frac{\pi^2 E}{12(1-\nu^2)}(\frac{t}{b})^2 \tag{161}$$

For uniform compression the buckling factor k_σ=4.

$$\sigma_{cr,p} = 4\frac{\pi^2 * 210000}{12(1-0,3^2)}(\frac{16}{1962/2})^2 = 202N/mm^2 \tag{162}$$

This will give a plate slenderness:

$$\bar{\lambda_p} = \sqrt{\frac{f_y}{\sigma_{cr,p}}} = \sqrt{\frac{355}{202}} = 1,32 \tag{163}$$

For $\bar{\lambda_p} > 0,673$ the reduction factor for internal compression elements like the flange at a box girder the effective width will be determined:

$$\rho_{loc} = \frac{\bar{\lambda_p} - 0,055(3+\psi)}{(\bar{\lambda_p})^2} \tag{164}$$

$$\rho_{loc} = \frac{1,32 - 0,055(3+1)}{(1,32)^2} = 0,63 \tag{165}$$

Now we know how much of the subpanels that can be utilized in design. The effective width can be calculated from the formula:

$$b_{eff} = \rho_{loc} * b_c \tag{166}$$

This gives effective widths for the compression flange:

$$b_{1,eff} = 0,63 * 981 = 618mm \tag{167}$$

$$b_{2,eff} = 0,63 * 981 = 618mm \tag{168}$$

Finally we can calculate effective widths with the effect of longitudinal stiffeners:

Width	**Width for gross area**	**Effective area**
b$_1$, $edge$	$\frac{b_1}{2}$=490,5mm	$\frac{b_{1,eff}}{2}$=309mm
b$_1$, inf	$\frac{b_1}{2}$=490,5mm	$\frac{b_{1,eff}}{2}$=309mm
b$_2$, inf	$\frac{b_2}{2}$=490,5mm	$\frac{b_{2,eff}}{2}$=309mm
b$_2$, $edge$	$\frac{b_2}{2}$=490,5mm	$\frac{b_{2,eff}}{2}$=309mm

Table 8: Final effective width calculation flange

The next step is to check for interpolation between plate and column like buckling. For plate like buckling the plate slenderness is defined as:

$$\bar{\lambda_p} = \sqrt{\beta_{A,c} \frac{f_y}{\sigma_{cr,p}}} \tag{169}$$

The parameter $\beta_{A,c}$ will be determined in the following manner:

$$\beta_{A,c} = \frac{A_{c,eff,loc}}{A_c} \tag{170}$$

The effective areas and gross cross sections areas for the compression flange will be calculated to:

$$A_{c,eff,loc} = b_{1,inf,eff} t_f + b_{2,inf,eff} t_f + A_{sl,1} \tag{171}$$

$$A_{c,eff,loc} = 309 * 16 + 309 * 16 + 280 * 20 = 15488mm^2 \tag{172}$$

$$A_c = b_{1,inf} t_f + b_{2,inf} t_f + A_{sl,1} \tag{173}$$

$$A_c = 490,5 * 16 + 490,5 * 16 + 280 * 20 = 21296mm^2 \tag{174}$$

$$\beta_{A,c} = \frac{A_{c,eff,loc}}{A_c} = \frac{15488}{21296} = 0,73 \tag{175}$$

The plate slenderness is now:

$$\bar{\lambda_p} = \sqrt{0,73\frac{355}{480}} = 0,65 \tag{176}$$

The column slenderness will be calculated from:

$$\bar{\lambda_c} = \sqrt{\beta_{A,c}\frac{f_y}{\sigma_{cr,c}}} \tag{177}$$

The elastic critical stress for column buckling at the compression flange:

$$\sigma_{cr,sl} = \frac{\pi^2 E I_{sl,1}}{A_{sl,1}a^2} \tag{178}$$

For calculation of I_{sl} see appendix E.

The parameter $\beta_{A,c}$ will be determined in the following manner:

$$\beta_{A,c} = \frac{A_{sl,1,eff}}{A_{sl,1}} \tag{179}$$

$$A_{sl,1,eff} = A_{c,eff,loc} = 15488mm^2 \tag{180}$$

$$A_{sl,1} = A_c = 21296mm^2 \tag{181}$$

$$\beta_{A,c} = \frac{15488}{21296} = 0,73 \tag{182}$$

Elastic critical stress for the compression flange:

$$\sigma_{cr,c} = \frac{\pi^2 * 210000 * 1,27 * 10^8}{21296 * 6000^2} = 343N/mm^2 \tag{183}$$

Column slenderness for the compression flange:

$$\bar{\lambda_c} = \sqrt{0,73\frac{355}{343}} = 0,87 \tag{184}$$

Interpolation between plate and column buckling for the compression flange the reduction of the thickness shall be calculated in accordance to:

$$\rho_c = \xi(2-\xi)(\rho - \chi_c) + \chi_c \tag{185}$$

This equation is only valid if the following equation is fulfilled:

$$\xi = \frac{\sigma_{cr,p}}{\sigma_{cr,c}} - 1, for: 0 \leq \xi \leq 1 \tag{186}$$

$$\xi = \frac{\sigma_{cr,p}}{\sigma_{cr,c}} - 1 = \frac{480}{343} - 1 = 0,40 \tag{187}$$

This means that an interpolation between the buckling states must be executed. χ_c will be taken as $\rho = 0{,}63$. This is a conservative approach as the post critical reserve in the stiffened panel is neglected, while post critical resistance in subpanels remain active.

$$\rho_c = \chi_c = 0,63 \tag{188}$$

This will lead to reduced thickness of effective area localized at the compression flange.

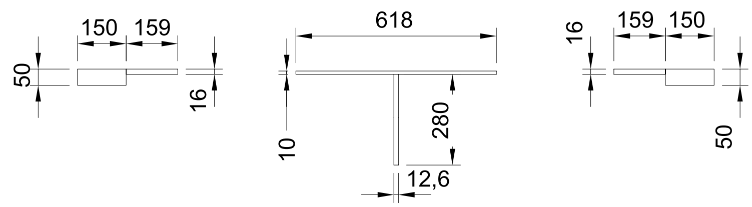

Figure 63: Effective area flange

Effective cross section resistance:

NS-EN 1993 1-5 states that the effective cross section based on the effective width should be able to withstand direct stresses from bending moment. Figure 64 illustrates the effective cross section of the main girder due to direct stresses at launching.

The maximum compressive stress in the main girder will then be:

$$\sigma_{max,Ed} = \frac{M_{Ed}}{W_{z,y=0}} = \frac{22564 * 10^6 Nmm}{1,37 * 10^8 mm^3} = 163,1 N/mm^2 \tag{189}$$

The moment utilization is then:

$$\eta_1 = \frac{\sigma_{max,Ed}}{f_y/\gamma_{m0}} = \frac{163,6}{355/1,05} = 0,48 \tag{190}$$

This result implies that direct stresses will not govern design resistance in the launching stage of the MSS. This particular result was expected as the main girder must withstand larger bending moments in a concreting stage. The additional contribution to is due to self weight of concrete that is casted to form a bridge deck.

Section name/ID:	Reduced cross section at Main Girder

i	b_i	h_i	z_i	y_i	
1	150	50	0	246	*
2	150	50	1812	246	*
3	159	16	150	280	*
4	14	248	68	296	*
5	10	193	1882	296	*
6	1800	24	82	3696	*
7	20	200	672	3496	*
8	20	200	1272	3496	*
9	200	16	82	3088	*
10	200	28	82	1988	*
11	200	16	82	888	*
12	200	16	1682	3088	*
13	200	28	1682	1988	*
14	200	16	1682	888	*
15	12,6	280	970,8	0	*
16	14	292	68	604	*
17	14	317	68	896	*
18	14	474	68	1522	*
19	14	1700	68	1996	*
20	10	227	1882	669	*
21	10	233	1882	869	*
22	10	349	1882	1647	*
23	10	1700	1882	1996	*
24	159	16	1653	280	*
25	618	10	707	280	*
26					
27					
28					
29					
30					

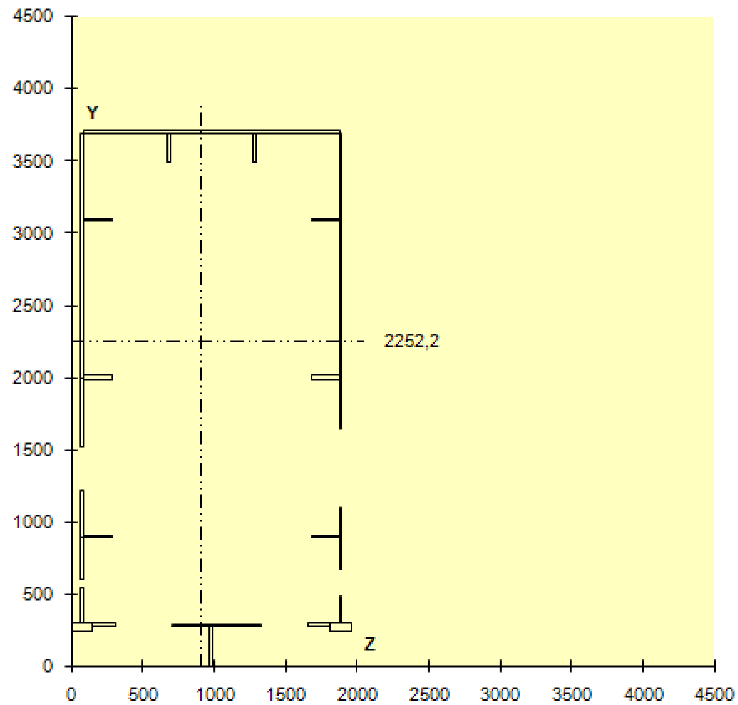

Section properties:

A =	174450	mm^2	I_z =	310,56E+09	mm^4
g =	1396	kg/m	I_y =	99,19E+09	mm^4
b =	1962	mm	$Wz_{(y=h)}$ =	211,58E+06	mm^3
h =	3720	mm	$Wz_{(y=0)}$ =	137,89E+06	mm^3
z_t =	902,5	mm	$Wy_{(z=o)}$ =	109,90E+06	mm^3
y_t =	2252,2	mm	$Wy_{(z=b)}$ =	93,62E+06	mm^3

Figure 64: Effective cross section main girder

6.2 Shear buckling

Input parameter	Definition	Value
a	Distance between rigid transverse stiffeners	6000mm
t_w	Thickness of the web	14mm
h_w	Height of the web	3400mm
t_f	Thickness of the flange	16mm
b_f	Breadth of the flanges	1800mm
f_{yw}	Yield strength web	$355N/mm^2$
f_{yf}	Yield strength flange	$355N/mm^2$
E	Young's modulus	$210000N/mm^2$
ν	Poisson's ratio	0,3
V_{Ed}	Design shear load	1381,5kN
γ_{m1}	Material factor	1,1

Table 9: Input data for calculation of shear loading

Shear buckling of the web panels with longitudinal stiffeners must be checked if the following criterion is fulfilled:

$$\frac{h_w}{t_w} \geq 31\frac{\epsilon}{\eta}\sqrt{k_\tau} \tag{191}$$

$$k_\tau = 5,34 + 4,00(\frac{h_w}{a})^2 + k_{\tau,sl} \tag{192}$$

$$k_{\tau,sl} = 9(\frac{h_w}{a})^2 + (\frac{I_{sl}}{t^3 h_w})^{3/4} > \frac{2,1}{t}(\frac{I_{sl}}{h_w})^{1/3} \tag{193}$$

For calculation of I_{sl} see appendix B.

$$k_{\tau,sl} = 9(\frac{3400}{6000})^2 + (\frac{1,14 * 10^8}{14^3 * 3400})^{3/4} > \frac{2,1}{14}(\frac{1,14 * 10^8}{3400})^{1/3} \tag{194}$$

$$k_{\tau,sl} = 9,42 > 4,83 \tag{195}$$

$$k_\tau = 5,34 + 4,00(\frac{3400}{6000})^2 + 9,42 = 16,04 \tag{196}$$

Check required if:

$$\frac{3400}{14} \geq 31\frac{0,81}{1,2}\sqrt{16,04} \tag{197}$$

$$242,85 \geq 83,80 \tag{198}$$

This would mean that a shear check is required for the inner web at the main girder. The design resistance will be calculated from:

$$V_{b,Rd} = V_{bw,Rd} + V_{bf,Rd} \leq h_w t_w \frac{\eta f_{yw}}{\sqrt{3}\gamma_{m1}} \tag{199}$$

$$V_{b,Rd} = V_{bw,Rd} + V_{bf,Rd} \leq 3400 * 14 \frac{1,2 * 355}{\sqrt{3} * 1,1} = 10642kN \tag{200}$$

Contribution from the web:

$$V_{bw,Rd} = \chi_w h_w t_w \frac{f_{yw}}{\sqrt{3}\gamma_{m1}} \tag{201}$$

The plate slenderness for shear buckling $\bar{\lambda_w}$ should be calculated for global shear buckling of the entire web panel with the effect of longitudinal stiffeners and local shear buckling of subpanels. Plate slenderness for shear buckling is defined as:

$$\bar{\lambda_w} = max(\frac{h_w}{37,4 t_w \epsilon \sqrt{k_\tau}}; \frac{h_{wi}}{37,4 t_w \epsilon \sqrt{k_{\tau i}}}) \tag{202}$$

Global shear calculation:

$$\bar{\lambda_w} = \frac{3400}{37,4 * 14 * 0,81 * \sqrt{16,04}} = 2,00 \tag{203}$$

Local shear calculation means a shear check of the subpanels between longitudinal stiffeners. The shear buckling factor is now calculated to:

$$k_\tau = 5,34 + (\frac{1100}{6000})^2 = 5,47 \tag{204}$$

$$\bar{\lambda_w} = \frac{1100}{37,4 * 14 * 0,81 * \sqrt{5,47}} = 1,10 \tag{205}$$

This would lead to that a global shear phenomenon is the most critical. The reduction factor for an intermediate transverse stiffener is now calculated to:

$$\chi_w = 1,37/(0,7 + \bar{\lambda_w}) = 1,37/(0,7 + 2) = 0,51 \tag{206}$$

Final contribution from the web:

$$V_{bw,Rd} = 0,51 * 3400 * 14 * \frac{355}{\sqrt{3} * 1,1} = 4523kN \tag{207}$$

The shear resistance from flanges are given as:

$$V_{bf,Rd} = \frac{b_f t_f^2}{c} * \frac{f_{yf}}{\gamma_{m1}} (1 - (\frac{M_{Ed}}{M_{f,Rd}})^2) \tag{208}$$

The distance c between the two plastic hinges in the flange is defined as:

$$c = a(0,25 + \frac{1,6 b_f t_f^2 f_{yf}}{t_w h_w^2 f_{yw}}) \tag{209}$$

$$c = 6000(0,25 + \frac{1,6 * 1800 * 16^2 * 355}{14 * 3400^2 * 355}) = 1527mm \tag{210}$$

The moment resistance from the flanges are determined in the following manner:

$$M_{f,Rd} = \frac{M_{R,k}}{\gamma_{m0}} = min(A_{f,1}f_{yf,1}h_f; A_{f,2}f_{yf}h_f)/\gamma_{m0} \tag{211}$$

The flange with the smallest cross sectional effective area to withstand direct stresses is the compressive flange. This flange has an effective area calculated in chapter 6.1 and has a size equal to:

$$A_{f,1} = 2 * 150 * 50 + 2 * 159 * 16 + 608 * 10 + 12,6 * 280 = 29696mm^2 \tag{212}$$

The inner moment arm:

$$h_f = h_w + t_{f,1}/2 + t_{f,2}/2 = 3400 + 16/2 + 24/2 = 3420mm \tag{213}$$

This will give a moment resistance equal as the following:

$$M_{f,Rd} = \frac{M_{R,k}}{\gamma_{m0}} = (29696 * 355 * 3420)/1,05 = 36050kNm \tag{214}$$

The shear resistance from flanges will be determined as:

$$V_{bf,Rd} = \frac{1800 * 16^2}{1527} * \frac{355}{1,1}(1 - (\frac{22564}{36050})^2) = 36,1kN \tag{215}$$

Total shear resistance main girder:

$$V_{b,Rd} = V_{bw,Rd} + V_{bf,Rd} = 4523kN + 36,1kN = 4559,1kN \tag{216}$$

This will give a shear utilization:

$$\eta_3 = \frac{V_{Ed}}{V_{b,Rd}} = 1381,5/4559,1 = 0,30 \tag{217}$$

As you can see shear forces at the web will not either govern ULS capacity at launching. At the concreting stage the main girder will experience larger shear forces due to self weight of concrete.

6.3 Patch loading

To calculate the main girders capacity at present configuration I‘ve used formulas from L.Davaine (2004). Input parameters in the calculation are the following:

Input parameter	Definition	Value
a	Distance between rigid transverse stiffeners	6000mm
t_w	Thickness of the web	14mm
h_w	Height of the web	3400mm
t_f	Thickness of the flange(launching rail)	50mm
s_s	Loaded length	1300mm
b_1	Distance between flange and first longitudinal stiffener	600mm
f_{yw}	Yield strength web	355N/mm^2
f_{yf}	Yield strength flange	355N/mm^2
E	Young's modulus	210000N/mm^2
ν	Poisson's ratio	0,3
F_{Ed}	Design patch load	2763kN
γ_{m1}	Material factor	1,1

Table 10: Input data for calculation of patch loading

The elastic patch load F_{cr} will be calculated from:

$$F_{cr} = \frac{F_{cr,1}F_{cr,2}}{F_{cr,1} + F_{cr,2}} \tag{218}$$

Where:

$$F_{cr,1} = 0,9k_{F,1}E\frac{t_w^3}{h_w} \tag{219}$$

$$k_{F,1} = 6 + 2(\frac{h_w}{a})^2 + [5,44\frac{b_1}{a} - 0,21]\sqrt{\gamma_s} \tag{220}$$

$$\gamma_s = 10,9\frac{I_{sl,1}}{h_w t_w^3} \leq 13(\frac{a}{h_w})^3 + 210(0,3 - \frac{b_1}{a}) \tag{221}$$

$I_{sl,1}$ is the second moment of area of the longitudinal stiffener closest to the loaded flange including contributing parts of the web ($15\epsilon t_w$) for out of plane bending. For the calculation of this parameter see appendix A.

$$\gamma_s = 10,9\frac{3,22*10^7}{3400*14^3} \leq 13(\frac{6000}{3400})^3 + 210(0,3 - \frac{600}{6000}) \tag{222}$$

$$\gamma_s = 10,9\frac{I_{sl,1}}{h_w t_w^3} \leq 13(\frac{a}{h_w})^3 + 210(0,3 - \frac{b_1}{a}) \tag{223}$$

$$\gamma_s = 37,6 \leq 113 \tag{224}$$

$$k_{F,1} = 6 + 2(\frac{3400}{6000})^2 + [5,44\frac{600}{6000} - 0,21]\sqrt{37,6} = 8,66 \tag{225}$$

$$F_{cr,1} = 0,9*8,66*210000*\frac{14^3}{3400} = 1320kN \tag{226}$$

And:

$$F_{cr,2} = k_{F,2}\frac{\pi^2 E}{12(1-\nu^2})(\frac{t_w^3}{b_1}) \quad (227)$$

$$k_{F,2} = (0,8\frac{s_s+2t_f}{a}+0,6)(\frac{a}{b_1})^{0,6(\frac{s_s+2t_f}{a})+0,5} \quad (228)$$

$$k_{F,2} = (0,8\frac{1300+1,6*50}{6000})(\frac{6000}{600})^{0,6(\frac{1300+2*50}{6000})+0,5} = 3,43 \quad (229)$$

$$F_{cr,2} = 3,43\frac{\pi^2 * 210000}{12(1-0,3^2)}(\frac{14^3}{600}) = 2977kN \quad (230)$$

Finally the elastic patch load can be determined:

$$F_{cr} = \frac{1320 * 2977}{1320+2977} = 914kN \quad (231)$$

Then the yield load F_y for patch loading must be determined:

$$F_y = l_y t_w f_{yw} \quad (232)$$

While the effective loaded length l$_y$ for load application through one flange is determined by:

$$l_y = s_s + 2t_f(1+\sqrt{m_1}) \leq a \quad (233)$$

$$m_1 = \frac{f_{yf}b_f}{f_{yw}t_w} \quad (234)$$

$$m_1 = \frac{355*150}{355*14} = 10,7 \quad (235)$$

$$l_y = 1300 + 2*50(1+\sqrt{10,7}) = 1727mm \leq 6000mm \quad (236)$$

$$F_y = 1727*14*355 = 8583kN \quad (237)$$

The patch slenderness is the calculated to:

$$\bar{\lambda_F} = \sqrt{F_y/F_{cr}} = \sqrt{8583/913} = 3,064 \quad (238)$$

The reduction factor χ_F will now be calculated with this formula:

$$\chi_F = \frac{1}{\phi_F + \sqrt{\phi_F^2 + \bar{\lambda_F}}} \leq 1,2 \quad (239)$$

Where:

$$\phi_F = 0,5(1+0,21(\bar{\lambda_F}-0,8)+\bar{\lambda_F}) \quad (240)$$

$$\phi_F = 0,5(1 + 0,21(3,064 - 0,8) + 3,064) = 2,269 \tag{241}$$

$$\chi_F = \frac{1}{2,269 + \sqrt{2,269^2 + 2,414}} = 0,199 \leq 1,2 \tag{242}$$

The ultimate resistance against patch loading is therefore:

$$F_{R,d} = \chi_F * \frac{F_y}{\gamma_{m1}} = 0,199 \frac{8583kN}{1,1} = 1560kN \tag{243}$$

With the new proposed design code from Mattias Clarin (2007) the elastic buckling load has to be taken as:

$$F_{cr} = F_{cr,1} = 1320kN \tag{244}$$

This will induce patch slenderness:

$$\bar{\lambda_F} = \sqrt{F_y/F_{cr}} = \sqrt{8583/1320} = 2,549 \tag{245}$$

The reduction factor will be determined to:

$$\phi_F = 0,5(1 + 0,21(2,549 - 0,8) + 2,549) = 1,985 \tag{246}$$

$$\chi_F = \frac{1}{1,985 + \sqrt{1,985^2 + 2,549}} = 0,222 \leq 1,2 \tag{247}$$

The ultimate resistance against patch loading:

$$F_{R,d} = \chi_F * \frac{F_y}{\gamma_{m1}} = 0,222 \frac{8583kN}{1,1} = 1732kN \tag{248}$$

This will give a utilization of patch loading equal to:

$$\eta_2 = \frac{F_{Ed}}{F_{R,d}} = \frac{2763}{1732} = 1,59 \tag{249}$$

Obviously design resistance of patch loading will give too small resistance. The main reason for this is the effect of the transversal stiffeners c/c 750mm. They will most definitely prevent local failure modes at the web area located near the compression flange. Their effect is vital for the configuration of the main girder and can not be neglected. As analysis in ANSYS suggest they will spread the patch load at a larger area at the subpanel. Bearing this in mind it is safe to conclude that this calculation method must be discarded when analyzing the main girder capacity.

6.4 Interactions

Bending moment and shear force in a web panel:

As stated before the main girder will experience larger values of direct stresses and shear forces at a concreting stage. Bearing this in mind it is expected that this interaction will not need to be executed. The web alone will able to withstand all the shear and an interaction will not be necessary if the following criterion is fulfilled:

$$\eta_3 = \frac{V_{Ed}}{V_{bw,Rd}} \leq 0,5 \tag{250}$$

Result from chapter 6.2 shows that $V_{bw,Rd}$= 4523 kN and the criterion will therefore be fulfilled:

$$\eta_3 = \frac{1381}{4523} = 0,31 \leq 0,5 \tag{251}$$

The flanges alone will as well be able to resist the hogging moment because:

$$M_{Ed} \leq M_{f,Rd} \tag{252}$$

$$22564kNm \leq 36050kNm \tag{253}$$

The moment resistance of the flanges is calculated in chapter 6.2 By this calculations it is shown that this interaction will not be necessary to perform.

Bending moment and patch loading:

In order to evaluate if the main girder‘s web will have an ULS capacity that satisfies design in NS-EN 1993 1-5 requirements based on interaction of forces must be performed. This interaction should be neglected if the patch load resistance is obtained by design formula in NS-EN 1993 1-5 due to shortcomings of method. However it can be of interest to use results from the ANSYS analysis. As all the test data on patch loading in Eurocode 3 are based on cross sections that are subjected to bending moments less than 0,4 times the bending resistance the ULS capacity found in the nonlinear analysis could have been used in this interaction. Unfortunately this is however not the case for the ANSYS analysis. Chapter 6.1 states that bending utilization η_1 is 0,48 of the main girder at launching. When you have this low utilization of direct stresses an interaction is not necessary to perform. With these comments it is safe to conclude that the bending moment and patch loading interaction will not need to be executed because the design resistance against patch loading alone will govern design.

7 Conclusions

As this master thesis' main objective was to determine the ULS capacity against buckling at the main girder's web ANSYS analysis were executed. These analysis had a configuration in accordance to given guidelines in NS-EN 1993 1-5. Boundary conditions and loading at the web were thoroughly investigated and should be sufficiently documented in the this thesis. Nonlinear analysis were executed based on engineering assumptions on how to simulate a stress pattern equal to the true stress pattern. Biaxial loading at a plate element with multiple stiffeners arrangement will experience a complex state of stress. Eurocode 3 will have a satisfactory calculation method to deal with the direct stresses from the bending moment so this effect will not be as interesting as the support reaction from the launching wagon. From the original arrangement at the reference project the design resistance obtained by ANSYS analysis is found to be:

$$F_{Rd} = \frac{F_{Rk}}{\gamma_{m1}} = \frac{4267,8kN}{1,1} = 3879kN \tag{254}$$

Imperfections were based on a critical mode that display instability at a local subpanel. This result must be discussed as it is very important for the resistance against buckling. Results obtained from calculations made in accordance to the reduced cross section method indicates that only a local buckling phenomenon is associated with instability caused by the direct stresses at the inner web. No reduction of the cross section is needed to account for global buckling. This indicates that the longitudinal stiffeners localized in the compression zone will have enough bending stiffness which mean that they will not buckle with the plate panel. This is an important feature in the design as there is no need to change their dimensions because a longitudinal stiffener will be optimized when they prevent global buckling. An increase of their bending stiffness will of course give a higher buckling capacity due to increased torsional rigidity of the stiffener, but to use this in a design process is not beneficial due to increased weight of structure and cost of steel. If capacity should be increased more longitudinal stiffeners may be used, transverse stiffeners may be implemented or even an increase of the plate thickness. The longitudinal stiffeners are as well checked for torsional buckling and this will not interfere with the capacity.

The other effect is of course how the support reaction will effect the stress pattern in the panel. In a launching stage this is the dominant loading and their effect must be carefully interpreted. What is evident is that the transverse stiffener c/c 750mm will provide the plate panel with an increased resistance against patch loading. No local failure mode is initialized and the stiffeners sucessfully transfer the load to the critical subpanel. Calculations in accordance to methods described in Eurocode 3 will not take this effect into account and must be discarded in design. Their effect will as well contribute to rotational stiffness and the support reaction is modelled fixed in ANSYS. This is however not completely correct as some rotation may occur, but in combination that there are some rotational stiffness at the upper flange which is modelled as simply supported, this is viewed as conservative design at Strukturas.

As the results from the ANSYS analysis indicates there are capacity present at this panel against instability. The utilization against patch loading will be:

$$\eta_2 = \frac{2763}{3879} = 0,71 \tag{255}$$

This indicates sufficient resistance at this project. An alternative arrangement is as well analyzed so this result can be used in other MSS-projects which endure larger support reactions. This transverse is a rigid intermediate stiffener loaded in shear. With nonlinear analysis in ANSYS the collapse load is determined to be:

$$F_{Rd} = \frac{F_{Rk}}{\gamma_{m1}} = \frac{6451,3kN}{1,1} = 5832kN \tag{256}$$

Clearly a higher capacity is associated with this stiffening arrangement due to the additional stiffness added. The reason for this is that the stiffener would provide a restraint at the panel. Eurocode 3 states that panels may be analyzed as separate panels if the stiffener is defined as rigid. This will mean that a smaller buckling length is associated with the critical mode which of course relates to higher resistance.

A Appendix A: Calculation of $I_{sl,1}/I_{st}$

Section name/ID:	I,sl/Ist

i	b_i	h_i	z_i	y_i	
1	340,2	14	0	0	*
2	16	200	163,1	14	*
3					
4					
5					
6					
7					
8					
9					
10					
11					
12					
13					
14					
15					
16					
17					
18					
19					
20					
21					
22					
23					
24					
25					
26					
27					
28					
29					
30					

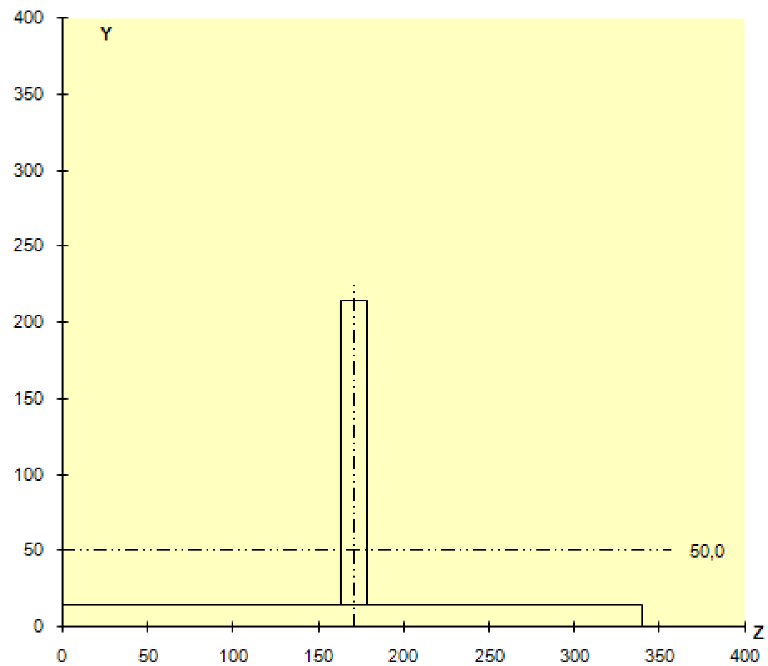

Section properties:

A =	7963	mm^2	I_z =	32,66E+06	mm^4
g =	64	kg/m	I_y =	46,01E+06	mm^4
b =	340	mm	$Wz_{(y=h)}$ =	199,13E+03	mm^3
h =	214	mm	$Wz_{(y=0)}$ =	653,16E+03	mm^3
z_t =	170,5	mm	$Wy_{(z=o)}$ =	269,83E+03	mm^3
y_t =	50,0	mm	$Wy_{(z=b)}$ =	271,10E+03	mm^3

Figure 65: $I_{sl,1}/I_{st}$: Stiffener 16×200mm + contributing plating inner web

B Appendix B: Calculation of I_{sl}

Section name/ID:	I,sl

i	b_i	h_i	z_i	y_i	
1	340,2	14	0	0	*
2	16	200	163,1	14	*
3	340,2	14	360		*
4	28	200	513,1	14	*
5	340,2	14	720		*
6	16	200	883,1	14	*
7					
8					
9					
10					
11					
12					
13					
14					
15					
16					
17					
18					
19					
20					
21					
22					
23					
24					
25					
26					
27					
28					
29					
30					

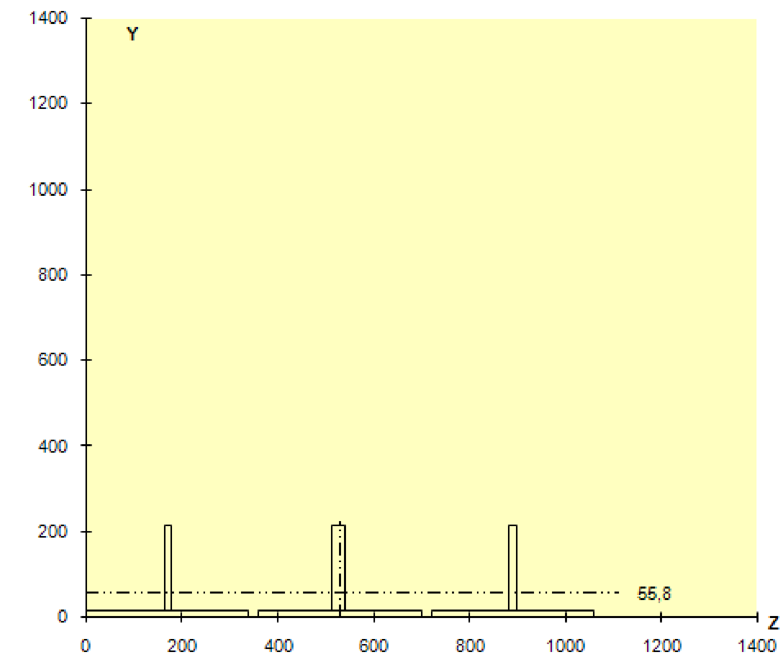

Section properties:

A =	26288	mm^2	I_z =	114,91E+06	mm^4
g =	210	kg/m	I_y =	2,20E+09	mm^4
b =	1060	mm	$Wz_{(y=h)}$ =	726,54E+03	mm^3
h =	214	mm	$Wz_{(y=0)}$ =	2,06E+06	mm^3
z_t =	529,7	mm	$Wy_{(z=o)}$ =	4,16E+06	mm^3
y_t =	55,8	mm	$Wy_{(z=b)}$ =	4,15E+06	mm^3

Figure 66: I_{sl}: All longitudinal stiffeners contribution shear buckling

C Appendix C: I_{sl}: Column buckling inner web

Section name/ID:	I,sl

i	b_i	h_i	z_i	y_i	
1	765	14	0	0	*
2	16	200	374,5	14	*
3					
4					
5					
6					
7					
8					
9					
10					
11					
12					
13					
14					
15					
16					
17					
18					
19					
20					
21					
22					
23					
24					
25					
26					
27					
28					
29					
30					

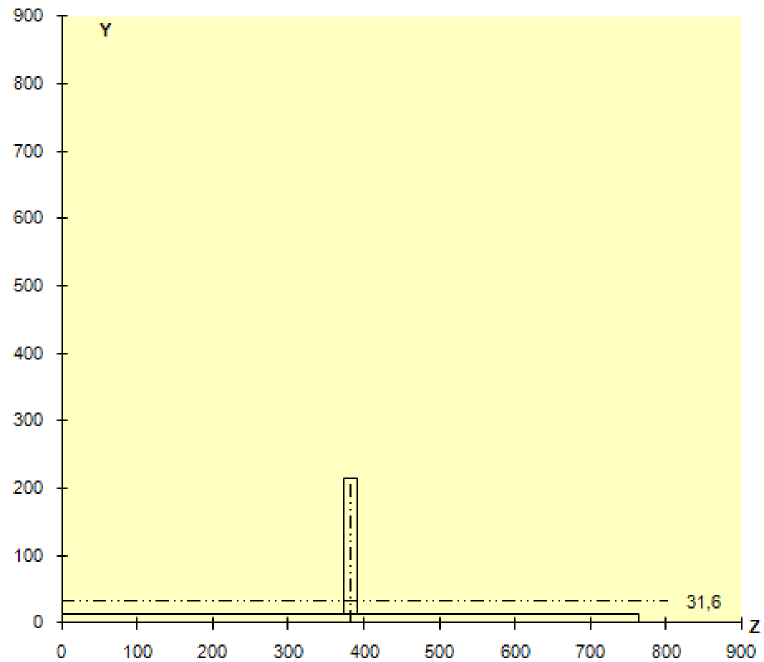

Section properties:

A =	13910	mm^2	I_z =	39,05E+06	mm^4
g =	111	kg/m	I_y =	522,38E+06	mm^4
b =	765	mm	$Wz_{(y=h)}$ =	214,11E+03	mm^3
h =	214	mm	$Wz_{(y=0)}$ =	1,24E+06	mm^3
z_t =	382,5	mm	$Wy_{(z=o)}$ =	1,37E+06	mm^3
y_t =	31,6	mm	$Wy_{(z=b)}$ =	1,37E+06	mm^3

Figure 67: I_{sl} at column buckling inner web

D Appendix D: I_{sl}: Column buckling outer web

Section name/ID:	I,sl

i	b_i	h_i	z_i	y_i	
1	765	10	0	0	*
2	16	200	374,5	10	*
3					
4					
5					
6					
7					
8					
9					
10					
11					
12					
13					
14					
15					
16					
17					
18					
19					
20					
21					
22					
23					
24					
25					
26					
27					
28					
29					
30					

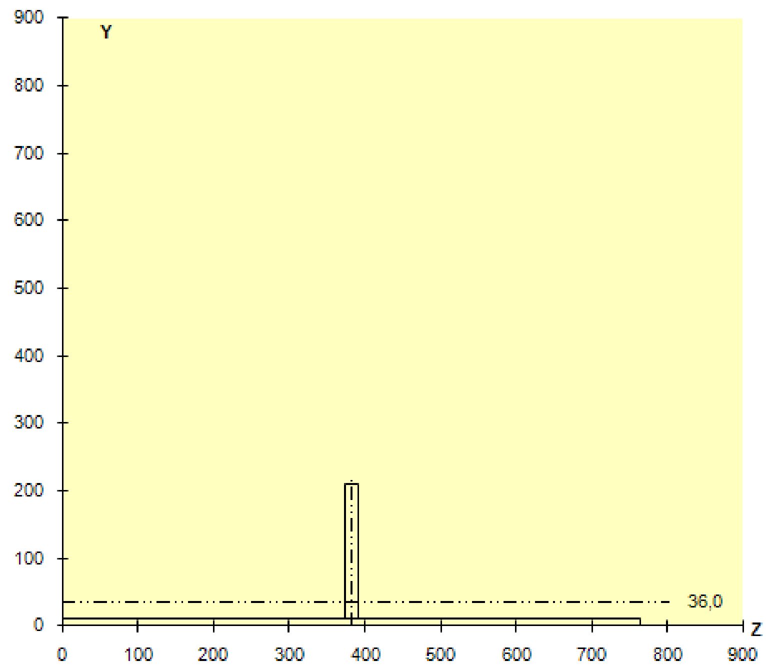

Section properties:

A =	10850	mm^2	I_z =	35,61E+06	mm^4
g =	87	kg/m	I_y =	373,15E+06	mm^4
b =	765	mm	$Wz_{(y=h)}$ =	204,59E+03	mm^3
h =	210	mm	$Wz_{(y=0)}$ =	989,92E+03	mm^3
z_t =	382,5	mm	$Wy_{(z=o)}$ =	975,55E+03	mm^3
y_t =	36,0	mm	$Wy_{(z=b)}$ =	975,55E+03	mm^3

Figure 68: I_{sl} at column buckling buckling outer web

E Appendix E: I_{sl}: Column buckling compression flange

Section name/ID:	I,sl

i	b_i	h_i	z_i	y_i	
1	981	16	0	0	*
2	20	280	480,5	16	*
3					
4					
5					
6					
7					
8					
9					
10					
11					
12					
13					
14					
15					
16					
17					
18					
19					
20					
21					
22					
23					
24					
25					
26					
27					
28					
29					
30					

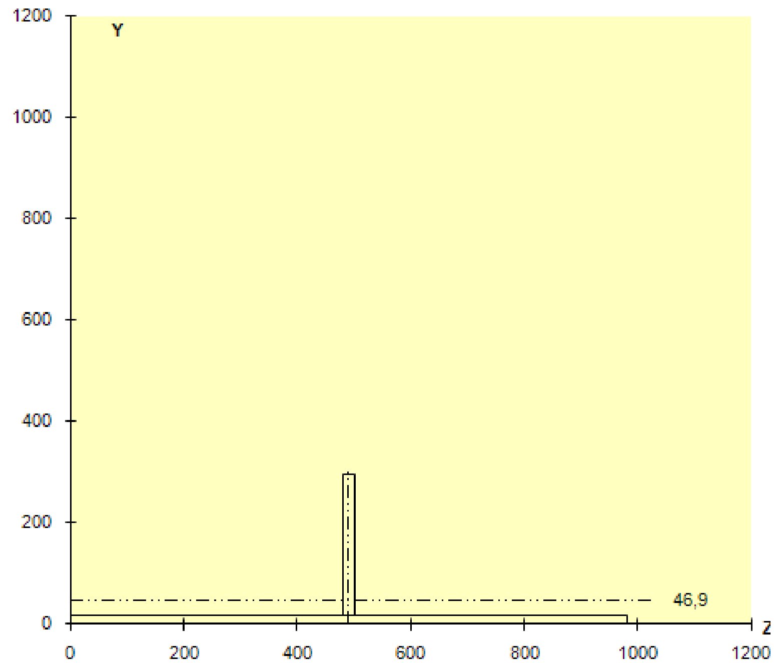

Section properties:

A =	21296	mm^2	I_z =	127,33E+06	mm^4
g =	170	kg/m	I_y =	1,26E+09	mm^4
b =	981	mm	$Wz_{(y=h)}$ =	511,19E+03	mm^3
h =	296	mm	$Wz_{(y=0)}$ =	2,71E+06	mm^3
z_t =	490,5	mm	$Wy_{(z=o)}$ =	2,57E+06	mm^3
y_t =	46,9	mm	$Wy_{(z=b)}$ =	2,57E+06	mm^3

Figure 69: I_{sl} at column buckling compression flange

F Appendix F: Input EBPlate

Appendix illustrates calculation sheet from EBPlate v 2.01. These calculations have in order to obtain the critical elastic stress with the effect of smeared stiffener for plate like buckling. The following pdf pages is related to structural element:

Inner web: page 89-96

Outer web: page 97-104

Compression flange: page 105-112

cticm

EBPlate

(v2.01)

Elastic Buckling of Plates

CALCULATION SHEET

Firm : Strukturas
Username : ThomasML
Contract : Master thesis
Contract item :
Note : Inner web
Date : 09.05.2011

PLATE'S CHARACTERISTICS

Dimensions :

Width	a	= 6.00 m
Height	b	= 3.40 m
Thickness	t	= 14.0 mm

Material characteristics :

Young's Modulus	= 210000. MPa
Poisson's Ratio	= 0.30

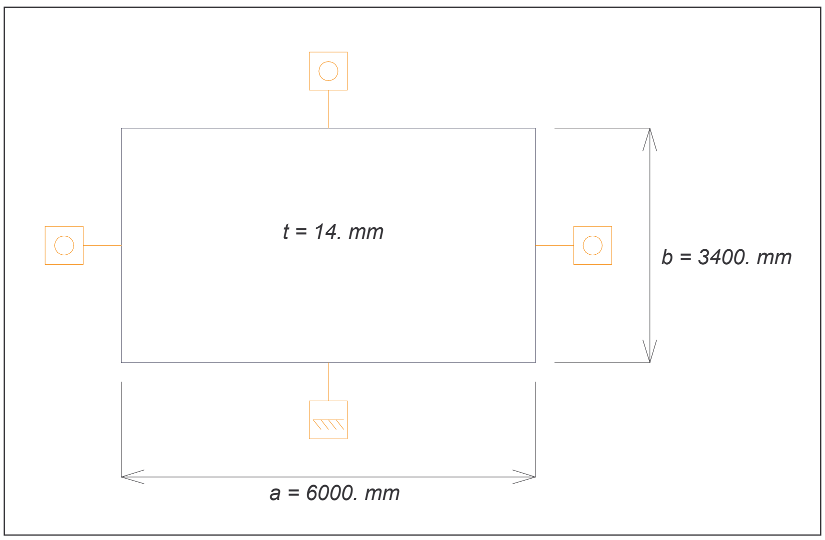

Figure 1 : Plate's dimensions and boundaries conditions

Boundaries conditions :

Side	Free	Clamped	Elastic restraints
Top	X		
Left	X		
Bottom		X	
Right	X		

STIFFENING CONDITIONS

Isotropy / Orthotropy :

The plate is isotropic.

Reference flexural plate rigidity : *D = 52769.23 N.m*

Stiffeners :

The plate is stiffened by 3 stiffeners.

			Parameters				*Dimensions*			
I	*O*	*XY (cm)*	δ	γ	θ	*Type*	*d1 (mm)*	*d2 (mm)*	*d3 (mm)*	*d4 (mm)*
1	H	x = 60.0	0.06723	36.76	0.1229	T 5	200.	16.		
2	H	x = 170.0	0.1176	54.58	0.6588	T 5	200.	28.		
3	H	x = 280.0	0.06723	36.76	0.1229	T 5	200.	16.		

I : Indice
O : Orientation
XY : Location
H : Horizontal
V : Vertical
T 1 : General Shape
T 2 : Angle
T 3 : Tee
T 4 : Trapezoidal section
T 5 : Single sided flat bar
T 6 : Double sided flat bar

Note :
The flexural inertia of the predefined type stiffeners is calculated taking into account an effective width of the plate. This width is equal to 10 times the thickness of the plate on each side of the connections of the stiffener.

I	L_W *(mm)*	z_W *(mm)*
1	296.0	46.6
2	308.0	60.5
3	296.0	46.6

L_W : Total width of the plate taken into account for the calculation of the flexural rigidity
z_W : Location of the neutral axis about the medium line of the plate

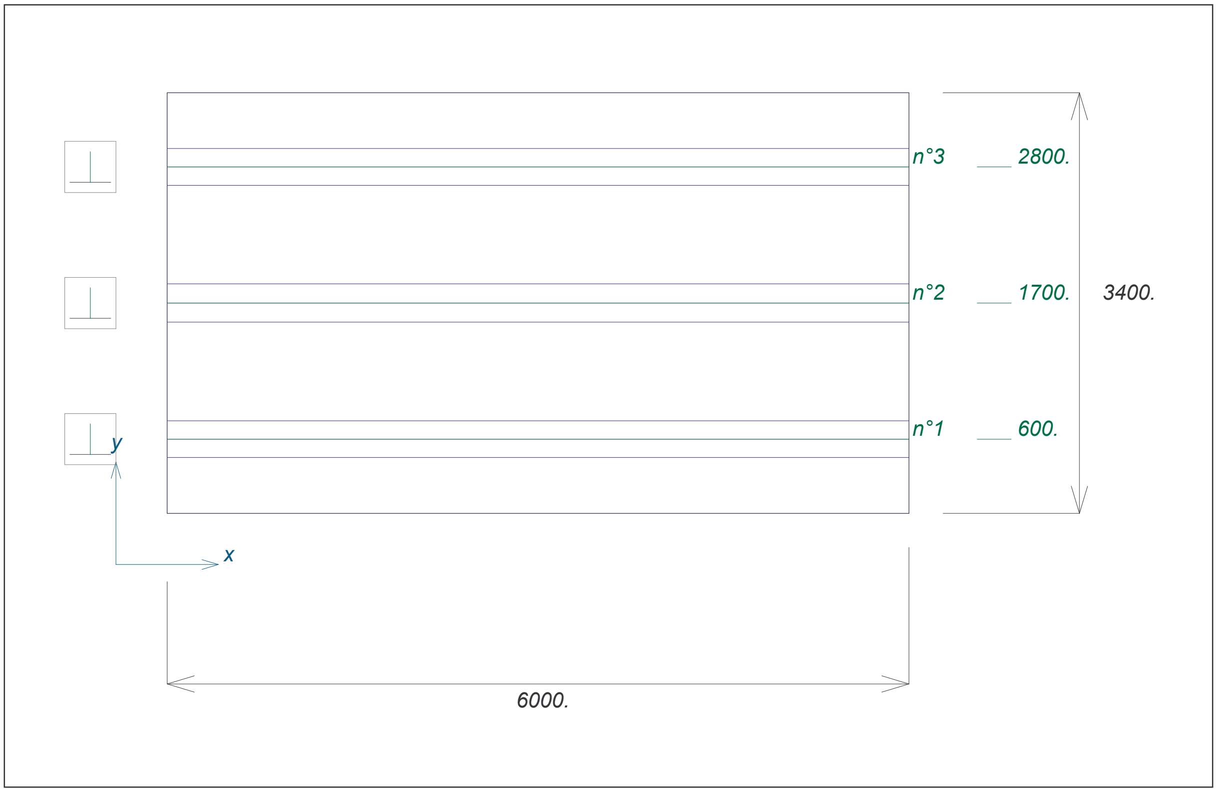

Figure 2 : Stiffeners

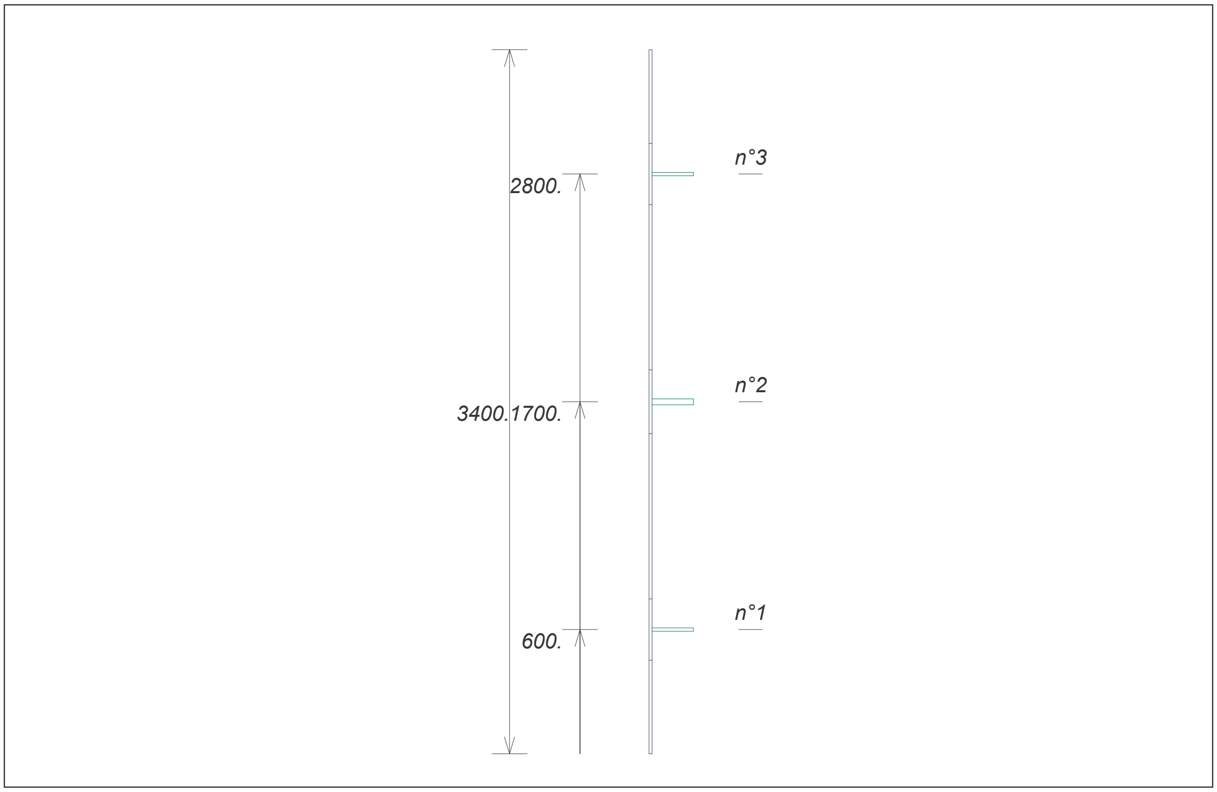

Figure 3 : Plate section with longitudinal stiffeners

STRESSES

Analytical stresses :

Analytical stresses will be calculated from this data.

Longitudinal stresses :

σ_{xt} = -99.9 MPa
σ_{xb} = 102.0 MPa

Transversal stresses :

σ_{yut} = 0.0 MPa
σ_{yub} = 0.0 MPa

Patch Loading stresses :

σ_{ypt} = 0.0 MPa c_t = 0.0 mm
σ_{ypb} = 0.0 MPa c_b = 0.0 mm

Local longitudinal stresses due to patch loading are not taken into account.
Local shear stresses due to patch loading are taken into account.

Shear stress :

τ = 0.0 MPa

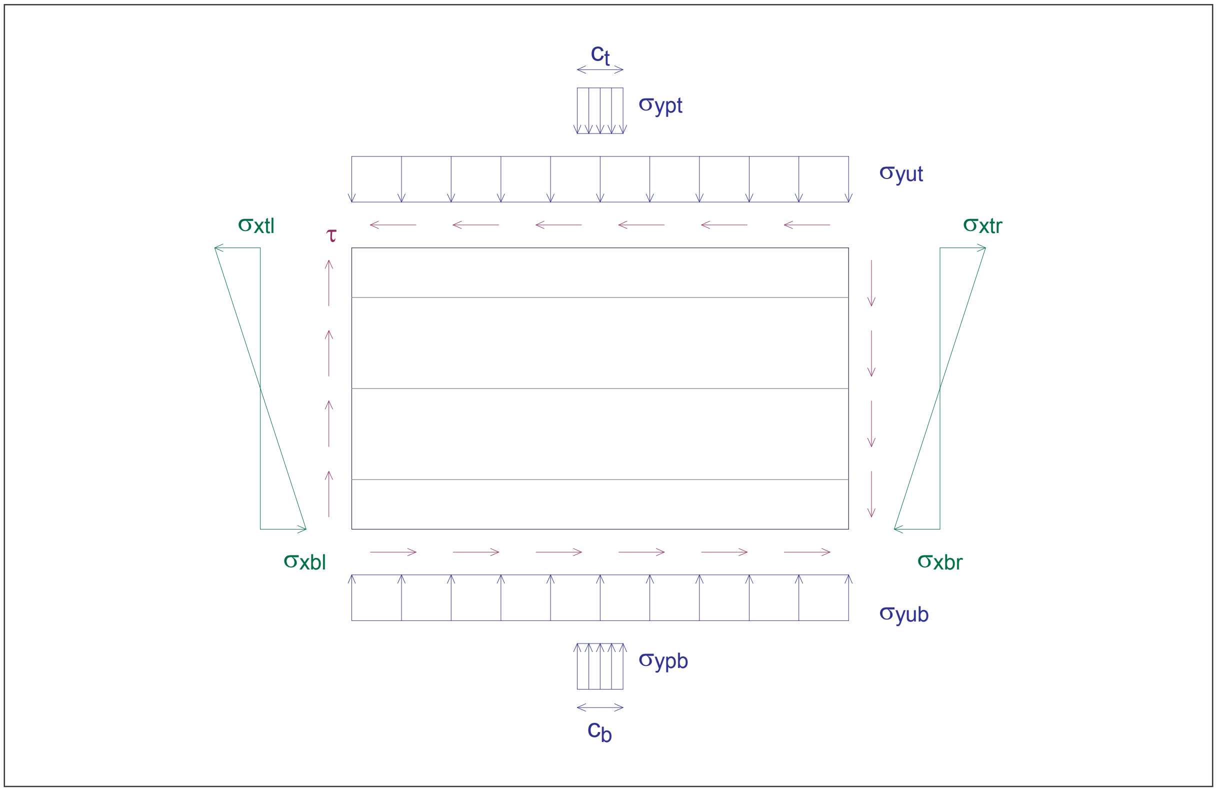

Figure 4 : Analytical stresses

Longitudinal stresses in the plate, defined by user (meshed stresses) :

No stresses defined in the plate.

Transverse stresses in the plate, defined by user (meshed stresses) :

No stresses defined in the plate.

Shear stresses in the plate, defined by user (meshed stresses) :

No stresses defined in the plate.

RESULTS

Calculation options :

Matrices dimensions :

Level of complexity : 1 (Low complexity case)
Matrices dimensions : 15 x 8

Number of modes :

Desired modes : First buckling mode
Number of calculated modes : 1

Plate behaviour :

Calculation of the global buckling mode, buckling of all subpanels being prevented

Results :

Reference stress :

σ_E = 3.22 MPa

Critical multiplier of the first buckling mode :

$\Phi_{cr,p}$ = 12.374

Critical stresses and buckling coefficients of the first buckling mode :

Longitudinal stresses :

$\sigma_{xtl.cr}$ = -1236.19 MPa k_{xtl} = -384.141

$\sigma_{xbl.cr}$ = 1262.18 MPa k_{xbl} = 392.216

$\sigma_{xtr.cr}$ = -1236.19 MPa k_{xtr} = -384.141

$\sigma_{xbr.cr}$ = 1262.18 MPa k_{xbr} = 392.216

cticm

EBPlate

(v2.01)

Elastic Buckling of Plates

CALCULATION SHEET

Firm : Strukturas
Username : ThomasML
Contract : Master thesis
Contract item :
Note : Outer web
Date : 09.05.2011

PLATE'S CHARACTERISTICS

Dimensions :

Width	*a*	*= 6.00 m*
Height	*b*	*= 3.40 m*
Thickness	*t*	*= 10.0 mm*

Material characteristics :

Young's Modulus	*= 210000. MPa*
Poisson's Ratio	*= 0.30*

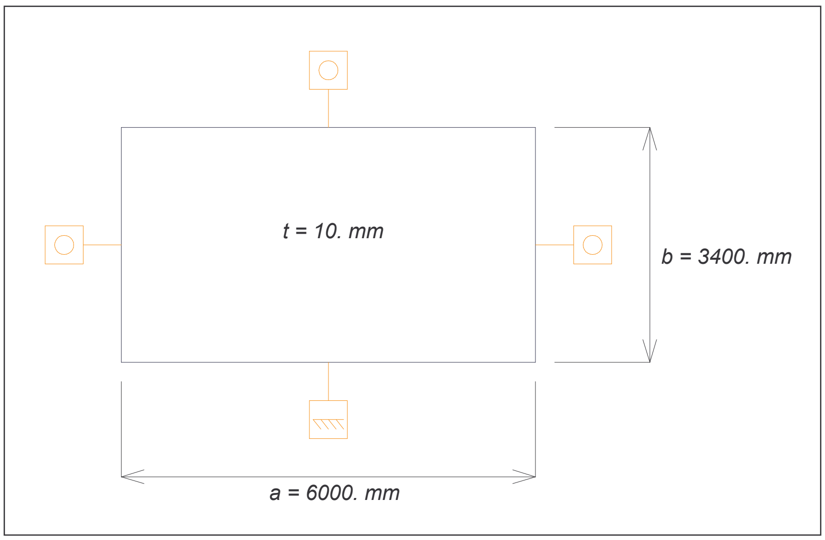

Figure 1 : Plate's dimensions and boundaries conditions

Boundaries conditions :

Side	Free	Clamped	Elastic restraints
Top	X		
Left	X		
Bottom		X	
Right	X		

STIFFENING CONDITIONS

Isotropy / Orthotropy :

The plate is isotropic.

Reference flexural plate rigidity : *D = 19230.77 N.m*

Stiffeners :

The plate is stiffened by 3 stiffeners.

			Parameters				*Dimensions*			
I	*O*	*XY (cm)*	δ	γ	θ	*Type*	*d1 (mm)*	*d2 (mm)*	*d3 (mm)*	*d4 (mm)*
1	H	x = 60.0	0.09412	79.98	0.3373	T 5	200.	16.		
2	H	x = 170.0	0.1176	93.14	0.6588	T 5	200.	20.		
3	H	x = 280.0	0.09412	79.98	0.3373	T 5	200.	16.		

I :	Indice	O :	Orientation	XY :	Location
H :	Horizontal	V :	Vertical		
T 1 :	General Shape	T 2 :	Angle	T 3 :	Tee
T 4 :	Trapezoidal section	T 5 :	Single sided flat bar	T 6 :	Double sided flat bar

Note :
The flexural inertia of the predefined type stiffeners is calculated taking into account an effective width of the plate. This width is equal to 10 times the thickness of the plate on each side of the connections of the stiffener.

I	L_W *(mm)*	z_W *(mm)*
1	216.0	62.7
2	220.0	67.7
3	216.0	62.7

L_W : Total width of the plate taken into account for the calculation of the flexural rigidity
z_W : Location of the neutral axis about the medium line of the plate

Figure 2 : Stiffeners

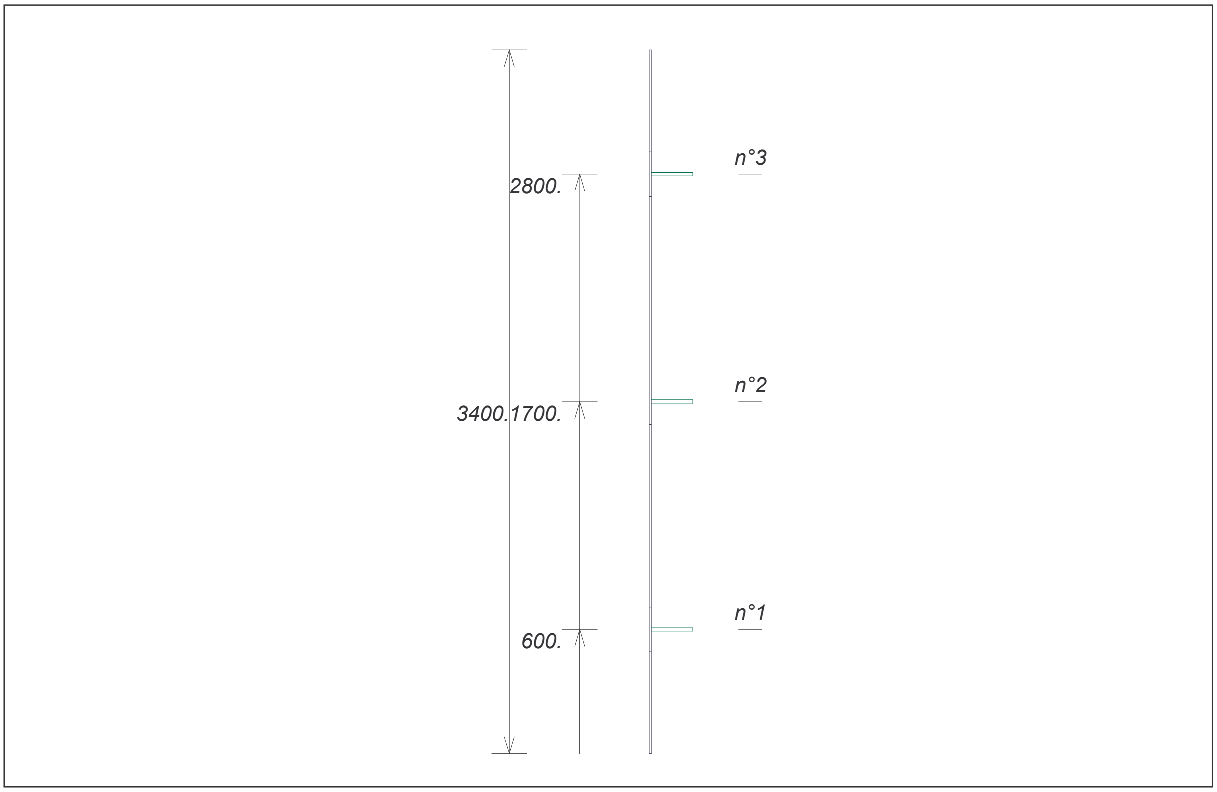

Figure 3 : Plate section with longitudinal stiffeners

STRESSES

Analytical stresses :

Analytical stresses will be calculated from this data.

Longitudinal stresses :

σ_{xt} = -99.9 MPa
σ_{xb} = 102.0 MPa

Transversal stresses :

σ_{yut} = 0.0 MPa
σ_{yub} = 0.0 MPa

Patch Loading stresses :

σ_{ypt}	= 0.0 MPa	c_t	= 0.0 mm
σ_{ypb}	= 0.0 MPa	c_b	= 0.0 mm

Local longitudinal stresses due to patch loading are not taken into account.
Local shear stresses due to patch loading are taken into account.

Shear stress :

τ = 0.0 MPa

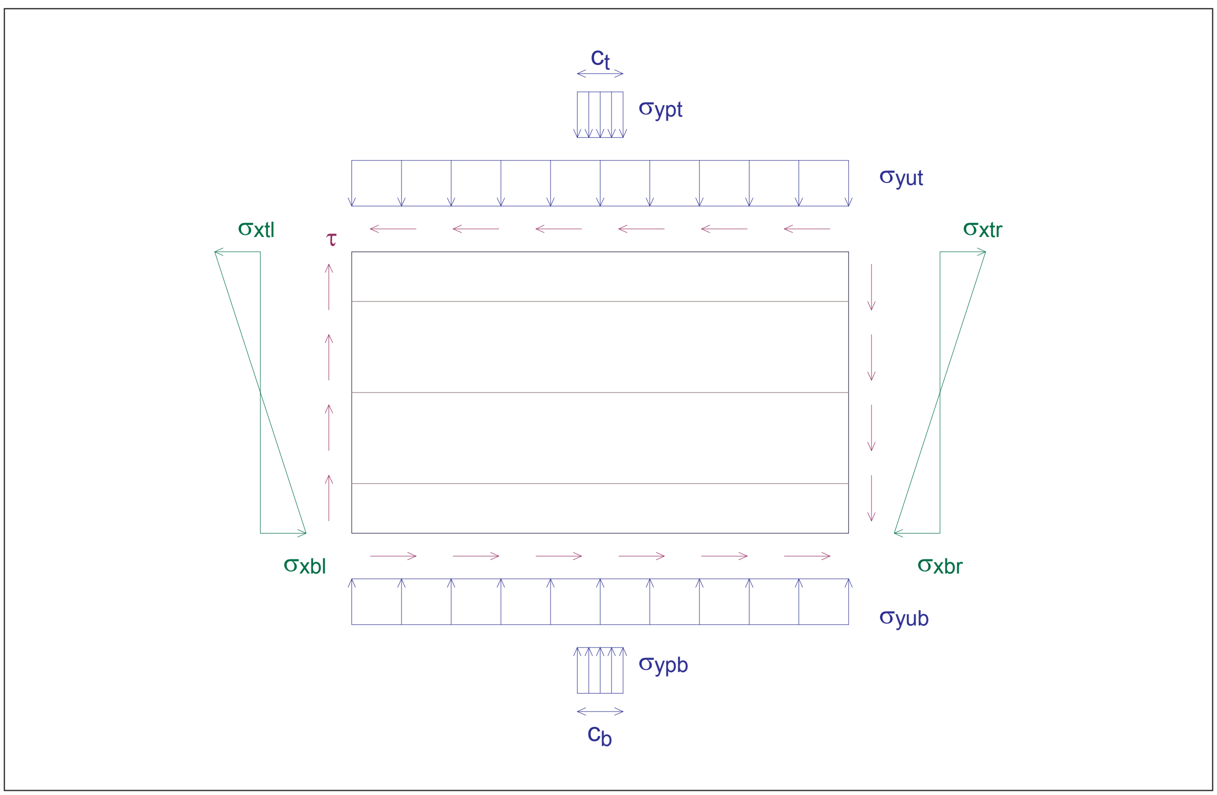

Figure 4 : Analytical stresses

Longitudinal stresses in the plate, defined by user (meshed stresses) :

No stresses defined in the plate.

Transverse stresses in the plate, defined by user (meshed stresses) :

No stresses defined in the plate.

Shear stresses in the plate, defined by user (meshed stresses) :

No stresses defined in the plate.

RESULTS

Calculation options :

Matrices dimensions :

User defined dimensions
Matrices dimensions : 15 x 8

Number of modes :

Desired modes : First buckling mode
Number of calculated modes : 1

Plate behaviour :

Calculation of the global buckling mode, buckling of all subpanels being prevented

Results :

Reference stress :

σ_E = 1.64 MPa

Critical multiplier of the first buckling mode :

$\Phi_{cr,p}$ = 8.465

Critical stresses and buckling coefficients of the first buckling mode :

Longitudinal stresses :

$\sigma_{xtl.cr}$ = -845.70 MPa	k_{xtl} = -515.083
$\sigma_{xbl.cr}$ = 863.48 MPa	k_{xbl} = 525.911
$\sigma_{xtr.cr}$ = -845.70 MPa	k_{xtr} = -515.083
$\sigma_{xbr.cr}$ = 863.48 MPa	k_{xbr} = 525.911

EBPlate

(v2.01)

Elastic Buckling of Plates

CALCULATION SHEET

Firm : Strukturas
Username : ThomasML
Contract : Master thesis
Contract item :
Note : Compression flange
Date : 09.05.2011

PLATE'S CHARACTERISTICS

Dimensions :

Width	a	= 6.00 m
Height	b	= 1.66 m
Thickness	t	= 16.0 mm

Material characteristics :

Young's Modulus	= 210000. MPa
Poisson's Ratio	= 0.30

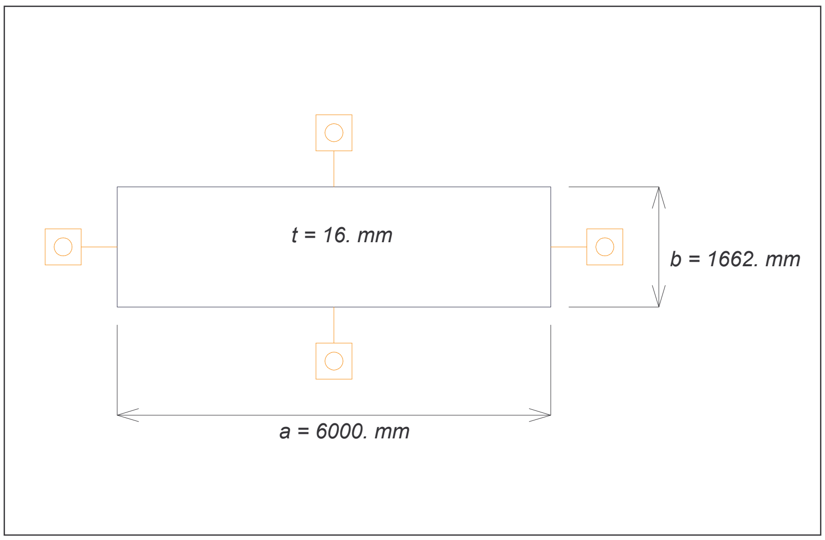

Figure 1 : Plate's dimensions and boundaries conditions

Boundaries conditions :

Side	Free	Clamped	Elastic restraints
Top	X		
Left	X		
Bottom	X		
Right	X		

STIFFENING CONDITIONS

Isotropy / Orthotropy :

The plate is isotropic.

Reference flexural plate rigidity : $D = 78769.24$ N.m

Stiffeners :

The plate is stiffened by 1 stiffener.

I	O	XY (cm)	Parameters δ	Parameters γ	Parameters θ	Type	Dimensions d1 (mm)	Dimensions d2 (mm)	Dimensions d3 (mm)	Dimensions d4 (mm)
1	H	x = 83.1	0.2106	155.8	0.4607	T 5	280.	20.		

I : Indice; O : Orientation; XY : Location
H : Horizontal; V : Vertical
T 1 : General Shape; T 2 : Angle; T 3 : Tee
T 4 : Trapezoidal section; T 5 : Single sided flat bar; T 6 : Double sided flat bar

Note :
The flexural inertia of the predefined type stiffeners is calculated taking into account an effective width of the plate. This width is equal to 10 times the thickness of the plate on each side of the connections of the stiffener.

I	L_W (mm)	z_W (mm)
1	340.0	75.1

L_W : Total width of the plate taken into account for the calculation of the flexural rigidity
z_W : Location of the neutral axis about the medium line of the plate

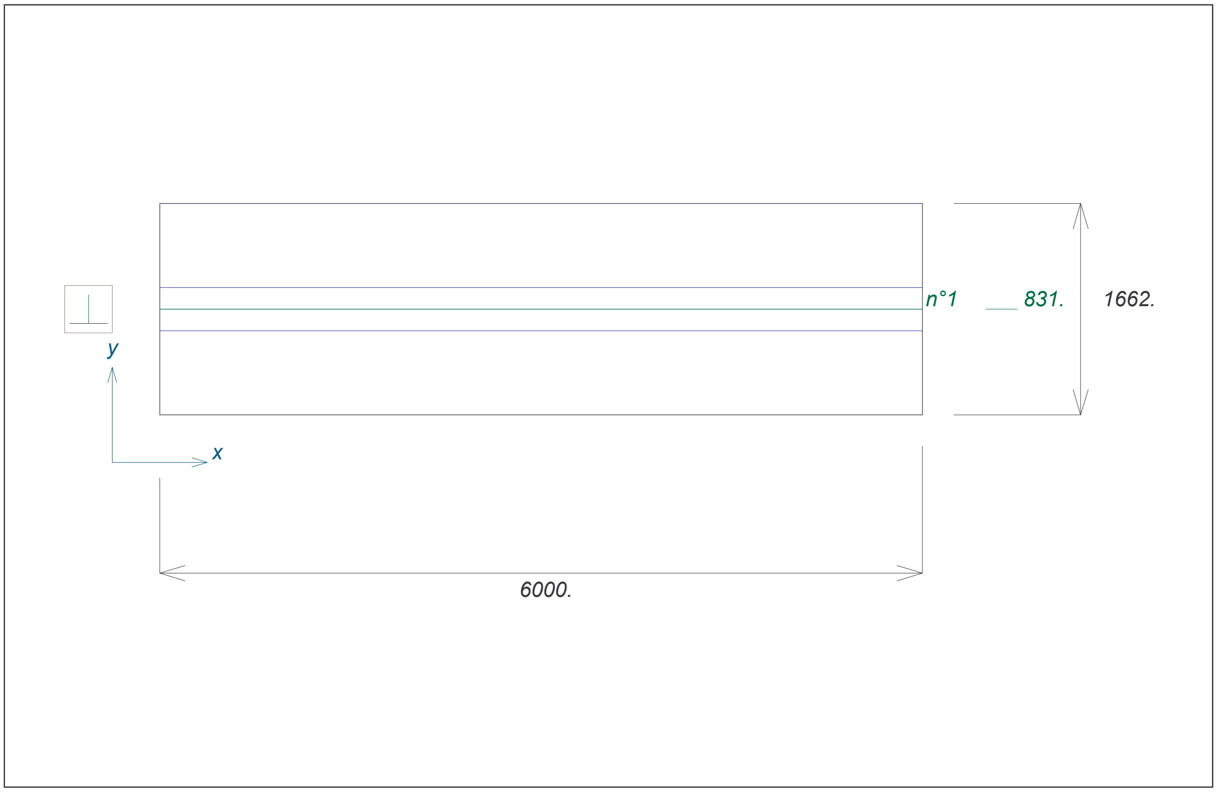

Figure 2 : Stiffeners

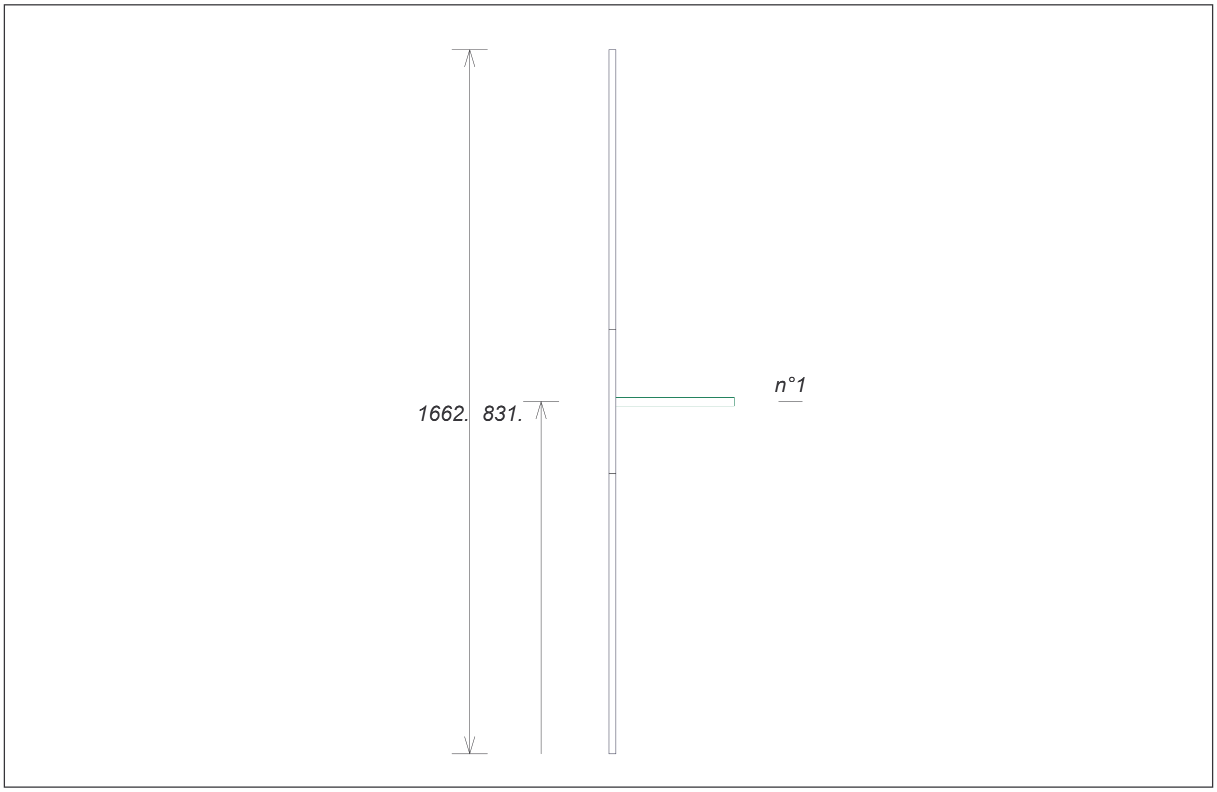

Figure 3 : Plate section with longitudinal stiffeners

STRESSES

Analytical stresses :

Analytical stresses will be calculated from this data.

Longitudinal stresses :

σ_{xt} = 102.0 MPa
σ_{xb} = 102.0 MPa

Transversal stresses :

σ_{yut} = 0.0 MPa
σ_{yub} = 0.0 MPa

Patch Loading stresses :

σ_{ypt} = 0.0 MPa c_t = 0.0 mm
σ_{ypb} = 0.0 MPa c_b = 0.0 mm

Local longitudinal stresses due to patch loading are not taken into account.
Local shear stresses due to patch loading are taken into account.

Shear stress :

τ = 0.0 MPa

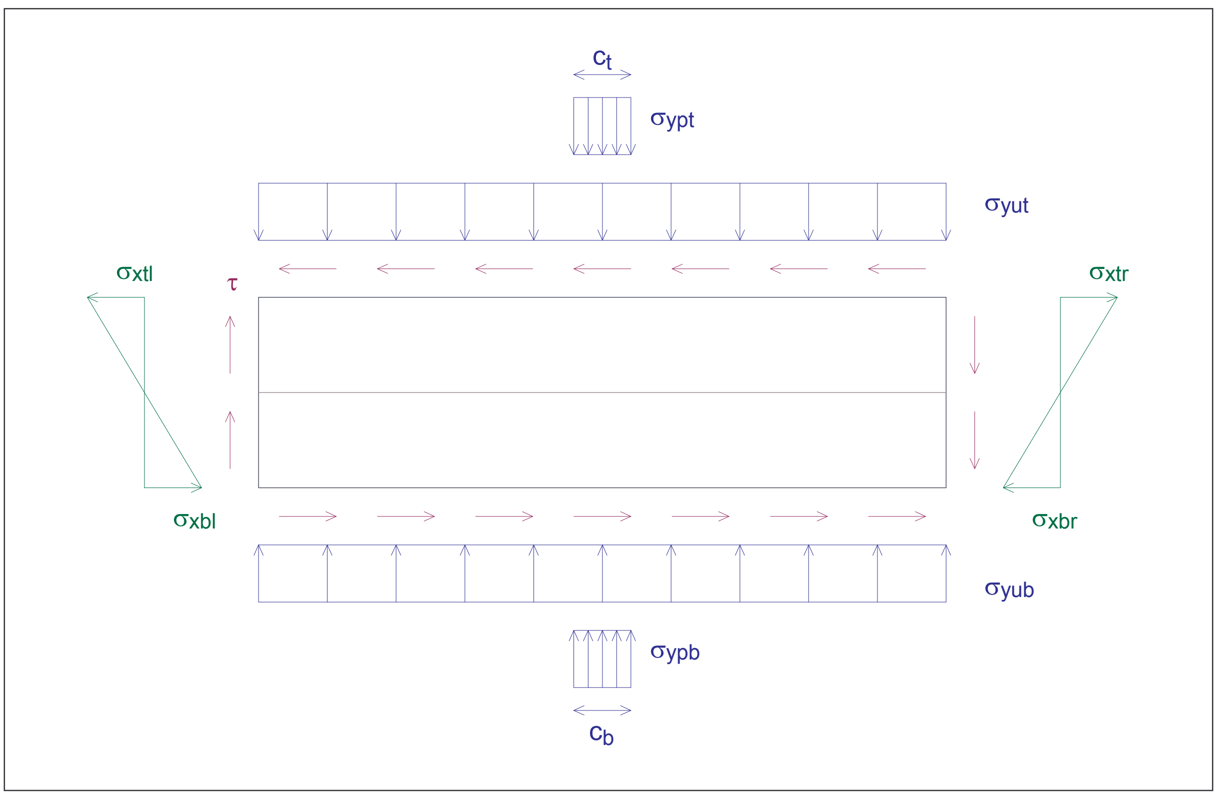

Figure 4 : Analytical stresses

Longitudinal stresses in the plate, defined by user (meshed stresses) :

No stresses defined in the plate.

Transverse stresses in the plate, defined by user (meshed stresses) :

No stresses defined in the plate.

Shear stresses in the plate, defined by user (meshed stresses) :

No stresses defined in the plate.

RESULTS

Calculation options :

Matrices dimensions :

Level of complexity : 1 (Low complexity case)
Matrices dimensions : 22 x 6

Number of modes :

Desired modes : First buckling mode
Number of calculated modes : 1

Plate behaviour :

Calculation of the global buckling mode, buckling of all subpanels being prevented

Results :

Reference stress :

σ_E = 17.59 MPa

Critical multiplier of the first buckling mode :

$\Phi_{cr,p}$ = 4.707

Critical stresses and buckling coefficients of the first buckling mode :

Longitudinal stresses :

$\sigma_{xtl.cr}$ = 480.07 MPa k_{xtl} = 27.292

$\sigma_{xbl.cr}$ = 480.07 MPa k_{xbl} = 27.292

$\sigma_{xtr.cr}$ = 480.07 MPa k_{xtr} = 27.292

$\sigma_{xbr.cr}$ = 480.07 MPa k_{xbr} = 27.292

References

[1] EN 1993-1-5, Eurocode 3: Design of steel structures, Part 1-5: Plated structural elements

[2] JRC Scientific and Technical Reports, Commentary and worked examples to EN 1993-1-5 “Plated structural elements”, First edition 2007, B.Johansson, R.Maquoi, G.Sedlack, C.Muller, D.Beg

[3] Design of plated structures, ECCS Eurocode Design Manuals, Eurocode 3: Design of steel structures, Part 1-5 Design of plated structures, Darko Beg, Ulrike Kuhlman, Laurence Davaine, Benjamin Braun

[4] EN 1993-1-1, Eurocode 3: Design of steel structures, Part 1-1: General rules and rules for buildings

[5] Patch loading resistance of longitudinally stiffened bridge girders, Davaine L, Raoul J, Aribert JM, 2004, Proceeding of the conference Steel Bridge 2004, Millau

[6] Plate buckling resistance, Patch loading of longitudinal stiffened webs and local buckling, Mattias Clarin, 2007, Doctorial thesis, Luleå University of Technology

[7] EBPlate v 2.01: A piece of software developed in the frame of the COMBRI research project. Its aim is to assess the elastic critical stresses of plates. The program is free and may be downloaded from the web site of cticm: www.cticm.com

[8] Stålkonstruksjoner, Arne Selberg, Tapir Forlag, 1972

[9] ANSYS Mechanical Structural Nonlinearities, Metal Plasticity, Lectures and workhops, Training Manual, ANSYS Inc., February 2010

[10] Knekning av søyler og rammer, Pål G. Bergan & Tor G.Syvertsen, Second edition, Tapir Forlag, 1989

[11] ANSYS Workbench 12.1 Relase Documentation, Customer Portal, Availible at the ANSYS website: www.ansys.com